UNIVERSITY OF KWAZULU-NATAL

SYNTHESIS, CHARACTERIZATION AND APPLICATION OF NOVEL NANO-MATERIALS FOR THE ELECTROCHEMICAL DETERMINATION OF ANTIMALARIAL DRUGS.

2019

BY: TIRIVASHE ELTON CHIWUNZE

(STUDENT No: 210551046)

Submitted in fulfillment of the requirements for the degree of

Doctor of Philosophy in Pharmaceutical Chemistry

Discipline of Pharmaceutical Science, College of Health Science,

University of KwaZulu-Natal, Durban, South Africa.

PREFACE

The experimental work described in this thesis was conducted at the Medicinal Chemistry laboratory at the School of Pharmaceutical Sciences, University of KwaZulu- Natal, Westville, South Africa, from May 2016 to December 2018, under the supervision of Dr. Rajshekhar Karpoormath.

This thesis has been prepared according to Format 4 (Thesis by publications) as outlined in the guidelines of College of Health Sciences, University of KwaZulu-Natal. The chapters consist of a general introduction, chapters in discrete research papers and a final discussion. Four chapters have been published and the remaining chapter has been submitted in peer-reviewed internationally accepted journal.

This work has not been submitted in any form for any degree or diploma to any tertiary institution, where use has been made of the work of others, it is duly acknowledged in the text.

Tirivashe Elton Chiwunze..  Date: 15/ 08/ 2019

As the candidate's supervisor I agree to the submission of the thesis:

Prof. Rajshekhar Karpoormath  Date…18/Aug./2019.....

ABSTRACT

This thesis reports the development of electroanalytical methods applicable for determination of selected antimalarial drugs; primaquine, mefloquine and amodiaquine. The electrochemical behaviour of the drugs were carried out using three differently modified glassy carbon electrodes (GCE) as working electrodes. First working electrode was modified using synthesized gold nano-urchins (AuNU/GCE) and was used for the determination of mefloquine and primaquine separately. The second and third working electrodes were both used for the quantification of amodiaquine and were modified using the following composites; multi-walled carbon nanotubes with poly(methyl orange) (MWCNT/PMO/GCE) and gold nanoparticles decorated graphene oxide with poly-cysteamine (rGO-AuNP/Poly-Cyst/GCE). All measurements were carried out with a Ag/AgCl (3 M KCl)) reference using cyclic voltammetry (CV), electrochemical impedance spectroscopy (EIS) linear sweep voltammetry (LSV), differential pulse voltammetry (DPV) and square wave voltammetry (SWV). The designed sensors showed enhanced voltammetric responses and very low limits of detection which are attributed to the high surface area and high conductivity of the nanomaterials. The proposed sensors also demonstrated practical utility in quantification of the antimalarial drug in pharmaceutical formulations and human urine sample. Thus, the present study demonstrates a promising and alternative approach for clinical analysis and quality control of primaquine, mefloquine and amodiaquine.

DECLARATION 1 – PLAGIARISM

I, **Tirivashe Elton Chiwunze,** declare that

i. The research reported in this thesis, except where otherwise indicated, is my original work.

ii. This thesis has not been submitted for any degree or examination at any other university.

iii. This thesis does not contain other person' data, pictures, graphs or other information, unless specifically acknowledged as being sourced from other persons.

iv. This thesis does not contain other persons' writing, unless specifically acknowledged as being sourced from other researchers. Where other written sources have been quoted, then:
   a. Their words have been re-written but the general information attributed to them has been referenced
   b. Where their exact words have been used, then their writing has been placed in italics and inside quotation marks, and referenced.

v. Where I have reproduced a publication of which I am an author, co-author or editor, I have indicated in detail which part of the publication was actually written by

vi. This thesis does not contain text, graphics or tables copied and pasted from the internet, unless specifically acknowledged, and the source being detailed in the thesis and in the References sections.

Signed:  ..... Date: 15/ 08/ 2019

DECLARATION 2 – PUBLICATION

DETAILS OF CONTRIBUTION TO PUBLICATIONS that form part and/or include research presented in this thesis (include publications in preparation, submitted, in press and published and give details of the contributions of each author to the experimental work and writing of each publication)

Publications

1. Thapliyal, Neeta, **Tirivashe E. Chiwunze**, Rajshekhar Karpoormath, Rajendra N. Goyal, Harun Patel, and Srinivasulu Cherukupalli. "Research progress in electroanalytical techniques for determination of antimalarial drugs in pharmaceutical and biological samples." *RSC Advances* 6, no. 62 **(2016)**: 57580-57602.

   Contributions: I did half the literature review and assisted in compiling the manuscript under the supervision of Dr. Neeta Bachheti Thapliyal and Dr Rajshekhar Karpoormath. Rest all the co-authors assisted me in improvisation, writing up and proof reading.

2. **Tirivashe E Chiwunze**, Neeta Bachheti Thapliyal, Venkata Narayana Palakollu, and Rajshekhar Karpoormath. "A Simple, Efficient and Ultrasensitive Gold Nanourchin Based Electrochemical Sensor for the Determination of an Antimalarial Drug: Mefloquine." *Electroanalysis* 29, no. 9 **(2017)**: 2138-2146.

   Contributions: I did all the experimental work, characterization and writing up of the manuscript under the supervision of Dr. Neeta Bachheti Thapliyal and Dr Rajshekhar Karpoormath. Rest all the co-authors assisted me in improvisation, writing up and proof reading.

3. Thapliyal, Neeta, **Tirivashe E. Chiwunze**, Rajshekhar Karpoormath, and Srinivasulu Cherukupalli. Thapliyal. "Fabrication of highly sensitive gold nanourchins based electrochemical sensor for nanomolar determination of primaquine." *Journal of Materials Science and Engineering: C* 74 **(2017)**: 27-35.

   Contributions: I assisted in all the experimental work, characterization and writing up of the manuscript under the supervision of Dr. Neeta Bachheti Thapliyal and Dr Rajshekhar Karpoormath. Rest all the co-authors assisted me in improvisation, writing up and proof reading.

4. **Tirivashe E Chiwunze**, Venkata Narayana Palakollu, Atal A.S. Gill, Francis Kayamba, Neeta Bachheti Thapliyal and Rajshekhar Karpoormath. "A highly dispersed multi-walled carbon nanotubes and poly(methyl orange) based electrochemical sensor for the determination of an anti-malarial drug: Amodiaquine". *Journal of Materials Science and Engineering: C* 97 **(2019)** 285-292

   Contributions: I did all the experimental work, characterization and writing up of the manuscript under the supervision of Dr. Neeta Bachheti Thapliyal and Dr Rajshekhar Karpoormath. Rest all the co-authors assisted me in improvisation, writing up and proof reading.

5. **Tirivashe Elton Chiwunze**, Venkata Narayana Palakollu, Neeta Bachheti Thapliyal, Atal A.S. Gill, Francis Kayamba , Rajshekhar Karpoormath, Thobeka Persevearance Vilakazi, Wendy Zulu, Aphelele Ngubane, Kajal Mohanlal, and Nokwanda Zenani Dhlamini. "A Novel Electrochemical Sensor Based on Gold Nanoparticles Decorated Reduced Graphene Oxide and Poly-Cysteamine Composite for the Determination of Amodiaquine". This manuscript has been submitted and its under review at the *Journal of Measurments.*

   Contributions: I did all the experimental work, characterization and writing up of the manuscript under the supervision of Dr. Neeta Bachheti Thapliyal and Dr Rajshekhar Karpoormath. Rest all the co-authors assisted me in improvisation, writing up and proof reading.

Conference contributions

1. **Oral presentation**: A Simple, Efficient and Ultrasensitive Gold Nanourchin Based Electrochemical Sensor for the Determination of an Antimalarial Drug: Mefloquine. College of Health Sciences Research Symposium, held at Nelson R Mandela School of Medicine Campus, Durban, South Africa, from 8th to 9th September **2016 and 2017**.

2. **Oral presentation**: A Simple, Efficient and Ultrasensitive Gold Nanourchin Based Electrochemical Sensor for the Determination of an Antimalarial Drug: Mefloquine. UKZN Nanotechnology Platform Symposium held at MH Joosub Hall-Westville Campus Durban, South Africa, on the 22nd of November **2017**

3. **Oral presentation**: A Novel Electrochemical Sensor Based on Gold Nanoparticles Decorated Reduced Graphene Oxide and Poly-Cysteamine Composite for the Determination of Amodiaquine 4th International Symposium on Electrochemistry, held at University of Johannesburg, Johannesburg, South Africa, from 3rd to 5th April **2018**.

4. **Poster presentation**: A Simple, Efficient and Ultrasensitive Gold Nanourchin Based Electrochemical Sensor for the Determination of an Antimalarial Drug: Mefloquine. ICONAN 2018, International Conference on Nanomedicine and Nanobiotechnology, held in Rome, Italy, from 26th to 28th September **2018**.

5. **Poster presentation**: A Sensitive Electrochemical Sensor Based on Gold Nanoparticles Decorated Graphene Oxide and Poly-Cysteamine Composite for the Determination of Amodiaquine. UKZN Nanotechnology Platform Symposium Senate Chamber-Westville Campus Durban, South Africa, on the 9th of October **2018**

6. **Oral presentation**: A Highly Dispersed Multi-walled Carbon Nanotubes and Poly(methyl orange) Based Electrochemical Sensor for the Determination of an Anti-Malarial Drug: Amodiaquine. College of Health Sciences Research Symposium, held at Nelson R Mandela School of Medicine Campus, Durban, South Africa, from 11th to 12th October **2018**.

Other publications

1. Palakollu, V. Narayana, **Tirivashe E. Chiwunze**, Atal AS Gill, Neeta Thapliyal, Shital M. Maru, and Rajshekhar Karpoormath. "Electrochemical sensitive determination of isoprenaline at β-cyclodextrin functionalized graphene oxide and electrochemically generated acid yellow 9 polymer modified electrode." *Journal of Molecular Liquids* (2017). *248*, 953-962.

2. Palakollu, Venkata Narayana, Neeta Thapliyal, **Tirivashe E. Chiwunze**, Rajshekhar Karpoormath, Sivanandhan Karunanidhi, and Srinivasulu Cherukupalli. "Electrochemically reduced graphene oxide/Poly-Glycine composite modified electrode for sensitive determination of l-dopa." *Materials Science and Engineering: C* 77 (2017): 394-404.

Signed:  Date: 15/ 08/ 2019

DEDICATION

I dedicate this to my parents, my

mom (Rhoda Chiwunze)

and

dad (Cornelius Chiwunze).

ACKNOWLEDGEMENTS

First of all, I want to thank God for his grace that has brought me this far. I want to thank my parents Rhoda and Cornelius Chiwunze for their support, encouragement and the belief they had in me. I would not be here if it wasn't for them.

I also wish to express my sincere gratitude to my supervisors Dr Rajshekhar Karpoormath for his guidance, patience and support during the course of this research. I sincerely thank Dr Neeta Bachheti Thapliyal for taking me under her wing and mentoring me through my whole Ph.D and always encouraging me to keep on going and working hard, you were like my guardian angel and always a voice of encouragement.

I also would like to thank:

My fellow colleagues, Dr Venkata Narayana Palakollu, Atal A.S. Gill, Zondi Nate Francis Kayamba, Cleopus Mavela, Dr Nisar and the rest of SMCRG.

My Siblings Tirivafi, Gamuchirai, Ruvimbo, Rutendo Chiwunze; Kudzai Kativu and Charity Njangu for their moral support and all the love they showed me. You guys showed me the real meaning of family and for that I will forever be indebted to you.

My friends Sifiso Makhathini, Rufaro Razuwika, Chiedza Munyeza, Mxolisi Shokhela, Siphokazi Zondi, Oneal Mtutu, Johaness Nyamadzawo, Michelle Chaitezvi, Rumbidzai Jiri, , Tinashe Mukau, Faith Kashora Tawanda Mandizvo, Tonderai Muginyi, Graig Gatsi.

My nephew and nieces (Engelberth, Anashe Chiwunze and Mudiwa Ngonyamo); and lastly but not least my brother in law Nyasha Ngonyamo and my sisters in law Beatrice and Marvelous.

TABLE OF CONTENTS

LIST OF FIGURES

Chapter 1:

Chapter 2:

Chapter 3

Chapter 4:

Chapter 5:

LIST OF TABLES

Chapter 2:

Chapter 3

Chapter 4:

Chapter 5:

Chapter 6:

LIST OF SCHEME

Chapter 5

Chapter 6

LIST OF ABBREVIATIONS

Abbreviations

AA-EGMA: Acrylic acid-ethylene glycol methacrylate

Ag-CWEs: Silver coated wire electrodes

Anodized BDD: Anodized boron-doped diamond electrode

ART-MIM/G/GCE: Artemisinin-imprinted membranes on the surface of graphene modified glassy carbon electrode

ACT: Artemisinin-based combination therapy

AuNUs: Gold nanourchins

AuNPs: Gold nanoparticles

AQ: Amodiaquine

ASV: adsorptive stripping voltammetry

Au RDE: Gold rotating disk electrode

BEHA: bis(2-ethylhexyl) adipate

Bi-SPCE: Bismuth film coated screen-printed carbon electrode

CPE/STH: Hemin immobilized on a titanium oxide modified silica based carbon paste electrode

CSP: Circumsporozite protein

C: Capacitance

Cyst: cysteamine

Cu-NW/CPE, $Cu(OH)_2$: nano-wire modified carbon paste electrode

CV: Cyclic voltammetry

CPE: Carbon paste electrode

CTAB: cetyltrimethylammonium bromide

Cu-CWEs: copper coated wire electrodes

Cu-NW/CPE: $Cu(OH)_2$ nano-wire-modified carbon paste electrode

DB24C8: dibenzo(24-crown-8)

DB30C10: dibenzo(30-crown-10)

DBP: dibutylphthalate

DNA: Deoxyribonucleic acid

DHFR: Dihdrofolate reductace

DDT: Dichloro-Diphenyl-Trichloroethane

DC: Doxycycline

DC-HRP on antiDC- ProtG-MBs/SPCE: Horseradish peroxidase conjugated doxycycline on antibody immobilized on the surface of protein G functionalized magnetic beads based screen printed carbon electrode (immunosensor)

DDP: didecyl phthalate

DHP: dihexadecyl hydrogen phosphate

DME: Dropping mercury electrode

DNA/SPCE: DNA modified screen printed carbon electrode

dsDNA-MB-MWNTs/GCE: Calf thymus double stranded DNA, methylene blue and multiwall carbon nanotubes modified glassy carbon electrode

DOP: Dioctyl phthalate

DOPP: dioctyl phenyl phosphonate

DPP: Differential pulse polarography

DPV: Differential pulse voltammetry

dsDNA/CPE: dsDNA-modified carbon paste electrode

EIS: Electrochemical impedance

Ep: Peak potential

ΔEp: Peak potential separation

EDX: Energy-dispersive X-ray

EGMRA-MIP/GCE: Ethylene glycol maleic rosinate acrylate based molecularly imprinted polymer modified glassy carbon electrode

FE-SEM: Field emission scanning electron microscopy

[FeT(o-glu)PPCl]/AuNPs/GCE: Fe(III) coordinating glycosylated porphyrin in gold nanoparticles-chitosan film modified glassy carbon electrode

FIA: Flow injection amperometry

G/PANI/SPCE: Graphene/polyaniline modified screen-printed carbon electrode

GCE: Glassy carbon electrode

GMEP: Global Malaria eradication programme

GC/PPy/PVC: Polypyrrole film immobilized on a glassy carbon electrode in plasticized polyvinyl chloride membrane

GrO/PANI/HRP/ITO electrode: graphene–polyaniline–horseradish peroxidase modified ITO electrode

Hg(Ag)FE: silver amalgam film electrode

HBsAg: Hepatitis B surface antigen

HPLC: High-performance liquid chromatography

Ip: Peak current

KTCPB: potassium tetrakis(4-chlorophenyl) borate

LOQ: Limit of quantification

LOD: Limit of detection

LSV: Linear sweep voltametry

MO: Methyl orange

MWCNTs: Multiwalled carbon nanotubes

MQ: Mefloquine HMDE: hanging mercury drop electrode

MAA: methacrylic acid

MIP/sol-gel/MWNT/Au: Multi-wall carbon nanotube layer with a thin molecularly imprinted sol-gel film modified gold electrode

MIPPy/PGE: Molecularly imprinted non-imprinted polypyrrole modified pencil graphite electrode

MWCNTs/GCE: Multi-walled carbon nanotubes modified glassy carbon electrode

MWCNTs-RTIL/GCE: multiwall carbon nanotubes- room-temperature ionic liquid modified glassy carbon electrode

NaTPB: Sodium tetraphenylborate

Ni/GCE: Nickel-modified glassy carbon electrode

p-(AHNSA)/GCE: poly(4-amino-3-hydroxynaphthalene sulfonic acid)-modified glassy carbon electrode

PHA/AuNPs/HRP/ITO: Horse-radish peroxidase immobilized polyhydroxyalkanoate–gold nanoparticle composite on indium-tin oxide electrode

Ppy-PCNFe/Pt: polypyrrole-pentacyanoferrate modified platinum electrode

PVC: Polyvinyl chloride

PQ: Primaquine

PMO: Polymerised methyl orange

PCR: Polymerase chain reaction

PBS: Phosphate buffer solution

QA/QC: Quality assurance and quality control

Qn_3PM: ion pair of quininium and phosphomolybdate

Qn_3PT: ion pair of quininium and phosphotungstate

QnRn: ion pair of quininium and reineckate

RuO-RuCN/GCE: Ruthenium oxide-ruthenium cyanide film on a glassy carbon electrode

RDTs: Rapid diagnostic test

rGO: Reduced graphene oxide

Rs: Resistance of the electrolyte solution

Rct: Charge-transfer resistance

RSD: Relative standard deviation

SEM: Scanning electron microscopy

SWCNTs/GCE: Single-walled carbon nanotubes modified glassy carbon electrode

SWV: Square wave voltammetry

TCP: tricresyl phosphate

THF: Tetrahydrofuran

TEM: Transmission electron microscopy

US: United States

UV-Vis: Ultraviolet-visible

W: Warburg impedance

WHO: World health organisation

CHAPTER 1

1. Introduction

1.1 Malaria – Overview

Malaria is an infectious disease caused by *Plasmodium* parasites. It has also been known by other names such as biduoterian fever, blackwater fever, falciparum malaria, plasmodium, Quartan malaria, and tertian malaria [1]. Transmission is through a bite of an infected female Anopheles mosquito. Malaria has clinical symptoms that range from fever, chills, and flu-like illness to more severe complications such as cerebral malaria, pulmonary edema, acute renal failure, severe anemia, and hypoglycemia [2]. It is preventable and curable although, if severe malaria is not treated it may lead to cerebral malaria and death. Malaria has been in existence for over 2,000 years, but the greater milestones took place in the 19th century[3]. In 1880, a Nobel Laureate winner, Laveran discovered that the *Plasmodium* parasite was responsible for causing malaria [4]. There are five known *Plasmodium* species that are capable of infecting humans namely. *P. falciparum P. vivax, P. ovale, P. malariae* and *P. knowlesi* [5]. *P falciparum* causes severe malaria and has been responsible of most malaria deaths. It is predominantly found in the sub-Saharian region. *P. vivax, P. ovale, and P. malariae* normally cause non-lethal, mild form of malaria and the strains are mainly common in the South-America and the Asia-Pacific regions [6, 7]. *P. knowlesi* species scarcely causes disease in humans although it is major cause of malaria in monkeys [8].

The World Health Organization (WHO) report in 2016, indicated an estimated 216 million cases and 445 000 deaths of malaria in 91 countries [9]. Both mortality and morbidity were the highest in the African region accounting for an average of 91 % globally. It was followed by South East Asia region that accounted for 6% of all the malaria deaths. Malaria is mostly widespread in poor tropical and subtropical areas of the globe. About 40 % of the world population is at risk of contracting malaria. It is more prevalent in Sub-Saharan Africa. This can be alluded to a number factor that includes [9]:

- The conducive warm climate that is ideal for the Anopheles mosquitoes to breed and survive all year round.
- The parasite species *P. falciparum*, which is the strain that is most likely to cause severe malaria and death, is predominant in the areas.
- Scarce resources and socio-economic instability have hindered efficient malaria control activities.

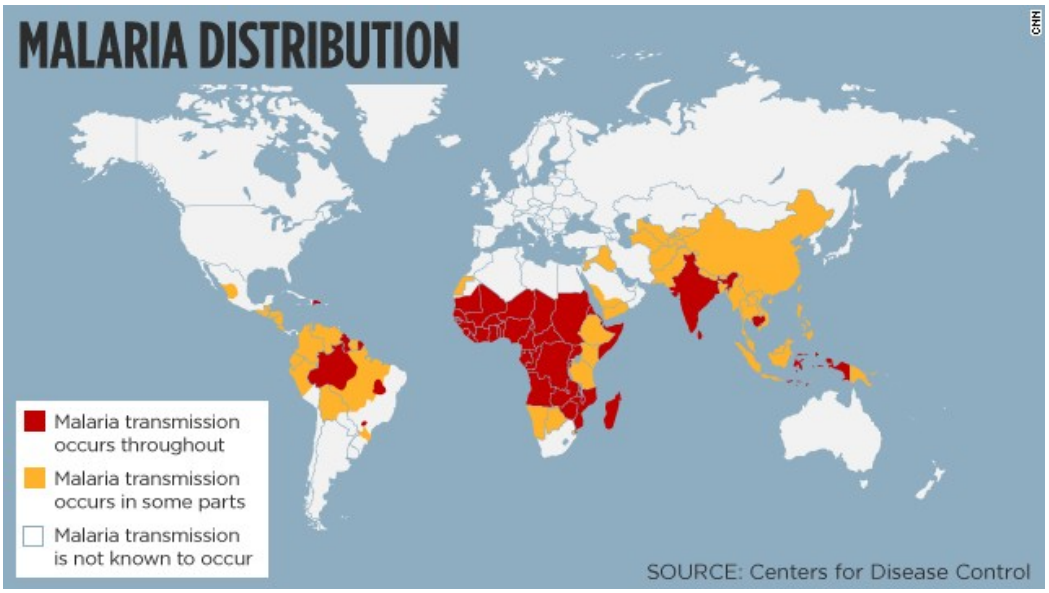

Fig. 1 Show a global profile of malaria transmission [10].

1.2 Plasmodium Lifecycle

The *plasmodium* parasites' lifecycle takes place into two host; mosquito and human. Figure 3 depicts an illustration of various stages involved in the plasmodial life cycle designated by steps A to F. It typically begins with a bite by an infected female anopheles mosquito. The mosquito draws blood from the human host at the same time injecting infected saliva containing the *plasmodium* sporozoites (A). The sporozoites are then trafficked to the liver where they infect the hepatic cells (B). They remain in the liver for 9-16 days. They multiple by asexual fusion and mature into tissue schizonts that contain thousands of merozoites (C). In the case of *P.vivax* some sporozoites develop into hypnozoites which lie dormant in the liver for up to 60 days and cause a relapse. After 5 days, the tissue schizonts rupture releasing the merozoites into the blood stream (D). At this point they enter the erythrocytes stage and reproduce asexually. It is at this stage that the clinical symptoms of malaria can occur. (E) The merozoites multiply inside the red blood cells until they rupture. Some of the newly released merozoites go on to infect other healthy erythrocytes (intra-erythrocytic cycle) and others undergo transformation into male and female gametocytes (F). The *plasmodium* continues its cycle when a female anopheles mosquito feeds on the infected human host and ingests the gametocytes that circulate in the peripheral blood of the host (G). In the mosquito mid gut (F) the male and female gametocytes reproduce sexually forming zygotes that multiply to form infective sporozoites. The sporozoites are transferred to the mosquito's salivary glands where they are injected into another human host perpetuating the cycle [11].

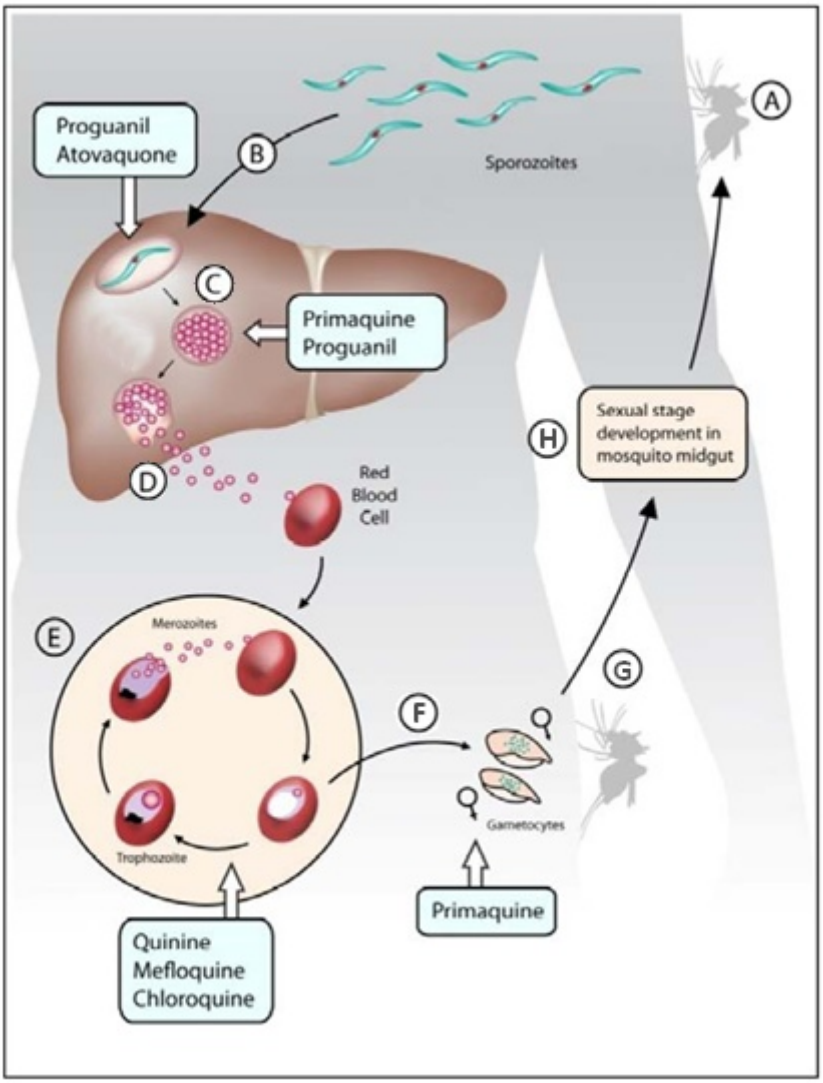

Fig. 2 Schematic illustration of the lifecycle of *P. falciparum*, showing all the various stages involved and associated antimalarial drugs target sites. (A) an infected female Anopheles mosquito bites human, takes a blood meal and injects sporozoites, (B) sporozoites are transported to the liver and replicate, (C) sporozoites mature into tissue schizonts containing merozoites,(D) merozoites are released in the host's blood stream, (E) infect the host's erythrocytes and reproduce asexually, (F) transformation into male and female gametocytes, (G) during the next meal by female Anopheles mosquito the gametocytes are taken up and (H) sexual reproduction takes place in the mosquito mid gut forming infectious sporozoites, completing the lifecycle [11].

1.3 Malaria Control and Prevention

Malaria is a preventable and treatable disease although, it is difficult to control mainly due to the adaptive nature of the parasite and the vector associated with the disease. Prevention of malaria infection involves three essential elements of the parasites' life cycles; the vector (mosquito), the host (human) and the agent (parasite) [12]. The vector control element largely involves stopping the mosquitoes from multiplying by reducing the breeding sites where possible i.e. destroying the vector in the larval stage and preventing mosquito bites to humans. The second element is the most important link in the malaria control chain as it primarily involves the host (human). Early diagnosis and prompt treatment of malaria stops the progression of the disease and reduce morbidity and mortality in areas with high risk of transmission. Lastly, the third element focuses on the antimalarial agents; ensuring treatment compliance by patients helps kill the asexual forms of the parasite hence stopping the progression of the disease and also lowering the parasitic load which reduces the risk of transmission to a vector during a blood feed. **Fig. 3** illustrates the control chain of malaria which is a complex chain of measures that often work together.

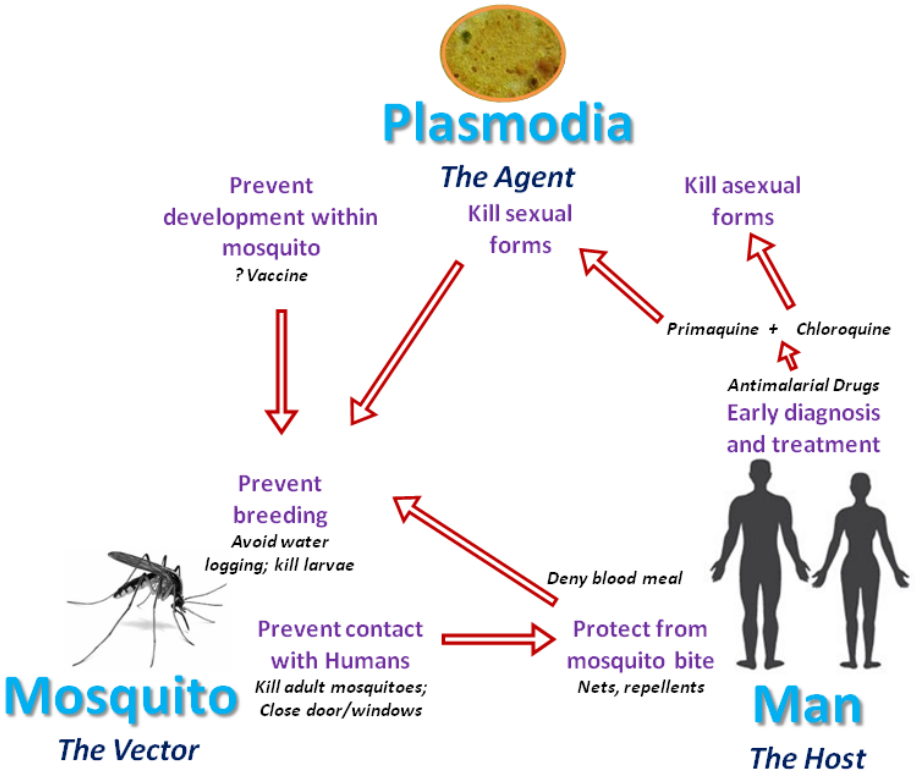

Fig. 3 Control strategy of malaria.

Typically, malaria diagnosis is carried out either by examining blood smears with microscopes or antigen-based rapid diagnostic tests (RDTs) [13, 14]. Although these techniques are effective, they cannot identify drug resistance profile of *Plasmodium falciparum*. In addition, other methods based on detecting the parasite's DNA by use of polymerase chain reaction assays (PCR) have been developed [13, 15, 16]. However, the technology is expensive and complex of which the most malaria prevalent areas are developing countries and cannot afford.

In the 1950s, a campaign called the Global Malaria Eradication Programme (GMEP) was launched [17]. It aimed at wiping out malaria completely around the globe. GMEP was motivated by the breakthrough discovery of dichloro-diphenyl-trichloroethane (DDT) [18, 19] and its effectiveness in killing the mosquitoes, and the widespread deployment of chloroquine, a cheap and effective antimalarial drug [20]. The mission was a partial success as it managed to eliminate malaria only in certain regions of the world, mostly developed countries with

temperate climates. The campaign‘s global failure was due to the GMEP being less effective in some parts of the world such as Africa and Asia where malaria is most prevalent today. These regions had logistic and administrative challenges that hindered progress for the campaign. The controversies surrounding the use of DDT [21] as an insecticide and the declining efficacy of chloroquine against *P. falciparum* resulted in the program being abandoned and the eradication of malaria being considered impractical. After the failure of the GMEP, efforts were shifted to the development of malaria vaccines. Although WHO has not yet licensed an effective antimalarial vaccine, there are several vaccines under development that are in the late stages of clinical trials. One such promising vaccine is RTS,S (Mosquirix) which was engineered by fusing the circumsporozoite proteins (CSP) from the parasite *P. falciparum* with a portion of hepatitis B surface antigen (HBsAg) and a chemical adjuvant to improve the immunologic response [22]. The lack of an effective vaccine leaves chemoprophylaxis as the best option in reducing the risk of contracting malaria.

1.4 Chemoprophylaxis

Chemoprophylaxis is the use of anti-malaria drugs to prevent malaria infections. It kills the parasite in the hepatocytes or erythrocytes stage. WHO recommends all people travelling to malaria endemic regions to take chemoprophylaxis [23]. However, chemoprophylaxis offers up to 90% anti-malarial protection. Additionally, it is essential to take strict precautions to avoid mosquito bites as well. The choice of the chemoprophylaxis regimen differs from region to region; it is determined by the nature of the drug resistance and *plasmodium* species rampant in that area. Malaria chemoprophylaxis is classified into two groups based on their site of action in the parasite’s lifecycle; liver stage (causal prophylaxis) and blood stage (suppressive prophylaxis).

Causal prophylactic drugs act on the parasite in the liver stage [24]. Currently, primaquine and Malarone (atovaquone-proguanil) are the only drugs that act on the hepatocytes stage and can

avert the formation of hyponozoites [25]. Nonetheless, only primaquine can kill the hyponozoites directly [26]. The advantage of this prophylaxis is that it does not require the travelers to continue medicating after leaving the endemic areas since the drugs would have eradicated the parasites at the early infectious and the dormant hyponozoites stages. Thus, causal prophylaxis offers the most effective prevention against all *Plasmodium* species and it is very crucial in the cases of *P. vivax* and *P. ovale* [24].

Suppressive prophylactics are drugs that act on the parasites within the intra-erythrocytic cycle [24]. They are among the earliest and most common antimalarial drugs. These include Quinine, Mefloquine and Chloroquine. Since these drugs kill the parasites within the red blood cells only, they must be continued for 4 more weeks after leaving the endemic areas to avoid infection that may emerge from the liver as late as 2–4 weeks after exposure. The drugs are only effective with *P. falciparum* infection. For *vivax* and *ovale* infections, they can only offer primary prevention, and are unable to prevent relapse from the dormant liver stage (hypnozoites) [27].

1.5 Currently Used Antimalarial Drugs

Different antimalarial drugs have been used for the treatment of malaria. For many years chloroquine was effective and the drug of choice, until recently when *P. falciparum* developed resistance and rendered it ineffective [28]. Several other drugs are used for treatment and prevention (prophylaxis). Various drugs are active against different stages or targets in the life cycle of the parasite. The most common drugs include quinine and its derivatives, chloroquine, amodiaquine, pyrimethamine, proguanil, sulfonamides, mefloquine, atovaquone, primaquine, artemisinin and its derivatives. Below is a list of most commonly used antimalarial drugs; some of which are used in combination therapy in regions where widespread drug resistance is evident.

1.5.1 Chloroquine (1)

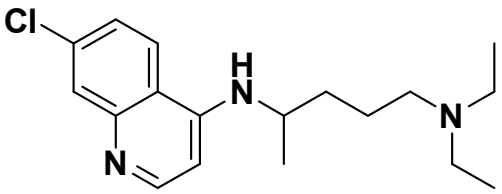

(1)

Fig. 4 Chloroquine

Chloroquine is a 4-aminoquinoline compound that was discovered by Hans Andersag in 1934 [29]. Its proposed mechanism of action is to inhibit heme polymerase activity. Heme polymerase facilitates polymerization of toxic heme to no-toxic haemozoin. Hindering the activity of polymerase allows the accumulation of free heme, which poisons and causes the death of the parasite. Chloroquine was effective against all strains of Plasmodium, although in the recent years, resistance has emerged in all the strains [28].

1.5.2 Quinine (2)

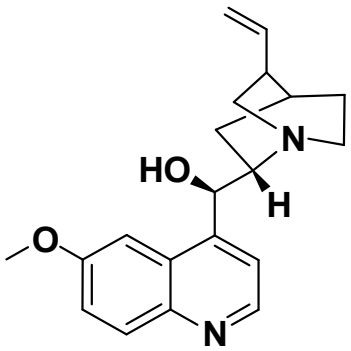

(2)

Fig. 5 Quinine

Quinine is an alkaloid extracted from the barks of the cinchona tree. The antimalarial properties of the cinchona barks were discovered as early as 1632 by the natives of the Andean regions of South America. Isolation of quinine, an active component from the bark extracts was only carried out in 1820 [30]. Quinine acts as a blood schizonticide and weak gametocide against

P.vivax and *P. malariae*. It is also used to treat acute cases of severe *P. falciparum* infection. It kills the plasmodium parasites in a similar fashion as the other quinine derivatives by accumulating in the food vacuoles and inhibiting the heme polymerase enzyme, thus resulting in the build-up of cytotoxic heme [31]. Side effects associated with Quinine include a reversible high-tone hearing loss, mild headache, muscle weakness, vomiting and unusual sweating.

1.5.3 Mefloquine (3)

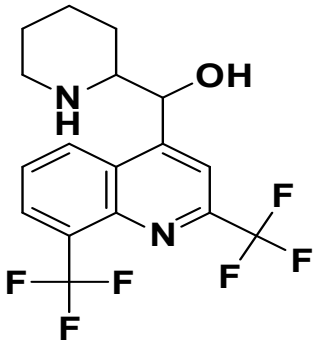

(3)

Fig. 6 Mefloquine

Mefloquine is an orally administered blood schizontocide that was developed during the Vietnam War by the US army to protect its soldiers from the multi-drug resistant *P. falciparum* strain [32]. By the time mefloquine was made accessible to the general population, cases of resistance had already manifested. Today it is used in combination with Artesunate to treat resistant strains. The mechanism of action is not fully understood but it is proposed to involve the formation of a mefloquine-toxic heme complex that damages the parasitic food vacuoles [31]. There are several side effects linked to the use of mefloquine that range from abdominal pains, diarrhoea, vomiting, nausea to neurological disorders such as hallucination, insomnia, convulsion and anxiety disorders [5]

1.5.4 Primaquine (4)

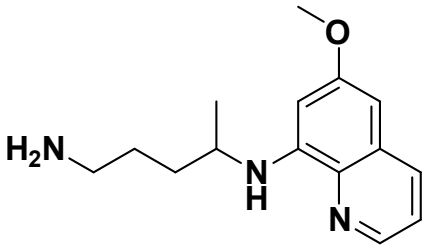

(4)

Fig. 7 Primaquine

Primaquine is a highly active 8-aminoquinoline compound that was first synthesized in 1946 in the USA [33]. It is highly effective against all forms of malaria and the only clinically available drug that can prevent relapse of malaria. The mode of action is not well established but it has been proposed that primaquine helps to create oxygen-free radicals that interrupt the plasmodial electron transport chain during respiration [34]. Primaquine causes very few side effects, such as nausea, heartburn, vomiting, anaemia, stomach cramps and loss of appetite [35].

1.5.5 Amodiaquine (5)

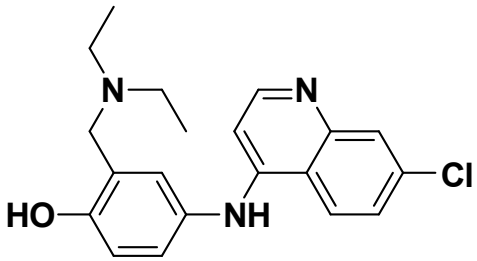

(5)

Fig. 8 Amodiaquine

Amodiaquine is a Mannich base that belongs to the family of 4-aminoquinolines [36]. It is structurally similar to chloroquine and is believed to have the same mechanism of action. It is used to treat uncomplicated cases of malaria and it has shown to have less toxic effects on HIV positive patients compared to the other antimalarial drugs. Despite these advantages,

amodiaquine is associated with certain side effects such as, abdominal cramps, nausea, vomiting and itchiness [37].

1.5.6 Pyrimethamine (6)

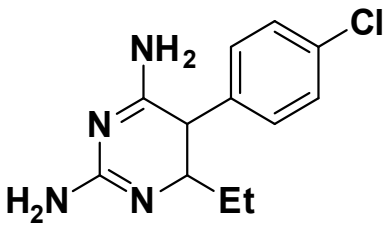

(6)

Fig. 9 Pyrimethamine

Pyrimethamine is a synthetic derivative of pyrimidine used for the treatment of protozoal infections and acute cases of malaria. It is ideally used in combination with sulfadiazine and both drugs are antifolates [38]. They both act as competitive inhibitors of dihydrofolate reductase (DHFR), a key enzyme involved in the production of tetrahydrofolic acid within the parasites [39]. Pyrimethamine is associated with certain side effects such as, folic acid deficiency, skin rash sore throat, flu symptoms, trouble breathing; irregular heartbeats, and hypersensitivity reactions [40].

1.5.7 Proguanil (7)

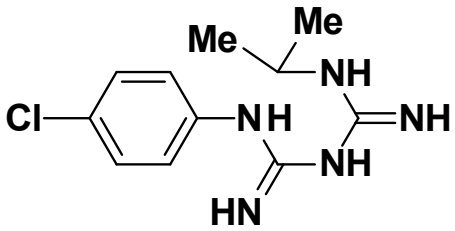

(7)

Fig. 10 Proguanil

Proguanil is a prophylactic antimalarial drug that is effective against *P. falciparum* and *P. vivax* strains. It is taken in combination with atovaquone to treat chloroquine-resistant and multi-drug resitant strains [41]. Its mode of action involves inhibiting the enzyme, dihydrofolate reductase which is responsible for producing a cofactor tetrahydrofolate, required for DNA and proteins synthesis by the parasite [39].

1.5.8 Sulphadoxine (8)

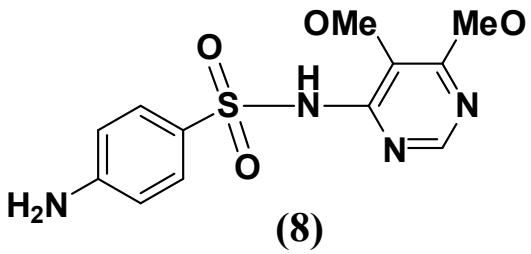

(8)

Fig. 11 Sulphadoxine

Sulphadoxine is a sulphonamide drug used in conjunction with pyrimethamine for the treatment of malaria [42]. Previously, it was used as prophylactic but due to the elevated levels of resistance, it was removed from the routinely recommended list. The mode of action is the same as that of pyrimethamine [43].

1.5.9 Atovaquone (9)

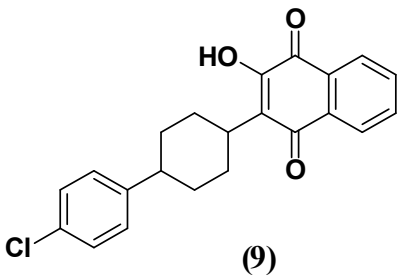

(9)

Fig. 12 Atovaquone

Atovaquone is a synthetic drug that belongs to the class of naphthoquinones [44]. It is an analogue of ubiquinone and it is used in the treatment and prevention of taxoplasmosis, mild

pneumocystis pneumomia and malaria [45]. It is usually used in combination with proguanil to prevent and treat malaria. The combination is commonly known as Malarone. Atovaquone mechanism involves the inhibition of mitochondrial transport by interrupting the interaction between ubiquinone and the plasmodial cyctochrome bc1 complex, which halts the production of pyrimidine [46].

1.5.10 Hydroxychloroquine (10)

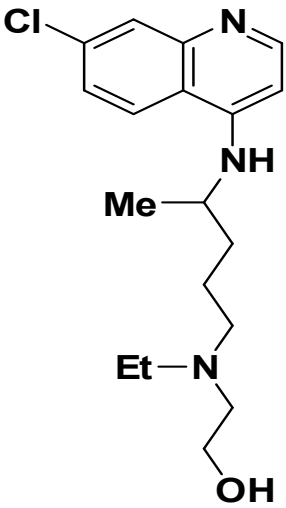

(10)

Fig. 13 Hydroxychloroquine

Hydroxychloroquine is an antimalarial drug with similar pharmacokinetic properties to those of chloroquine [47]. It is used to treat cases of chloroquine sensitive malaria. The hydroxy group makes it more water soluble which results in it being well absorbed in the digestive tract as compared to chloroquine [48]. It also has an ultra-long half-life of 23 days and a low blood clearance.

1.5.11 Doxycycline (11)

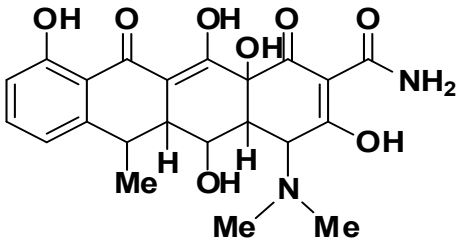

(11)

Fig. 14 Doxycycline

Doxycycline belongs to the class of antibiotics called tetracycline. It is a broad-spectrum antibiotic used for the treatment of a variety of infections caused by bacteria and other parasites [49]. It is used in conjunction with another schizontocidal agent for the treatment of malaria. Also it is effective as a prophylaxis in areas with multidrug-resistant *P. falciparum* malaria [50]. It is known to have adverse drug reactions such as photosensitivity, vaginitis, thin skin, nausea and vomiting [51].

1.5.12 Artemisinin (12)

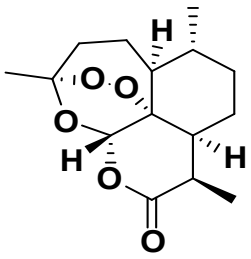

(12)

Fig. 15 Artemisinin

Artemisinin is an antimalarial lactone derived from Qing Hao a Chinese herb. The Chinese have been using it for over 1000 years for the treatment of fevers. Artemisinin was first isolated from a plant in 1971 [52]. It has shown to be effective against all drug resistant strains of *P. falciparum.* It is used in artemisinin-based combination therapy (ACT) where it is used in

conjunction with other antimalarial such as mefloquine, chlorproguanil/dapsone, piperaquine, lumefantrine and amodiaquine [53]. Its mechanism of action in not certain but it is believed to involve the cleavage of the endoperoxide bond through a reaction with haeme. This results in the production of free radicals which alkylate parasitic proteins [54]. All artemisinin derivatives are thought to have the similar mechanism of action. There are few side effects associated with artemisinin such as nausea, headaches, abnormal bleeding, itching and dark urine.

1.5.13 Dihydroartemesinin (13)

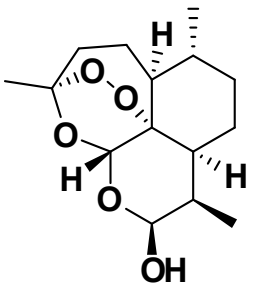

(13)

Fig. 16 Dihydroartemisinin

Dihydroartemisinin also known as artenimol is the active metabolite of all artemisinin derivatives. It is the most unstable and most effective artemisinin compound. Its mechanism of action in not certain but it is believed to be the same as all other artemisinin compounds. It has a strong blood schizonticidal action and reduces gametocyte transmission [55].

1.5.14 Artemether (14)

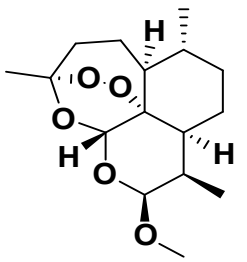

(14)

Fig. 17 Artemether

Artemether is a methyl derivative of dihydroartemisinin. It is synthesized by the reduction of dihydroartemisinin. It has a similar mode of action to that of artemisinin, but it has demonstrated a reduced ability as a hypnozoiticidal compound. Artemether and artesunate are the most broadly used artemisinin compounds, for treating uncomplicated cases of *P. falciparum* [56].

1.5.15 Arteether (15)

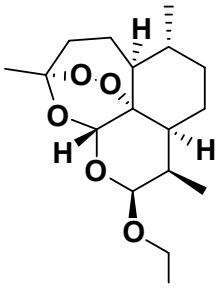

(15)

Fig. 18 Arteether

Arteether is an ethyl ether derivative of artemisinin that can be prepared by the reduction of dihydroartemisinin. It is an efficient schizontocidal drug used in combination therapy for cases of uncomplicated resistant *P. falciparum* [57].

1.5.16 Artesunate (16)

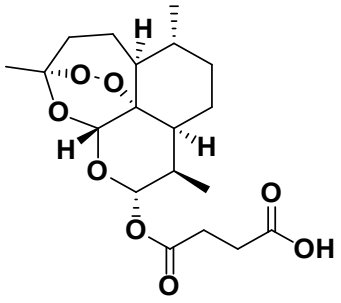

(16)

Fig. 19 Artesunate

Artesunate is an artemisinin derivative that is highly water-soluble. It is a semi-synthetic drug that is prepared by reacting dihydroartemisinin and succinic acid anhydride in an alkaline medium. It is highly effective against multi-drug resistant strains because of its instantaneous bioavailability. It is usually used in combination with mefloquine [58].

1.6 Antimalarial quality control

The quality of medicine is a major concern for global health, especially in developing countries. Most African countries lack the capacity to strictly adhere to the quality assurance and quality control (QA/QC) systems of drug regulatory measures because of limited human and financial resources [59]. The QA/QC systems involve the activities undertaken to ensure the quality of medicines, starting from development, manufacturing, distribution, marketing and procurement stages. Substandard medications have compromised efficacy, in some cases they have a detrimental effect on the lives of patients as they prolong the illness and put a strain on the patients' health and finances. Most malaria cases can be resolved with proper drugs containing the right amount of the active pharmaceutical ingredient, however it is reported that 30% of antimalarial medication on the global market are either counterfeit or of inferior quality [59]. China and India are responsible for most of the bogus antimalarial tablets. ~ 38% to 53% of the drugs produced in these countries are classified as counterfeits [60].

Drug counterfeit is a global predicament that affects almost every country from the richest to the poorest; but it has a worse adverse effect on the third world and developing countries. Poor-quality drugs have greatly contributed to the development of resistance in the malarial species. It deters and undermines all efforts and investments to eradicate malaria. Moreover, they can jeopardize a country's health care system, exhaust financial and human resources, and exacerbate health problems which can have devastating implication on a country's economic growth [61].

Majority of the bogus malarial drugs are found in Sub-Saharan Africa and South Eastern Asia [60, 62]. Paucity of well-established regulatory organizations and inadequate facilities to assess the quality of antimalarial drugs has been the major cause. The only way to combat this problem is to implement strict legislations to control the importation of medicines, hash punitive action for counterfeits and also strengthening of surveillance by ensuring that national quality control laboratories are sufficiently equipped to carry out the analysis. The development of a cheaper and more effective analytical technique is imperative.

Currently, various methods such as spectrophotometry [63], mass spectrometry [64], chromatography [65] and fluorimetry [66] are being used to monitor the quality of antimalarial drugs. However, the operational costs, both running and skilled personal for these analytical instruments are exorbitant for developing countries. Therefore, they cannot afford quality control laboratories with such instrumentation. Electrochemistry is one promising alternative, although it has not been fully explored as a quality control tool for antimalarial drugs. It provides a cheaper option; the instrumentation is simple, small, does not require sample preparation, no skilled personnel required and has the potential of being miniaturized into a hand-held device. This method has a potential to be applied in a wide matrix including biological samples such as human serum, urine and in recovery studies [67, 68].

1.7 Electrochemistry

Electrochemistry is a section of physical chemistry that studies the relationship of a chemical process and its electrical phenomena [69]. It has a wide range of applications that include metal electroplating [70], production of energy from chemical reactions [71] and electrochemical analysis [72]. Electrochemical analytical techniques utilized in pharmaceuticals analysis usually use a potentiostat with a three-electrode electrochemical cell. It consists of a working electrode, a reference electrode, an auxiliary electrode and a supporting electrolyte as illustrated in Figure 20. A potentiostat is responsible of controlling the potential difference between the reference

electrode and the working electrode. Equally, it measures the current flow between the working electrode and auxiliary electrode thus the cell current is the measured variable and the voltage is the controlled variable.

A typical working electrode is an insulated rode with only a controlled conducting circular area exposed where electrochemical reactions take place. The controlled circular area can be a bare metal or fabricated with different materials to increase the conductivity. The reference electrode is used to measure the working electrode potential and has a constant redox potential when no current pass through it. The auxiliary electrode is basically an inert conductor that is needed to complete the circuit together with the working electrode. A supportive electrolyte is an electrically conductive solution containing chemical species that are not electroactive in the range of applied potentials. It is used to maintain a constant ionic strength and prevent ion migration of the analyte in the electric field [73].

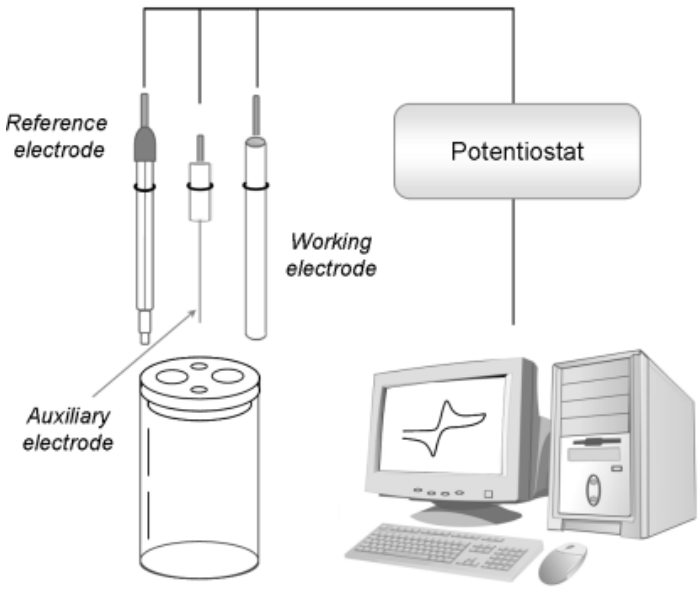

Fig. 20 A simplified illustration of an electrochemical instrumentation.

2. Study Rationale

Malaria is a devastating disease claiming millions of lives yearly. Prompt diagnosis and proper treatment of the disease remarkably lowers the associated morbidity and mortality rate. The large numbers of counterfeit drugs flooding the markets are making it difficult for patients to get proper treatment. It is undermining the fight against malaria. Development of new technologies for quality control of drugs is crucial. The challenge has motivated the integration of chemical sensors in designing monitoring techniques. Electrochemical sensors provide a promising alternative and cheaper way for drug analysis. Currently, methods used for quantification and quality control of antimalarial drugs are time-consuming, labour-intensive, costly and highly sophisticated techniques. However, the last few decades witnessed an upsurge in electrochemical methods for the determination and quantification of drugs in general. The use of nanoparticles in electrochemical techniques increases the selectivity and sensitivity, resulting in minimal or no sample preparation required. This method is a promising and efficient alternative for monitoring antimalarial drugs.

3. Aim and Research Objectives

This thesis focuses on the synthesis, characterization of novel nanomaterials, the study of their electrocatalytic properties and application in detection of antimalarial drugs, mefloquine, primaquine and amodiaquine.

Specific objectives of the study are:

1. To synthesize and characterize gold nanourchins.

2. To formulate a nanocomposite of MWCNT with PMO.

3. To synthesize graphene oxide decorated with gold nanoparticles and couple with cysteamine polymer.

4. To use nanomaterial to design and fabricate nanosensors that are selective and sensitive towards ant-malaria drugs Primaquine, Amodiaquine and Mefloquine.

5. To analyze real samples and validate developed methods.

4. Thesis Outline

The current thesis is presented in seven chapters. Four of which are presented as experimental manuscript and one as a review manuscript.

- **Chapter one** of the thesis is an introduction to the study and objectives coupled with the overview of the whole thesis.
- **Chapter two** of the thesis gives the literature review on basic strategies and recent developments in the electroanalysis of antimalarial drugs in various matrices and also introducing theoretical background of the commonly used electroanalytical methods for drug assays.
- **Chapter three** involves the synthesis of gold nanourchins (AuNUs) via seed-mediated method and characterization using ultraviolet-visible spectroscopy, energy-dispersive X-ray spectroscopy, field emission scanning electron microscopy, zeta-sizer and electrochemical techniques (electrochemical impedance spectroscopy and cyclic voltammetry). The synthesized gold nanourchins (AuNUs) were used as modifiers in the design of an electrochemical sensor for MQ.
- **Chapter four** examines the application of the modified GC electrode with gold nanourchins (AuNUs) for the detection of PQ. The developed sensor was successfully applied to determine the drug in human urine samples and pharmaceutical formulations demonstrating its analytical applicability in clinical analysis as well as quality control.
- **Chapter five** looks at the design of an AQ electrochemical sensor utilizing multiwall carbon nanotubes (MWCNT) and poly methyl orange composite as GC modifiers.

Various optimization studies on the electrooxidation of AQ were done together with recovery studies. A plausible electrochemical oxidation mechanism of AQ was proposed based on the data obtained.

- **Chapter six** reports a one pot synthesis of reduced graphene oxide decorated with gold nanoparticles. The reduced graphene oxide and gold nanoparticles composite coupled together with electrochemically produced cysteamine polymer were used as modifiers for the development of an electrochemical sensor for AQ.
- **Chapter seven** summarizes the main conclusions and recommendation of this work.

References

[1] K.T. Wariso, I.L. Oboro, Advances in microbiology 5 (2015) 351.

[2] A. Trampuz, M. Jereb, I. Muzlovic, R.M. Prabhu, Critical care 7 (2003) 315.

[3] L.J. Bruce-Chwatt, Journal of the Royal Society of Medicine 74 (1981) 531-536.

[4] F.E. Cox, Parasites & vectors 3 (2010) 5.

[5] G.C. Cook, A. Zumla, Manson's tropical diseases, Elsevier Health Sciences, 2008.

[6] I. Mueller, P.A. Zimmerman, J.C. Reeder, Trends in parasitology 23 (2007) 278-283.

[7] K. Mendis, B.J. Sina, P. Marchesini, R. Carter, The American journal of tropical medicine and hygiene 64 (2001) 97-106.

[8] N. White, Plasmodium knowlesi: the fifth human malaria parasite, The University of Chicago Press, 2008.

[9] World Health Organization, Fact Sheet: World Malaria Report 2015. http://www.who.int/malaria/media/world-malaria-report-2015/en/ (Accessed on 13/09/2018).

[10] Center of Disease Control and Prevention, Where Malaria Occurs, https://www.cdc.gov/malaria/about/distribution.html (Accessed on 03/04/2019).

[11] K.T. Andrews, T.N. Tran, N.C. Wheatley, D.P. Fairlie, Current topics in medicinal chemistry 9 (2009) 292-308.

[12] R.W. Steketee, The American journal of tropical medicine and hygiene 80 (2009) 879-880.

[13] N. Tangpukdee, C. Duangdee, P. Wilairatana, S. Krudsood, The Korean journal of parasitology 47 (2009) 93.

[14] A. Moody, Clinical microbiology reviews 15 (2002) 66-78.

[15] A. Moody, P. Chiodini, British journal of biomedical science 59 (2002) 228-231.

[16] S.P. Johnston, N.J. Pieniazek, M.V. Xayavong, S.B. Slemenda, P.P. Wilkins, A.J. da Silva, Journal of clinical microbiology 44 (2006) 1087-1089.

[17] J.A. Nájera, M. González-Silva, P.L. Alonso, PLoS medicine 8 (2011) e1000412.

[18] R.L. Metcalf, Journal of Agricultural and Food Chemistry 21 (1973) 511-519.

[19] W.M. Jarman, K. Ballschmiter, Endeavour 36 (2012) 131-142.

[20] I. Hastings, P. Bray, S. Ward, Science 298 (2002) 74-75.

[21] S. Sadasivaiah, Y. Tozan, J.G. Breman, The American journal of tropical medicine and hygiene 77 (2007) 249-263.

[22] K.J. Wilby, T.T. Lau, S.E. Gilchrist, M.H. Ensom, Annals of Pharmacotherapy 46 (2012) 384-393.

[23] K.C. Kain, G.D. Shanks, J.S. Keystone, Clinical infectious diseases 33 (2001) 226-234.

[24] E. Schwartz, Mediterranean journal of hematology and infectious diseases 4 (2012).

[25] B. Campo, O. Vandal, D.L. Wesche, J.N. Burrows, Pathogens and global health 109 (2015) 107-122.

[26] J. Arnold, A. Alving, E. HOCKWALD, C. Clayman, R. Dern, E. BBUTLER, C. Flanagan, G. Jeffery, Journal of laboratory and clinical medicine 46 (1955) 391-397.

[27] J.K. Baird, Travel medicine and infectious disease 11 (2013) 60-65.

[28] W. Peters, Experimental parasitology 17 (1965) 80-89.

[29] K. Krafts, E. Hempelmann, A. Skórska-Stania, Parasitology research 111 (2012) 1-6.

[30] J. Achan, A.O. Talisuna, A. Erhart, A. Yeka, J.K. Tibenderana, F.N. Baliraine, P.J. Rosenthal, U. D'Alessandro, Malaria journal 10 (2011) 144.

[31] D.J. Sullivan, H. Matile, R.G. Ridley, D.E. Goldberg, Journal of Biological Chemistry 273 (1998) 31103-31107.

[32] K.J. Palmer, S.M. Holliday, R.N. Brogden, Drugs 45 (1993) 430-475.

[33] N. Vale, R. Moreira, P. Gomes, European journal of medicinal chemistry 44 (2009) 937-953.

[34] P.H. Schlesinger, D.J. Krogstad, B.L. Herwaldt, Antimicrobial agents and chemotherapy 32 (1988) 793.

[35] D. Clyde, Bulletin of the World Health Organization 59 (1981) 391.

[36] K.J. Raynes, P.A. Stocks, P.M. O'Neill, B.K. Park, S.A. Ward, Journal of medicinal chemistry 42 (1999) 2747-2751.

[37] L. Salako, Bulletin of the World Health Organization 62 (1984) 63.

[38] H.E. Segal, P. Chinvanthananond, B. Laixuthai, E.J. Pearlman, A.P. Hall, P. Phintuyothin, A. Na-Nakorn, B.F. Castaneda, Transactions of the Royal Society of Tropical Medicine and Hygiene 69 (1975) 139-142.

[39] I. Rollo, British journal of pharmacology and chemotherapy 10 (1955) 208-214.

[40] A. Mbaye, K. Richardson, B. Balajo, S. Dunyo, C. Shulman, P. Milligan, B. Greenwood, G. Walraven, The American journal of tropical medicine and hygiene 74 (2006) 960-964.

[41] I.K. Srivastava, A.B. Vaidya, Antimicrobial agents and chemotherapy 43 (1999) 1334-1339.

[42] W.H. Organization, The selection and use of essential medicines: report of the WHO Expert Committee, 2017 (including the 20th WHO Model List of Essential Medicines and the 6th Model List of Essential Medicines for Children), World Health Organization, 2017.

[43] L. Joyner, S. Kendall, British journal of pharmacology and chemotherapy 11 (1956) 454-457.

[44] L.I. LÓPEZ LÓPEZ, N. FLORES, S. Daniel, S.Y. SILVA BELMARES, A. SÁENZ GALINDO, Vitae 21 (2014) 248-258.

[45] C.M. Spencer, K.L. Goa, Drugs 50 (1995) 176-196.

[46] J.E. Siregar, G. Kurisu, T. Kobayashi, M. Matsuzaki, K. Sakamoto, F. Mi-ichi, Y.-i. Watanabe, M. Hirai, H. Matsuoka, D. Syafruddin, Parasitology international 64 (2015) 295-300.

[47] A.L. Scherbel, S.L. Schuchter, J.W. Harrison, Cleve Clin Q 24 (1957) 98-104.

[48] D.J. Browning, Pharmacology of chloroquine and hydroxychloroquine, Hydroxychloroquine and Chloroquine Retinopathy, Springer, 2014, pp. 35-63.

[49] H.-L. Yuan, N.-W. Lu, H. Xie, Y.-Y. Zheng, Q.-H. Wang, Infectious Diseases 48 (2016) 844-846.

[50] S. Andersen, A. Oloo, D. Gordon, O. Ragama, G. Aleman, J. Berman, D. Tang, M. Dunne, G. Shanks, Clinical infectious diseases 26 (1998) 146-150.

[51] S. Goetze, C. Hiernickel, P. Elsner, Skin pharmacology and physiology 30 (2017) 76-80.

[52] D.L. Klayman, Science 228 (1985) 1049-1055.

[53] F. Nosten, N.J. White, The American journal of tropical medicine and hygiene 77 (2007) 181-192.

[54] S.R. Meshnick, International journal for parasitology 32 (2002) 1655-1660.

[55] A.J. Lin, D.L. Klayman, W.K. Milhous, Journal of medicinal chemistry 30 (1987) 2147-2150.

[56] N.J. White, M. Van Vugt, F.D. Ezzet, Clinical pharmacokinetics 37 (1999) 105-125.

[57] A. Brossi, B. Venugopalan, L. Dominguez Gerpe, H. Yeh, J. Flippen-Anderson, P. Buchs, X. Luo, W. Milhous, W. Peters, Journal of medicinal chemistry 31 (1988) 645-650.

[58] L.B. Barradell, A. Fitton, Drugs 50 (1995) 714-741.

[59] P.N. Newton, M.D. Green, F.M. Fernández, N.P. Day, N.J. White, The Lancet infectious diseases 6 (2006) 602-613.

[60] A. Dondorp, P. Newton, M. Mayxay, W. Van Damme, F. Smithuis, S. Yeung, A. Petit, A. Lynam, A. Johnson, T. Hien, Tropical Medicine & International Health 9 (2004) 1241-1246.

[61] E. Custodio, M.Á. Descalzo, E. Villamor, L. Molina, I. Sánchez, M. Lwanga, C. Bernis, A. Benito, J. Roche, Malaria journal 8 (2009) 225.

[62] G.M. Nayyar, J.G. Breman, P.N. Newton, J. Herrington, The Lancet infectious diseases 12 (2012) 488-496.

[63] F.H.A. Nogueira, L.M. Moreira-Campos, R.L.C.d. Santos, G.A. Pianetti, Revista da Sociedade Brasileira de Medicina Tropical 44 (2011) 582-586.

[64] M.C. Bernier, F. Li, B. Musselman, P.N. Newton, F.M. Fernández, Analytical Methods 8 (2016) 6616-6624.

[65] S. Guo, M.P. Kyaw, L. He, M. Min, X. Ning, W. Zhang, B. Wang, L. Cui, The American journal of tropical medicine and hygiene 97 (2017) 1198-1203.

[66] N. Ranieri, P. Tabernero, M.D. Green, L. Verbois, J. Herrington, E. Sampson, R.D. Satzger, C. Phonlavong, K. Thao, P.N. Newton, The American journal of tropical medicine and hygiene 91 (2014) 920-924.

[67] E. Povedano, A. Valverde, V.R.V. Montiel, M. Pedrero, P. Yáñez-Sedeño, R. Barderas, P. San Segundo-Acosta, A. Peláez-García, M. Mendiola, D. Hardisson, Angewandte Chemie 130 (2018) 8326-8330.

[68] E.F. Marques, M.G.F. Sales, New devices to monitor oxidative stress biomarkers in point-of-care: a new tool for cancer prevention (2018) 91.

[69] B. Bhattacharyya, Electrochemical micromachining for nanofabrication, MEMS and nanotechnology, William Andrew, 2015.

[70] P.W. Seavill, K.B. Holt, J.D. Wilden, Green Chemistry 20 (2018) 5474-5478.

[71] G. Che, B.B. Lakshmi, E.R. Fisher, C.R. Martin, Nature 393 (1998) 346.

[72] H. Hwang, (2007).

[73] N. Eliaz, E. Gileadi, Physical Electrochemistry: Fundamentals, Techniques, and Applications, Wiley-Vch, 2018.

CHAPTER 2

Research Progress in Electroanalytical Techniques for Determination of Antimalarial Drugs in Pharmaceutical and Biological Samples

Neeta Thapliyal, [a] Tirivashe Chiwunze, [a] Rajshekhar Karpoormath,* [a] Rajendra N. Goyal,[b] Harun Patel[a] and Srinivasulu Cherukupalli[a]

[a]Department of Pharmaceutical Chemistry, College of Health Sciences, University of KwaZulu-Natal, Durban 4000, South Africa

[b]Department of Chemistry, Indian Institute of Technology Roorkee, Roorkee 247667, India

*Corresponding author

E-mail: karpoormath@ukzn.ac.za, rvk2006@gmail.com

Tel no.: +27(0)312607179, +27721107207; Fax No.: +27(0)312607792

RSC Advances

REVIEW

View Article Online
View Journal | View Issue

Cite this: *RSC Adv.*, 2016, **6**, 57580

Research progress in electroanalytical techniques for determination of antimalarial drugs in pharmaceutical and biological samples

Neeta Thapliyal,*[a] Tirivashe E. Chiwunze,[a] Rajshekhar Karpoormath,*[a] Rajendra N. Goyal,[b] Harun Patel[a] and Srinivasulu Cherukupalli[a]

Received 25th February 2016
Accepted 1st June 2016

DOI: 10.1039/c6ra05025e

www.rsc.org/advances

Antimalarial drugs play a crucial role in the treatment and cure of malaria. Electrochemical sensors have been the subject of extensive research in the field of drug analysis since many decades, and yet seem to project great potential for the future. The present review explores the basic strategies and recent developments in the electroanalysis of antimalarial drugs in various matrices. A discussion of the commonly used electroanalytical methods for drug assays is briefly discussed. The methods have been critically analysed highlighting their analytical performance and limitations. Nanomaterials, conducting polymers and presence of surfactants made significant contributions to voltammetric determination of antimalarial drugs suggesting promising future for use of chemically-modified electrode based sensors for the detection. Future progress in quantification of these drugs in biological fluids is expected to drastically improve the applicability of electrochemical methods for routine clinical analysis.

Abstract

Antimalarial drugs play a crucial role in the treatment and cure of malaria. Electrochemical sensors have been the subject of extensive research in the field of drug analysis since many decades, and yet seem to project great potential for the future. The present review explores the basic strategies and recent developments in the electroanalysis of antimalarial drugs in various matrices. A discussion of the commonly used electroanalytical methods for drug assays is briefly discussed. The methods have been critically analysed highlighting their analytical performance and limitations. Nanomaterials, conducting polymers and presence of surfactants made significant contributions to voltammetric determination of antimalarial drugs suggesting promising future for use of chemically-modified electrode based sensors for their detection. Future progress in quantification of these drugs in biological fluids is expected to drastically improve the applicability of electrochemical methods for routine clinical analysis.

1. Introduction

Malaria, a mosquito-borne infectious disease, continues to be one of the most severe health threats worldwide with an estimated 198 million cases of the disease in 2013, resulting in 5,84,000 deaths per year[1]. Almost half of the world's population is at risk of contracting malaria with most of the related deaths reported among children residing in sub-Saharan Africa, where a child succumbs to the disease every minute. Malaria is caused by parasitic protozoans of the genus Plasmodium with its five species (*Plasmodium vivax, Plasmodium falciparum, Plasmodium malariae, Plasmodium ovale* and *Plasmodium knowlesi*) affecting the human race, the most deadly being *P. falciparum*[2]. Prompt diagnosis and treatment of the disease remarkably lowers the associated morbidity and mortality rate. Antimalarial drugs play a vital role in reducing malaria transmission and restricting the spread of drug-resistant infecting species. Currently, there are four major drug classes used for the management of the disease, which include quinoline-related compounds, artemisinin derivatives, antifolates and antimicrobials. No single drug available is effective against all forms of the parasite's life cycle and hence a combination of drugs is recommended to combat the disease. Despite the availability of a wide arsenal of antimalarials, continuous efforts are in progress to develop and assay new drugs in order to improve the efficacy of the therapy. Resistance to antimalarial medicines pose a problem for effective malarial therapy;[3] however use of drugs still remain the most effective option for malaria treatment.

Development of new drugs with varying pharmacological action and therapeutic properties presents a challenging task to control the content of drugs as well as their metabolites in different media, including commercial formulations and biological fluids. Therapeutic drug monitoring (TDM) is a clinical strategy that measures drug concentration in a patient's bloodstream to monitor its compliance, efficacy and toxicity, thus optimizing and managing individual medication regimen. TDM also investigates occurrence of adverse effects and drug-

drug interactions. Hence robust, precise and accurate analytical methods are required to quantify the drugs in human body fluids. Besides, since therapeutic substances and preparations need to be free from any impurities and also to detect counterfeiting of medicines, quantitative analysis of drugs in commercial formulations is critical for effective quality control. Based on these facts it becomes imperative to emphasize on the development of analytical methodologies for quantification of antimalarial drugs in pharmaceutical as well as biological samples. A large number of methods have been reported for the assay of antimalarial drugs, most of which are time-consuming and involve labour-intensive, costly and highly sophisticated chromatographic techniques[4-13]. However, last few decades witnessed an upsurge in electrochemical methods for the detection and determination of these compounds. The electrochemical techniques are characterized by high selectivity and sensitivity, minimum or no sample preparation and extremely low detection limit, which is comparable to widely used chromatographic techniques. In addition, low cost instrumentation, portability and versatility for the analysis of a wide variety of species favours electrochemistry technique as the analytical method of choice[1]. Electrochemical analysis is now increasingly used for drug analysis in biological samples and their dosage forms. This work presents a critical review of the electrochemical methods reported in the literature for the determination of WHO recommended antimalarial drugs, namely chloroquine, quinine, mefloquine, piperaquine, primaquine, amodiaquine, lumefantrine, artemisinin, artemether, dihydroartemisinin, artesunate, atovaquone, proguanil, sulfadoxine, pyrimethamine, doxycycline and clindamycin. These methods constitute useful tools having practical applicability for quality control tests and/or routine TDM in clinical practice. The review is an attempt to critically discuss the electrochemical methods developed till date for quantitative analysis of the above-mentioned drugs revealing their advantages and limitations and throw light on the recent trends in antimalarial drug determination.

2. Brief account of most frequently used electroanalytical techniques

Electroanalytical techniques are powerful, versatile and simple techniques of analysis that offer wide linear concentration range, rapid analysis time, cost-effective instrumentation, possibility of miniaturization, low reagent consumption, suitability for real-time detection along with high sensitivity, precision and appreciable accuracy[14-16]. Among the various known electrochemical methods, voltammetry and potentiometry are the most prominent ones widely used for drug quantification.

2.1 Voltammetry

Voltammetry involves measurement of the current (i) generated upon application of a constant or varying potential (E) at the working electrode surface. Since the measured current is directly proportional to the bulk concentration of the analyte species, the method allows quantitative analysis of the analyte with extreme sensitivity. In some cases the current is recorded or the applied potential is varied over a period of time (t). When the current is recorded at a constant potential, the technique is termed amperometry. Thus, all voltammetric techniques can be defined as some function of current, potential and time. Since the applied potential electrochemically oxidizes or reduces the analyte species resulting in a change in its concentration at the electrode surface, voltammetry is considered as an active technique. The most widely used working electrodes are carbon, gold, silver, platinum and mercury. The advent of chemically modified electrodes have increased the scope of electrochemical sensing by improving electrode sensitivity allowing detection of a wide range of electroactive compounds upto a very low detection limit[17]. The technique is extensively employed for trace analysis of various inorganic and organic electrochemical species in different matrices (for example, clinical samples, pharmaceutical formulations, environmental samples, gasoline and oil)[18-20]. Numerous voltammetric techniques in electroanalytical chemistry, namely, cyclic, linear sweep,

differential, square wave and stripping voltammetry, have been developed in recent decades. A brief overview of the basic concepts of the various commonly employed electroanalytical techniques is summarized below.

2.1.1 Polarography

In voltammetric method, when the working electrode is formed by mercury drop falling continuously from a capillary tube in a preset frequency, the technique is referred to as polarography. Dropping mercury electrode (DME), static mercury drop electrode (SMDE) or hanging mercury drop electrode (HMDE) is used as the working electrode. In DME, mercury drops are steadily released as a result of gravity at the end of capillary. In HMDE, rotation of a micrometer screw forces the mercury out of the capillary tube in the form of a drop, while in SMDE a solenoid driven needle is used to adjust the mercury flow. Analytes are transferred from the bulk to the surface of the working electrode via diffusion mass transport. The applied potential is varied from initial to the final potential and the current is monitored as a function of applied voltage. A sigmoidal (S-shaped) current-voltage plot is obtained which is referred to as a polarograms. In polarography, Ilkovic equation is used which relates the diffusion current and the concentration of the reduced or oxidized species at the mercury electrode, as follows:

$$i_d = 706nCD^{1/2}\, m^{2/3}\, t^{1/6}$$

where i_d is the diffusion current (in μA); n is the number of electrons exchanged in the electrode reaction; C is the analyte concentration (in mol/cm^3); D is the diffusion coefficient of the analyte (in cm^2/s); m is the mass of mercury drop and t is the drop lifetime (in seconds).

Qualitative information can also be obtained from the half-wave potential of the polarograms. Though mercury displays advantages as a working electrode such as wide cathodic range and a renewable surface, it has several limitations that include its non-suitability for investigating

oxidizable species. Besides, potential risks of contamination, poisoning and disposal associated with the use of mercury have also emerged as a big problem.

2.1.2 Linear Sweep Voltammetry

Linear sweep voltammetry (LSV) is one of the simplest techniques in electroanalytical chemistry for the investigation of electrode reaction mechanism. A linearly changing potential between working and reference electrodes is applied from an initial value to a final value as a linear function of time. Thus, in LSV the potential is scanned between two potential limits (as initial E and final E) in one direction i.e. from negative to positive potential and positive to negative values in case of oxidation and reduction, respectively. When the corresponding oxidation or reduction potential of the electroactive species is reached, the molecules near the electrode surface are oxidized or reduced and the current rises sharply. The current then becomes diffusion controlled and begins to fall. The corresponding current response is recorded and the resulting current-potential curve is referred as a linear sweep voltammogram. For a reversible system in LSV, the peak current obtained is described by the Randles-Sevcik equation:

$$i_p = [2.69 \times 10^5]\, n^{3/2} A D^{1/2} C v^{1/2}$$

where i_p is the peak current (in μA), n is number of electrons involved, A is the electrode area (in cm^2), D is the diffusion coefficient of the species having oxidized or reduced (in cm^2/s), C is the species concentration (in mol/cm^3) and v is the scan rate (in V/s).

2.1.3 Cyclic Voltammetry

Cyclic voltammetry (CV) has emerged as one of the most exploited as well as the most versatile techniques in electrochemical studies. Usually the first experiment performed to investigate the electrochemical behavior of a compound at an electrode surface, it is used to study the fundamental aspects of the electrochemical processes and electron-transfer reactions,

understanding reaction intermediates, and obtaining stability of reaction product(s). The technique involves monitoring the current while varying the applied potential at a working electrode in both forward as well as reverse directions at a fixed sweep rate. In case of a reversible electrochemical process, as the potential ($E_{initial}$) moving towards the negative direction reaches the standard reduction potential, a cathodic current flows and the analyte is reduced. When the direction of the scan is reversed (E_{rev}) back to $E_{initial}$ moving towards positive potential, an anodic current starts to flow as the electrochemically generated reduced species is reoxidized. The observed current-potential curve is called as a cyclic voltammogram (CV). The peak current in CV is also governed by Randles-Sevcik equation mentioned earlier in the case of LSV.

2.1.4 Pulse Voltammetric Techniques

Pulse techniques were developed in order to suppress the capacitive current and thus lower the detection limits of the measurements. Here, the potential is varied in a series of steps (or pulse) following which the charging current has largely decayed. After the potential step, the measured current consists solely of the faradaic current (charging current being negligible). Thus, use of pulse-based technique allows for elimination of the unwanted capacitive current from the faradaic current.

2.1.4.1 Differential pulse voltammetry

Differential pulse voltammetry (DPV) is a prominent voltammetric technique extensively employed for quantitative analysis of electrochemically active species. It provides superior detection limits in comparison to LSV and CV, and also allows resolution of overlapping electrochemical processes. In this technique, the potential applied to the electrode is varied in a series of steps (or pulse) from an initial potential to an interlevel potential where it remains for approximately 50 milliseconds and then changes to the final potential. In the recurring pulses, the final potential is changed, and a constant difference is maintained between the initial and the

interlevel potential. The current is sampled twice, first just before application of each pulse and second time at the end of the pulse. The difference between these values is plotted as a function of the potential. Because of low limit of detection (~10^{-8} M), DPV is often the method of choice for analysis of pharmaceutical formulations and body fluids.

2.1.4.2 Square-wave voltammetry

Square-wave voltammetry (SWV) is one of the most powerful pulse techniques demonstrating a broader dynamic range and lower limit of detection. The potential wave form in SWV consists of a symmetrical square wave superimposed on a staircase (stepped) potential ramp in such a way that the forward square wave pulse coincides with the underlying staircase. The current is measured twice during each square-wave cycle, once at the end of the forward pulse, and then at the end of the reverse pulse. The difference between the two measurements is plotted versus the applied staircase potential. The resulting peak-shaped voltammograms displays excellent sensitivity and effective discrimination against background contributions. SWV is considered more sensitive than DPV because in it both forward and reverse currents are measured. Speed, excellent sensitivity and the rejection of background currents are some of the advantages of using SWV. Thus, the analysis time is reduced and analytical determinations can be made at very low concentrations. Applications of SWV include trace analysis of electrochemical species and its use with electrochemical detection in HPLC.

2.1.5 Stripping Techniques

Stripping voltammetry is an electroanalytical technique that involves concentration of the analyte species in the sample solution onto or into a working electrode surface. Generally, mercury is chosen as the working electrode for this technique. The preconcentration of analyte leads to exceptional sensitivity and low detection limits. The preconcentrated analyte is then stripped from the electrode by the application of a voltage scan and the current is measured during the stripping step. Stripping voltammetry is primarily a trace analytical technique.

Stripping voltammetry has been employed for analysis of organic molecules as well as metal ions. Generally, mercury is chosen as the working electrode. The three most commonly used methods are anodic stripping voltammetry (ASV), cathodic stripping voltammetry (CSV) and adsorptive striping voltammetry (AdSV).

In ASV, the analyte is deposited (or electroplated) onto the working electrode at negative potentials and then oxidized during an anodic potential sweep resulting in a sharp peak. During deposition, an amalgam is formed by the elemental metal and the mercury on the electrode. ASV can only be used to determine those metals that exhibit appreciable solubility in mercury. CSV is used to determine substances that form insoluble salts with mercurous ion. In this method, a positive potential is applied to the mercury electrode in the presence of such a substance resulting in the formation of an insoluble film on the electrode surface. Application of a potential scan in the negative direction reduces (or strips) the deposited film into the solution. The method is employed to detect inorganic anions and certain organic compounds. AdSV is similar to ASV and CSV except that here the preconcentration step is achieved simply by adsorption on the working electrode surface or by reactions at chemically modified electrodes. Many organic and inorganic species have been determined at micromolar and nanomolar concentration levels using this technique.

The analytical advantages of the various voltammetric techniques include excellent sensitivity with a very wide linear concentration range for both organic and inorganic species (10-12 to 10-1 M), rapid and easy analysis, simultaneous determination of several analytes, the ability to determine kinetic and mechanistic parameters, having a well-developed theory and thus the ability to rationally estimate the values of unknown parameters. However, this method is applicable to limited range of metals, and organic compounds present in the sample need to be completely destroyed prior to determining the inorganic species in solution.

2.2 Potentiometry

Potentiometry relates to measurement of the potential between two electrodes in an electrochemical system providing information about the quantity of the analyte species. These methods measure potential as a function of analyte activity or concentration and find use in a wide range of applications such as industrial quality control, environment pollution monitoring, food processing, agriculture and biomedical analysis[21-23]. There are two broad classes of potentiometric electrodes, namely the metallic electrodes and membrane electrodes. The potential of a metallic electrode is the result of a redox reaction at the electrode's surface. An electrode of the first kind responds to the concentration of its cation in solution. If another species is in equilibrium with the metal ion, the electrode's potential also responds to the concentration of that species. The potential of a membrane electrode is determined by a difference in the concentration of the solution on each side of the membrane. The recent potentiometric methods mostly use ion-selective electrodes (ISEs) that are capable of selectively binding the analyte ions attaining lower detection limits. ISEs are highly sensitive permselective membrane-based devices consisting of permselective ion-conducting materials. The membrane is generally water insoluble, mechanically stable, nonporous and is designed such that it will selectively bind the analyte ions. The key component of the membranes is a complexing agent capable of reversible binding with the target ion. It is generally called ionophore or electroactive material. Besides ionophore, other components of the membranes include solvent mediators or plasticizers and anionic or cationic additives which also affect the potentiometric characteristics of ISEs. A potential is developed across the membrane when it separates two solutions of different activity containing the same counter ion. The monitored cell potential is found to be directly proportional to the concentration or activity of the sample ions in aqueous solution under investigation. Ideally, the response of ISE should follow the given equation

$$E = K + \frac{2.303RT}{ziF} \log a_i$$

where E is the potential, K is a constant that includes all sample-independent potential contributions, R is the universal gas constant, F is the Faraday constant, T is the absolute temperature, and z_i and a_i are the ionic charge and activity of the ion, respectively. At 25 °C, the value of 2.303 RT/ z_iF is 0.059/z_i volts. The membrane is said to exhibit Nernstian response if the slope of a plot between cell potential and log activity comes out to be 0.059/z_i volts. The plot is then called Nernst plot and slope as Nernstian slope. ISEs provide rapid, accurate, low cost and on-line method of analysis. Limitations of the method include its dependency on temperature. Also, the ISE is usually fragile and can be fouled by solution components leading to sluggish and drifting response. Potentiometry with ISEs is one of the most promising analytical tools for determining various organic and inorganic species which has led to a constant increase in development of electrodes endowed with the ability to selectively identify a number of drugs for pharmaceutical and clinical analyses.

A comparison of voltammetric and potentiometric methods of analysis is presented in **Table 1**. Both methods have their respective advantages and disadvantages, along with different scopes of analytes and matrix effects, making them appropriate or advantageous for analysis of a specific analyte. Also, both techniques are well-suited for in-situ continuous monitoring and are accessible for miniaturization, integration and automation.

Table 1. A comparison of voltammetric and potentiometric methods of analysis

Technique	**Voltammetry**	**Potentiometry**
Type	Dynamic technique since it involves change in analyte concentration	Passive technique since it does not affect the concentration of the analyte in the sample
Method of operation	Measures oxidation or reduction current as a function of voltage	Measures potential at zero current
Analyte	Should either be electroactive or can be measured by an electroactive species in an indirect manner.	No such limitation.
Measurement	Measures concentration.	Measures activity rather than concentration.
Detection limits	~ 10^{-9} M or even lower (ca. 10^{-12} M).	~ 10^{-6} M but can be lower (ca. 10^{-8}M).
Principal applications	Quantitative analysis of electrochemically reducible organic or inorganic substances	Quantitative analysis of ions in solutions, pH.

3. Electrochemical methods for quantification of antimalarial drugs

Antimalarials have been categorised into different classes that include the quinoline derivatives, artemisinin derivatives, antifolates and antimicrobials. The essential pharmacokinetic properties of the antimalarials are summarized in **Table 2**. These antimalarials are well absorbed after oral administration and show high bioavailability. Each analytical technique is known to have its own characteristics that vary from one analyte to another. Method validation is a pre-requisite step to assess the performance characteristics of analytical methods. It provides reliable analytical data with the basic parameters being linearity, concentration range, limit of detection (LOD) and limit of quantification (LOQ). Hence, it is essential to consider the validation parameters for effective analysis of the various methods used to determine the drug. Keeping this in view, the validation characteristics reported for the electroanalytical methodologies discussed have been highlighted in the present review.

Table 2. A compilation of the peak plasma concentration (C_{max}), the peak time (*T*max, time at which C_{max} is observed after drug administration), the percent of urinary drug elimination (UE) and the associated adverse effects reported for anti-malarial drugs.

Antimalarial Drug	C_{max} (ng/mL)	T_{max} (hours)	UE (%)	Adverse effects/Overdose	Ref.
Chloroquine	63-263	1-8	39-67	ECG disturbance, leucopenia, methaemoglobinaemia, toxic psychosis peripheral neuropathy, retinopathy, keratopathy, myopathy, abdominal cramps, vomiting, diarrhoea, pruritus, alopecia, exfoliative dermatitis, purpuric skin reactions and hyperpigmentation	24-26
Quinine	5270-17900	1.0-5.9	20	Cinchonism, visual impairment, hypoglycaemia, tinnitus, hearing impairment, headache, diplopia, rash, dermatitis, vomiting, stomach pain, diarrhea, central nervous system toxicity, pulmonary edema, cardiac arrhythmia and death (in rare cases).	27, 28
Mefloquine	722-2259	4.5-31	9	Depression, anxiety, hallucinations, severe or stomach pain, nausea, vomiting, loss of appetite, dark urine, clay-colored stools, jaundice, hepatitis, mouth sores, weight loss, severe skin rash, polyneuropathy, bradycardia, visual impairment, thrombocytopenia, psychosis, seizures, acute brain syndrome.	28, 29
Amodiaquine	5.2-39.3	0.5-2.0	2.0	Gastrointestinal disturbances, cough, anorexia, insomnia, fatigue, neutropenia, hepatotoxicity, arrhythmia, bradycardia, pruritus, eye disorders. Bone marrow toxicity and hepatotoxicity.	28, 30
Primaquine	65-295	1.0-4.0	0.4-2.2	Gastrointestinal disorders, hypertension, cardiac arrhythmia, pruritus, headache, confusion, depression, haemolysis, leukopenia, granulocytopenia, methemoglobinemia (cyanosis).	28, 31
Piperaquine	71.6-730	3.0-6.0	<1%	Dizziness, headache, nausea, vomiting, anorexia, myalgia, cough, asthenia, arthralgia, abdominal distress, pyrexia, eosinophilia, QTc prolongation.	28, 32
Lumefantrine	5100-9800	6-8	Traces only	Headache, dizziness, loss of appetite, weakness, fever, chills, muscle/joint pain, nausea, cough, abdominal and chest pain, irregular heartbeat.	28, 33, 34

Artemisinin	211-1056	1-5	<1.0	Nausea, vomiting, abdominal pain, diarrhoea, abdominal pain, fever, darkening of urine, dizziness, hypertension, skin rashes, sweating, tinnitus, cardiovascular disturbances, hepatitis.	28, 35
Artesunate	47.5-223.2	0.5-1.5	Traces only	Transient and reversible reticulocytopenia, fever, rash, ataxia, bradycardia, transient first-degree heart block and reversible elevation of serum transaminases.	28, 36
Artemether	287-648	1.5-2.5	Traces only	Hypersensitivity reactions, gastrointestinal disturbances, bradycardia, neutropenia, reticulocytopenia and elevated liver enzyme activity,	28, 37, 38
Dihydroartemisinin	162-702	2-12	52	Headache, nausea, loss of appetite, dizziness, energy loss, muscle/joint pain, rash, coloured urine, jaundice, arthralgia, abdominal distress, neutropenia, pyrexia.	28, 37
Proguanil	560-751	4-6	30-69	Rash, abdominal pain, bloody urine, lower back pain, vomiting, diarrhoea, headache, loss of appetite, mouth sores or ulcers, nausea.	28, 39
Pyrimethamine	676-1190	1-4	20-40	Gastric distress, nausea, vomiting, loss of appetite, bloody urine, chest pain, irregular heartbeat, atrophic glossitis, blood dyscrasias, leucopenia, thrombocytopenia.	28, 38, 40
Sulfadoxine	57900-217800	4-63	3.0	Gastrointestinal disturbances, headache, rash, dizziness, skin reactions, hepatitis, leucopenia, thrombocytopenia, anaemia, haematuria.	28, 36
Clindamycin	2.5-14	0.75-3.0	10	Diarrhoea, anorexia, nausea, vomiting, abdominal discomfort, pruritis, anaphylaxis, blood dyscrasia, hepatotoxicity, polyarthritis.	28, 41
Doxycycline	3060-6900	1.5-6.0	35-60	Gastrointestinal effects, hypersensitivity reactions, thrombophlebitis, hypoplasia, enterocolitis and inflammatory lesions in the ano-genital region, candidal vaginitis, rash, dermatitis.	28. 42
Atovaquone	634-13270	5-6	<0.6	Vomiting, diarrhoea, abdominal pain, headache, cough, rash, fever.	28, 43

3.1 Quinoline derivatives

The antimalarial quinoline derivatives comprise of chloroquine, quinine, mefloquine, amodiaquine, primaquine, piperaquine and lumefantrine. The mechanism of action of quinoline antimalarials is not fully known; however these drugs are said to accumulate inside the acidic food vacuole by virtue of their weak base properties, where they interfere with haemoglobin digestion and inhibit the process of haem polymerization, thus facilitating an aggregation of cytotoxic haem eventually killing the parasite.

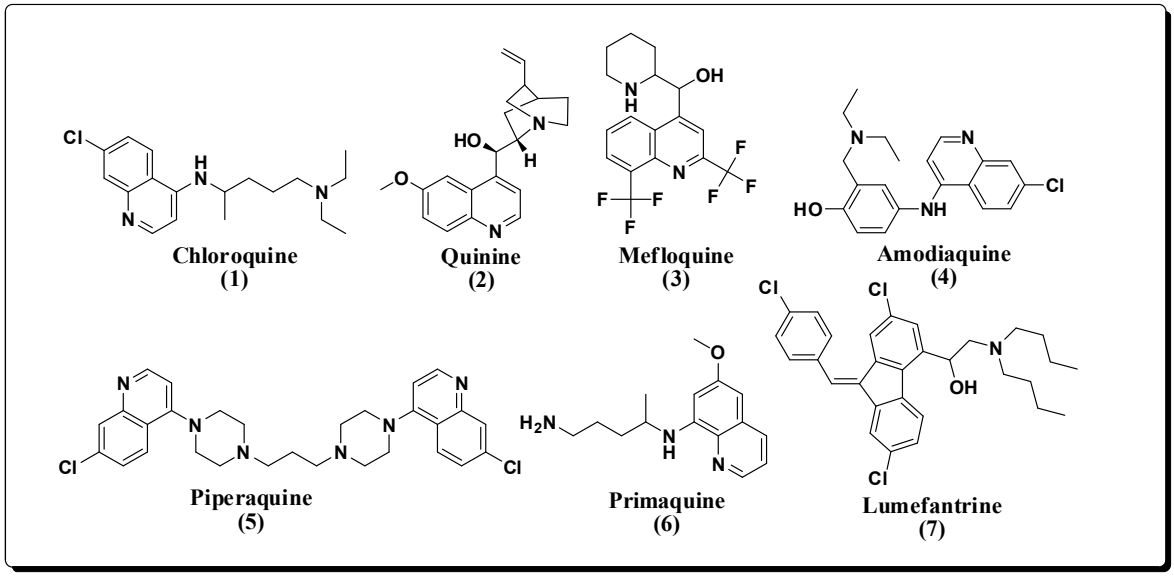

Fig. 1 Chemical structures of quinoline-based antimalarial drugs.

3.1.1 Chloroquine (1)

Chloroquine (CQ), a 4-aminoquinoline, was approved by the Food and Drug Administration (FDA) in 1949[44]. The drug remained a mainstay for the treatment and prophylaxis of malaria for more than four decades. Later, the emergence of CQ-resistant strains of *P. falciparum* limited its use to a great extent. However, it is still advised to control uncomplicated malaria due to *P. malariae, P. ovale, P. vivax and P. knowlesi*. Besides, CQ is also used to treat rheumatoid arthritis, amoebic hepatitis and lupus erythematosus[45]. The drug is usually well-tolerated at therapeutic doses and shows minimal toxicity.

The voltammetric behaviour of CQ was investigated at bare and dsDNA-modified carbon paste electrode (CPE) in acetate, Britton-Robinson (BR) and phosphate buffer solutions using cyclic CV and DPV[46]. Presence of dsDNA on the electrode surface facilitated a preconcentration process for CQ resulting in high sensitivity and an improved electrochemical signal. The oxidation peaks observed were assigned to be due to the irreversible oxidation of the nitrogen of alkylamino group and N-heterocyclic nitrogen of the aminoquinoline moiety of CQ molecule. The method was validated for analysis of the drug in serum without any sample pre-treatment with satisfactory recovery range. However, the determination of CQ content in pharmaceutical samples was not conducted. Also, the study did not report the effect of potential interferents as well as the relative affinity of various metabolites towards DNA which may adversely affect the quantification of the drug in biological fluids. Later, in 2009, a $Cu(OH)_2$ nanowire-modified CPE (Cu-NW/CPE) was developed for the electroanalytical determination of CQ in phosphate buffer (pH 5.5)[47]. The electrode was remarkably stable and yielded reproducible results. Though the method was successfully applied for the determination of CQ in pharmaceutical samples, it was not validated for quantification of the drug in human body fluids.

Various polyvinyl chloride (PVC) based CQ-selective electrodes were developed and evaluated for the assay of CQ in tablets[48-50]. The electrodes exhibited Nernstian behaviour and fast response times within a wide pH range. The lifetime of these sensors was found to be relatively short which was anticipated to be due to low lipophilic character of the sensing material having sodium tetraphenylborate (NaTPB) as the membrane additive. Later, an improved CQ potentiometric sensor was proposed that used a more lipophilic ion-exchanger, potassium tetrakis(4-chlorophenyl)borate (KTCPB)[51]. The electrode showed fast Nernstian response and superior lifetime with minor interference from alkali and alkaline earth metal ions. The developed sensor was then utilised for determination of the drug in synthetic tablets, artificial serum and biological fluids. Unsatisfactory results were obtained for biological fluids and serum samples which indicated the non-usability of the sensor in clinical samples. Another drawback

of the method was that the membrane surface swelled and cracked upon exposure to proteins and urine for more than 8 hours.

3.1.2 Quinine (2)

Quinine (Qn), a cinchona alkaloid, is the oldest antimalarial drug that continues to be in use since its discovery in the 17th century[27]. The drug exhibits schizonticidal action against intra-erythrocytic malaria parasites. With the advent of more effective artemisinin based combination therapies (ACT), Qn is presently recommended for the management of malaria in the first trimester of pregnancy or as an alternative when ACT is not available. Qn is also added to tonic type drinks as a flavouring agent[52].

Qn was determined in tonic waters (containing 23.5-118 mg Qn/L) in BR buffer (pH 3.7) using d. c. polarography at a dropping mercury electrode (DME)[53]. A multichannel taste sensor based on CPE modified with lutetium/praseodymium phthalocyanine complexes ($LuPc_2$/$PrPc_2$) or doped polypyrrole (Ppy) was constructed and evaluated to detect bitterness in beverages and food items caused by Qn, $MgCl_2$ and some phenolic compounds[54]. The doping agents used were potassium perchlorate, potassium ferricyanide (II), p-toluenesulfonic acid, lithium trifluromethane sulphonate, potassium hexafluorophosphate, sodium 1-decanesulfonate and sodium tetrasulphonate-phthalocyaninate of nickel (II). $LuPc_2$ modified electrode exhibited appreciable electrocatalytic activity in contrast to $PrPc_2$ electrode, which does not give any response to Qn. Poorly defined peaks were observed at doped Ppy electrodes. The principal component analysis of the obtained signals confirmed the capability of the electrodes for discrimination towards the bitter solutions[54].

The electrochemical oxidation of the drug was explored at a multiwall carbon nanotubes (MWCNTs) and room-temperature ionic liquid of 1-butyl-3-methylimidazolium hexafluorophate gel modified GCE (MWCNTs-RTIL/GCE) in 0.10 M phosphate buffer solution using CV and square wave voltammetry (SWV)[55]. No interference was observed

from substances commonly present in pharmaceutical preparations (K^+, Na^+, Cl^-, NO_3^-, SO_4^{2-}, glucose, saccharose and citrate) suggesting that the method was highly selective towards Qn. The feasibility of the proposed method for quantitative determination of Qn in pharmaceutical injection samples was successfully evaluated. Later, Awasthi *et al* studied the cyclic voltammetric behaviour of the drug at a polypyrrole-pentacyanoferrate/platinum (Ppy-PCNFe/Pt) electrode in aqueous medium[56]. The work was first of its kind for determination of the drug in absence of any supporting electrolyte. The electrochemical process was irreversible and showed diffusion as well as adsorption controlled behaviour at the electrode surface. However, a major drawback of the method was that a fresh electrode needed to be used for each new measurement since movements of ions into and out of the polymeric film was expected to change the composition of modified electrode. Further, at drug concentrations lower than 1.0 mM, a loss in electrochemical activity of Ppy-PCNFe/Pt electrode was observed due to deactivation of Ppy. No attempts were made to evaluate the analytical applicability of the method for analysis of Qn in any of the real samples. Poly(4-amino-3-hydroxynaphthalene sulfonic acid)-modified glassy carbon electrode (p-(AHNSA)/GCE) was fabricated by electropolymerization and used to determine Qn in 0.1 M phosphate buffer solution using SWV[57]. The detection limit obtained was found to be much lower as compared to the earlier reported methods for the quantification of the drug. The influence of potential interferents on the peak current response of the drug revealed significant interference from equimolar quinidine and 8-hydroxyquinoline. The analytical applicability of the method for Qn analysis was successfully validated in pharmaceutical preparations (tablets and injections) and spiked human urine samples. However, the stability, accuracy and reproducibility of the method were not mentioned. A molecularly imprinted polymer (MIP) film with methacrylic acid (MAA) as functional monomer and ethylene glycol maleic rosinate acrylate (EGMRA) as cross-linker was created on GCE surface via free radical polymerization method[58]. The prepared sensor showed sensitive and selective binding sites for Qn and was employed for Qn determination. Though cinchonine, cinchonidine, caffeine and theophylline did not affect the amperometric

response towards the drug, a significant interference was observed in presence of tenfold of quinidine. The method was found to be accurate, reproducible, stable and exhibited feasibility to determine Qn in tonic water with appreciable recovery percentage.

Dar *et al* studied the electrochemical behavior of Qn in presence of different surfactants viz., Tween-20, sodium dodecylbenzenesulfonate (SDBS) and cetyltrimethylammonium bromide (CTAB) using CV and SWV[59]. As compared to Tween-20 and SDBS, addition of CTAB to the solution containing Qn exhibited appreciable enhancement in reduction peak current, a greater shift in cathodic peak potential and a lower detection limit. The electrochemical process was diffusion-controlled and pseudo reversible at hanging mercury drop electrode (HMDE). The method displayed excellent accuracy, precision and reproducibility. No interferences from excipients such as gelatin, lactose, starch and magnesium stearate were observed. Further, the method was validated for the quantitative analysis of Qn in bark of *Cinchona officinalis*, commercial soft drinks (bitter lemon) and pharmaceutical formulations containing Qn. However, use of HMDE limits the use of the method. The electrode is bulky and involves potential risks of toxicity, contamination, poisoning and disposal associated with the use of metallic mercury. A bismuth-coated screen-printed carbon electrode (Bi-SPCE) was fabricated for voltammetric determination of Qn in tonic water[60]. The main drawback of the method was that a fresh Bi-SPCE was required for every measurement. Later, a nanocomposite based on calf thymus dsDNA, methylene blue (MB) and MWCNTs was coated onto the GCE surface to fabricate dsDNA-MB-MWCNTs/GCE for enantioselective recognition of Qn and quinidine[61]. The electrode was simple to prepare, stable as well as reproducible. However, the effect of interferents was not studied. Also, the method was not employed for quantitative analysis of the drug in real samples. Orata *et al* reported the use of polyaniline and bentonite modified carbon electrode in 1M H_2SO_4 to study the redox profiles of Qn in cinchona bark and malbet (a herbal medicine) using cyclic voltammetry[62]. Later, the same group explored the electrochemical behaviour of Qn at polyaniline, bentonite and Qn modified carbon graphite electrode

investigating the redox interaction of Qn with consumables (tea and milk), proteins/drugs (acetylsalicylic acid, tyrosine, cholesterol, leucine, paracetamol, iso-nicotinic acid, hydrocortisone and ferrous fumarate) and metal cations (Cu^{2+}, Co^{2+}, Zn^{2+} and Sn^{2+})[63]. However, in both the above-stated methods, quantitative analysis of Qn was not taken into consideration, with the work being primarily focussed on investigating the electrochemical behaviour of quinine using the modified electrodes.

The first potentiometric determination of Qn was reported by Kalman *et al* using an ion-selective membrane electrode where the drug was quantified in pharmaceutical preparations[64]. The proposed method provides an accuracy of 2.5%. Later, a picrate ion-selective electrode was fabricated for determination of micro-amounts of Qn along with other alkaloids in bulk as well as in pharmaceutical preparations[65]. Anzai *et al* investigated the performance characteristics of a Qn-sensitive membrane electrode based on the ion-association complex of Qn with tetraphenylborate (TPB) and tested its efficacy for determination of Qn in pharmaceutical preparations[66]. The electrodes displayed good selectivity towards Qn in presence of various potentially interfering inorganic and organic ions. However, alkaloids such as papaverine, quinidine and yohimbine showed serious interference. Another potentiometric technique using a silver sulphide ion-selective electrode was proposed for the determination of Qn and some other drugs/physiologically active substances[67]. Saad *et al* used wall-jet flow-through potentiometric flow injection analysis (FIA) detectors to test the efficiency of the developed membranes for analysis of the drug[68,69]. Qn selective sensors were fabricated based on a lipophilic ion-exchanger potassium tetrakis[3,5-bis(trifluoromethylphenyl)]borate (PTFB) in PVC membranes using dioctyl phthalate (DOP), 2-nitrophenyl phenyl ether (NPPE), and bis(2-ethylhexyl)adipate (BEHA) as plasticizers. The best performance was exhibited by the sensor containing BEHA. It was sensitive, fast-responding and exhibited near Nernstian response under batch injection analysis (BIA). Negligible interference by foreign species such as alkali and alkaline earth metal ions, sodium benzoate and sugars was noted. Analytical

applicability of the method was evaluated by determining Qn in spiked mineral water samples as well as other drinks (carbonated and bitter lemon drinks) yielding satisfactory results.

A TPB in PVC matrix based sensor was developed using different borate derivatives, KTCPB, potassiumtetrakis[3, 5 - bis(trifluromethyl)phenyl] borate (KTFPB) and NaTPB as the ion-exchangers and 2-nitrophenyl octyl ether (NPOE), dioctyl sebacate (DOS) and didodecyl phthalate (DDP) as plasticizers[70]. Selectivity measurements revealed no interference from metal cations (NH_4^+, K^+, Na^+ and Ca^{2+}), ephedrine, glycine and glutamic acid. The membrane fabrication in the proposed method did not require separate preparation of the Qn-borate ion-pair, which was an improvement over other earlier reported potentiometric methods. This was attributed to the fact that the QuH^+ cation, being more lipophilic than Na^+ or K^+ ions, could easily displace them from the sensing membrane. The KTCPB/DDP/PVC electrode gave the best response in terms of sensitivity and selectivity, and was successfully employed to determine Qn in tonic water as well as in orange, apple and white grape juices. The results obtained using standard addition technique showed high recovery and a low standard deviation suggesting the applicability of the method to determine Qn in coloured and benzoate containing substances. Molecular imprinted polymer technology was employed by Kamel *et al* to develop miniaturized planar PVC based polymeric membrane sensors containing Qn-MAA and/or acrylic acid (AA)-ethylene glycol methacrylate (EGMA) followed by application of the method for routine determination of Qn in soft drinks[71]. PVC membrane based silver (Ag) and copper (Cu) coated wire electrodes (CWEs) were constructed to determine quininium cation (Qn^+)[72]. Ion-pairs and ion associates of Qn^+ with reineckate (Rn^-), phosphotungstate (PT^{3-}) and phosphomolybdate (PM^{3-}) were used as the ion-exchangers. Ag-Qn_3PM CWE displayed best performance exhibiting appreciable selectivity, a Nernstian response alongwith good accuracy and precision. The method was then validated for micro determination of Qn_2SO_4 in pharmaceutical compounds containing Qn. The method does not give any information regarding detection limit. Also, gradual leaching of the electroactive ion-exchanger from the electrode

membrane surface was observed leaving it soaked for a day. Solid state CWEs possess the advantage of being more easily prepared as compared to the conventional electrodes. Also, it does not require an internal reference electrode.

A novel potentiometric technique, differential dynamic potentiometry (DiDP), was proposed to study the effect of β-cyclodextrin (β-CD) on the response of electrodes sensitive to Qn and other pharmaceutical drugs[73]. DiDP method consists of recording the dynamic potential difference between two ISEs. The responses in serial calibration mode were found to be characteristic for each individual drug including Qn. The effect of membrane plasticizers, 2-fluoro-2'-nitrodiphenyl ether (FNDPE), DOS, NPOE and tricresyl phosphate (TCP), on the electrode performance was monitored, with the TCP containing membrane showing the best response. The method was further used for quantitative analysis of Qn upto 1.0 mM. However, the selectivity and usability of the method in real samples was not investigated.

3.1.3 Mefloquine (3)

Mefloquine (MQ), a 4-methanol quinoline, was developed in the 1970s as a synthetic analogue of Qn[74]. Usually recommended for treatment of CQ-resistant *P. falciparum* malaria, the drug can be safely used during all trimesters of pregnancy. It is also considered a good prophylactic[75]. However, extensive resistance and serious adverse effects associated with MQ resulted in decline of its use.

The electro-reduction behavior and quantification of MQ was studied in BR buffer at a HMDE using CV, DPV and SWV techniques[76]. The analytical applicability of the method was verified in pharmaceutical dosage forms and biological samples. The method was fully validated and there was no possible interference from the excipients and endogenous substances found in tablets and biological fluids. A MQ ion-selective electrode was developed to determine the drug in blood plasma samples[77]. High MQ protein binding resulted in reduced drug

sensitivity and hence, poor potentiometric response was noted. Also, the method involved sample extraction prior to analysis of the drug in blood sample.

3.1.4 Amodiaquine (4)

Amodiaquine (AQ) is a mannich base 4-aminoquinoline having structure and mechanism of action similar to that of CQ. The drug is used as an alternative to CQ since it is effective against CQ-resistant *P. falciparum* parasites[78]. Reports of fatal adverse drug reactions in 1980s led to withdrawal of this drug as first-line of treatment for malaria in some countries[79]. Currently, AQ is widely employed in the combination therapy for control of malaria in Africa.

The cyclic voltammetric behaviour of AQ was investigated at a bare and DNA modified CPE in BR buffer (pH 4.0) studying the dynamics of DNA mediation in the transfer of electrons[80]. Well-defined anodic and cathodic peaks were obtained at both the electrodes. Though there was not much variation in peak potential, a remarkable improvement in peak current was observed at DNA modified CPE. Presence of guanine interfered with the voltammetric response of AQ. Analytical applicability of the method in real samples was not validated. Also, the detection limit, stability, accuracy and reproducibility of the electrode were not reported. Later, Valente *et al* developed a hemin-based electrode for voltammetric determination of the drug[81]. The electrooxidation process was irreversible and diffusion-controlled. The method was then validated for analysis of AQ in breast milk without any prior sample treatment.

Eight PVC membrane ion-sensitive electrodes were fabricated and investigated for potentiometric determination of AQ hydrochloride[82]. The sensing membrane was based on water-insoluble ion-pair complex formed between the cationic drug and NaTPB or KTCPB as the ion-exchanger. Various plasticizers namely, DOP, NPOE, bis(2-ethylhexyl)adipate (EHA) and dioctyl phenylphosphonate (DOPP) were investigated for fabricating the sensor and their performances were compared. A stable, fast and near-Nernstian response over a wide drug concentration range was exhibited by all the sensors. The overall best performance was

exhibited when KTCPB and DOP was used as the ion-exchanger and plasticizer, respectively. Upon evaluating the selectivity of the sensor, CQ, Qn, imipramine, promethazine and alkaloids were found to show serious interference on the potentiometric response of AQ. The drug was successfully determined in tablets and in the reconstituted powder without any sample treatment.

3.1.5 Primaquine (5)

Primaquine (PQ), an 8-aminoquinoline, was approved as an anti-malarial drug in 1952 by the FDA[83]. It is the only known drug that is capable of eliminating the intra-hepatic forms (schizonts and hypnozoites) of *P. ovale* and *P. vivax*. It also prevents the transmission of *P. falciparum* malaria by exhibiting potent gametocytocidal activity. Besides, PQ is also used as an alternative for primary prophylaxis against all species of malaria. The antimalarial activity of PQ is suggested to due to its reactive intermediates that interrupt the metabolism of parasitic mitochondria.

Arguelho *et al* investigated the electrochemical behavior of PQ in B-R buffer at a glassy carbon electrode (GCE) using linear, differential-pulse and square-wave voltammetry[84]. The electron transfer process was suggested to involve dimerization of the product of charge transfer. It was proposed that the electrochemical oxidation of PQ in aqueous solution involved the quinolinic ring. The method was then successfully validated for determination of the drug in pharmaceutical samples without any extraction steps. The observed detection limit was high (in millimolar range) and the method did not test the applicability of the electrode in human body fluids. Later, a differential pulse voltammetric method was presented for quantification of PQ at Cu-NW/CPE in tablets exhibiting a good recovery percentage[47]. The electrode showed good reproducibility and excellent stability. No interference from sorbitol, lactose, Na^+, and K^+ was observed towards the current response of the drug. The feasibility of the method for analysis of Qn in pharmaceutical preparations was successfully validated.

Macrocyclic crown ethers based ion-selective electrodes were developed as potentiometric sensors by Saad *et al* for the quantification of PQ[85]. Three macrocyclic crown ethers, namely dibenzo (18-crown-6), dibenzo (24-crown-8) (DB24C8) and dibenzo (30-crown-10) (DB30Cl0) were considered for electrode fabrication. Near-Nernstian responses were observed at DB24C8- and DB30C10-based membranes indicating that crowns with large cavity sizes are able to effectively encapsulate the bulky cation of PQ. The developed electrode showed good usability for about 30 days. However, after this period the membrane components of the electrode start leaching that lead to a sluggish and noisier response. Slight interference on the electrode response was observed in presence of CQ, sulfadimide and sulfacetamide. Also, the feasibility of the method for determination of the drug in real samples was not evaluated.

3.1.6 Piperaquine (6)

Piperaquine (PRQ) is a bisquinoline drug that was extensively used for more than two decades for the prophylaxis and treatment of malaria[86]. However, with the emergence of PRQ-resistant strains of *P. falciparum* and introduction of highly effective ACT, use of the drug as monotherapy gradually declined. In 1990s, PRQ was included as one of the components of the short-course ACTs. Lately, a combination of dihydroartemisinin and PRQ is being safely used for the treatment of uncomplicated malaria and effective malarial therapy as well as for providing prophylaxis for re-infection. To date, there has been no work reported on the electroanalytical determination of the drug.

3.1.7 Lumefantrine (7)

Lumefantrine (LF; also known as benflumetol) is a highly lipophilic fluorene derivative of aryl amino-alcohol group of drugs that is only administered in combination with artemether for the treatment of multi-drug resistant strains of *P. falciparum* malaria. The combination also shows high efficacy against the erythrocytic stage of *P. vivax* infection[87]. LF is believed to exert its antimalarial effect by impeding the formation of β-hematin by forming a complex with hemin

and inhibits synthesis of nucleic acid and protein. There is a sole electrochemical study reported in literature for determination of LF[88]. A carbon graphite working electrode was modified using antimalarial drug, coartem (LF/artemether). The electro-oxidation of LF occurred at a lower potential at the modified electrode as compared to the bare electrode showing electrocatalytic effect. The presence of bentonite as the host matrix catalysed the electro-oxidation of the drug with the oxidation occurring at a lower potential. However, no further work with respect to quantitative analysis of the drug was carried out.

3.2 Artemisinin and its derivatives

Artemisinin and its derivatives (**Fig. 2**) are considered as the most important antimalarial group of drugs owing to their rapid action, high efficacy, tolerability and limited resistance in malarial parasites. The derivatives include artesunate, artemether and dihydroartemisinin. They show a broad spectrum of activity and are effective against Qn resistant malaria parasites. At present, artemisinin based combination therapy (ACT) is recommended as the first-line of treatment for uncomplicated *P. falciparum* malaria, where one of the artemisinin derivatives is combined with a drug from a different class. These have the potential to delay antimalarial drug resistance when administered in combination with long-acting antimalarial drugs such as pyrimethamine or AQ. Available in oral, parenteral and suppository formulations, artemisinin and its derivatives exert their antimalarial effect on the ring-forming younger parasites reducing parasite numbers by a factor of approximately 10,000 per asexual cycle[89]. All artemisinins possess an endoperoxide moiety. Their antimalarial activity is believed to be due to activation of the drugs within the food vacuole of the intra-erythrocytic stage of the parasite, where reductive cleavage of the peroxide bond by heme liberated during digestion of haemoglobin generates reactive oxygen radicals. This induces oxidative stress and alkylates heme and vital parasite proteins causing damage to the parasite[90]. A recent study suggested that the artemisinin derivatives display antimalarial activity by inhibiting a *P. falciparum*-encoded sarcoplasmic-endoplasmic reticulum calcium ATPase[91].

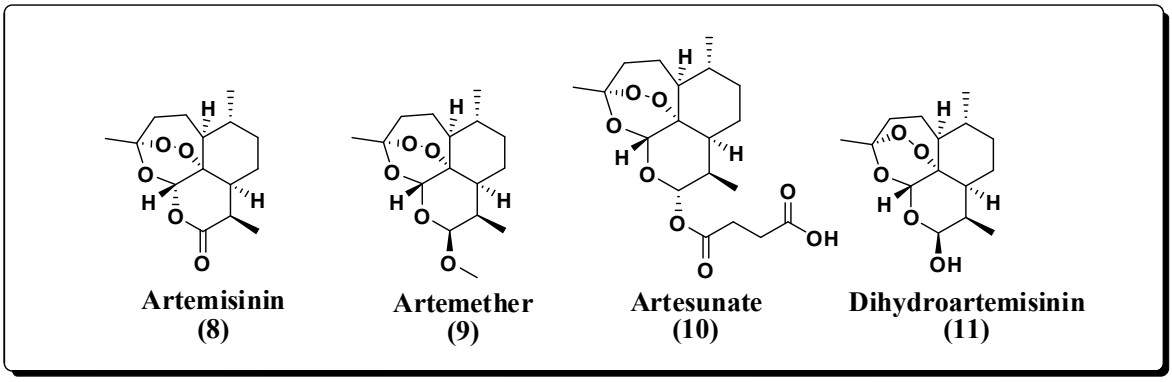

Fig. 2 Chemical structures of artemisinin and its derivatives.

3.2.1 Artemisinin (8)

Artemisinin (ARN) is a sesquiterpene lactone endoperoxide that was isolated in 1972 from *Artemisia annua*, a Chinese herb used to treat fever[90]. It was successfully used for the treatment of multi-drug resistant strains of falciparum malaria for more than two decades. Besides its efficacy against malaria, ARN also shows anticancer effects.

The interaction of ARN and haemoglobin was studied at layer-by-layer haemoglobin/poly(vinyl sulfonate) film modified glassy carbon and silver electrode[92]. The catalytic activity of the electrodes was suggested to be due to the breaking of the peroxide bond in ARN by the prosthetic group heme in haemoglobin. Though the report presented a new understanding for the antimalarial mechanism, it did not explore quantitative analysis of ARN. Debnath *et al* reported a differential pulse polarographic (DPP) method for the determination of ARN. The method was simple, sensitive, precise and was successfully used to quantify ARN in a traditional Chinese herbal drug *Artemisia annua L*[93]. However, the method used DME which has several limitations such as variation in the surface area of mercury (Hg) drop, higher charging current and high consumption of Hg. Also, Hg is poisonous and hence, it needs to be carefully handled. Later, the same group developed a DPV method to determine the drug in *Artemisia annua* extracts using a cobalt phthalocyanine modified CPE and a hemin modified electrode with Adeps neutralis (solid fat) as binder[94,95]. A DPP method was further proposed to determine

the amount of ARN in herbal tea preparation of *Artemisia annua*[96]. The tea prepared without cooking but shaking for 15 minutes gave high concentration of ARN. No interference was observed in the tea extract to estimate the drug. The method was simple and did not require any special separation technique or derivatization of ARN. Gong *et al* synthesized various glycosylated porphyrin metal complexes and employed as active material for developing amperometric sensor for ARN detection[97]. The working electrodes were prepared by incorporating different glycosylated porphyrin metal complexes including [ZnT(o-glu)PPCl], [FeT(o-glu)PPCl], [MnT(o-glu)PPCl] and T(o-glu)PPH_2 in gold nanoparticles/chitosan matrix film coated onto the GCE surface and their characteristic performance was investigated using amperometry. The electrode having [FeT(o-glu)PPCl] as the active material exhibited the best response in terms of selectivity and sensitivity. Among EDTA-Fe^{3+}, Fe^{3+}, CN^-, H_2O_2 and artemisinic acid, only CN^- was found to interfere in the amperometric response of ARN. The method was stable as well as reproducibility, and was successfully assessed for direct determination of ARN in plant extract samples.

The electrochemical behaviour of ARN was investigated at MWCNTs and dihexadecyl hydrogen phosphate modified glassy carbon electrode (MWCNTs-DHP/GCE) using CV and linear sweep voltammetry (LSV)[98]. No interference from other species (metal ions, ascorbic acid, vitamin E, vitamin B6, vitamin A, uric acid, lysine, tryptophan, cysteine and indole-3-acetic acid) was found towards the determination of ARN. The method was successfully applied to determine the content of ARN in *Artemisia annua* L. An amperometric sensor based on hemin immobilized on titanium oxide modified silica (STH) was developed and applied for determination of ARN in the crude extracts of *A. vulgaris L*[99]. The selectivity of the electrode for ARN was evaluated in presence of interferents such as EDTA-Fe^{3+}, Fe^{3+}, H_2O_2 and CN^-. None of the mentioned interferents affected the amperometric response of the drug. The modified electrode showed good stability and reproducibility. Phukon *et al* fabricated a sensitive and selective biosensor based on HRP immobilized natural polymer

polyhydroxyalkanoate with gold nanoparticle composite on indium-tin oxide (PHA/AuNPs/HRP/ITO) for the determination of ARN in bulk and spiked human serum[100]. Recently, a molecularly imprinted membrane based sensor was fabricated for analysis of ARN[101]. The sensor was constructed by first modifying the GCE with graphene (G) and then assembled with ARN imprinted membrane (ART-MIM) using in-situ polymerization technique using ethylene glycol dimethacrylate (EGDMA) as cross-linking agent and acrylamide (AM) as the functional monomer and. The ART-MIM/G/GCE sensor displayed higher selectivity towards ART as compared to its derivatives, dihydroartemisinin, artemether and artesunate. Also, a lower detection limit and a wider dynamic range were observed as compared to the earlier reported methods. The analytical applicability of the sensor was successfully validated for the determination of ART in *A. annua* L1[101].

3.2.2 Artesunate (9)

Artesunate (ARTS) is a hemisuccinate derivative of dihydroartemisinin, which is effective against multi-drug resistant *Plasmodium falciparum*. It is the only derivative that is available as a parenteral formulation for intravenous administration[102]. It is a potent blood schizonticide active against the ring stage of the malarial parasite. ARTS also exhibits cytotoxic activity against different cancer cell lines[103].

Jain *et al* investigated the electrochemical behaviour of ARTS at glassy carbon electrode in phosphate, BR and acetate buffer systems[104]. The best response was observed in phosphate buffer system containing 1.0% CTAB. No interference was observed from commonly encountered pharmaceutical excipients and endogenous substances usually present in biological samples. The method was successfully applied for determination of ARTS drug in tablets and spiked human serum, urine and plasma samples. Later, the same group fabricated MWCNTs modified electrode (MWCNTs/GCE) for quantitative analysis of ARTS in bulk and commercial formulations[105]. The method led to improved voltammetric parameters including the

detection limit. Recently, a horseradish peroxidase immobilized graphene oxide-polyaniline film based sensor was developed for analysis of ARTS in pharmaceutical dosage forms and biological fluids without any potential pharmaceutical excipients as well as the body fluid matrix interferences[106].

3.2.3 Artemether (10)

Artemether (ARM) is a semi-synthetic derivative of ARN used as an alternative for pre-referral treatment of severe malaria when parenteral ARTS is not available. ARM-LF combination was the first fixed dose oral combination of an ARN derivative with another antimalarial drug which upon administration, show improved efficacy against the erythrocytic stages of Plasmodium species[107]. The presence of electrochemically active peroxide (–O–O–) group in ARM leads to easy reduction of the drug at various electrodes.

The electrochemical behaviour of ARM was first studied at a GCE in presence of hemin. Hemin was found to catalyze the reduction process of ARM. However, the quantitative analyis of the drug was not performed[108]. Later, Debnath *et al.* investigated the polarographic behaviour of ARM at mercury electrode using DiPP[109]. None of the excipients commonly present in tablets/capsules was found to influence the peak current response of the drug, suggesting good specificity of the method. The analytical applicability of the method was successfully evaluated for analysis of the drug in tablets and capsules. Although the method was simple, accurate and precise, it has the disadvantages associated with the use of a mercury electrode. Orata *et al* chemically modified the carbon graphite working electrode surface with LF/ARM (coartem) for electrochemical study of the drugs[88]. The results suggested that ARM possesses redox active moieties. The drug also interacted electrochemically with amino acids. Bentonite was also used as the host matrix in the modified electrode to analyse ARM. However, the bentonite matrix was found to completely inhibit the redox activity of the drug. The study did not attempt to evaluate the analytical applicability of the modified electrode for quantification of ARM.

3.2.4 Dihydroartemisinin (11)

Dihydroartemisinin (DHA) is both an active metabolite of ARN derivatives in vivo and a semi-synthetic derivative of ARN therapeutically active against malaria. DHA in combination with PRQ, is one of the five ACTs recommended by WHO for the treatment of uncomplicated *P. falciparum* malaria. Wang *et al* reported the sole study on the voltammetric behaviour and determination of DHA[110]. The working electrode was single-wall carbon nanotube (SWCNT) modified glassy carbon electrode. The method was fast and simple. However, it did not test the feasibility of the modified electrode for quantification of the drug in real samples.

3.3 Antifolates

Since their discovery in the 1940s, antimalarial antifolates remain an important class of drugs for prophylaxis and treatment of malaria, both as single agents as well as in combinations. These drugs function by interfering with folate metabolism thus disrupting the pathway critical for the survival of the malaria parasite[111]. Though effective, antifolates may cause hematologic effects if ministered for a prolonged period of time[112]. Malaria haemolysis may lead to folic acid deficiency and megaloblastic anemia[113]. The chemical structures of antimalarial antifolates are shown in **Fig. 3**.

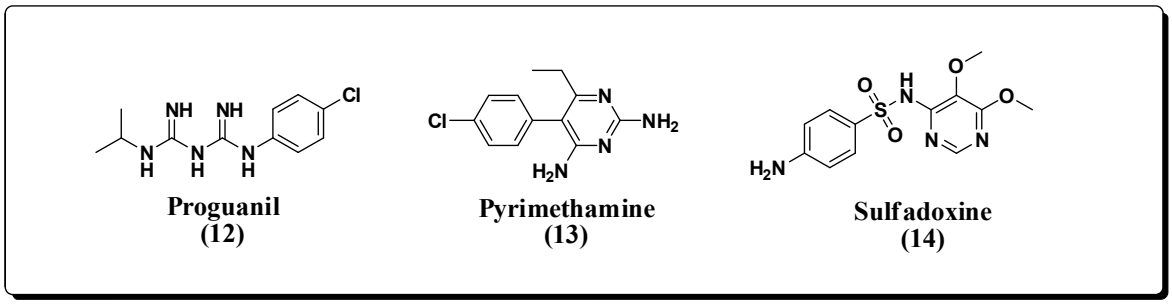

Fig. 3 Chemical structures of antimalarial antifolates.

3.3.1 Proguanil (12)

Proguanil (PG), a synthetic biguanide derivative of pyrimidine, is a prophylactic antimalarial drug. It is metabolized into its active metabolite, cycloguanil, which blocks dihydrofolate

reductase enzyme inhibiting folic acid metabolism[114]. This stops the reproduction of the malaria parasites, *P. falciparum* and *P. vivax*, in red blood cells. PG is usually taken in combination with atovaquone for malarial prophylaxis, to treat uncomplicated malaria in travellers outside malaria-infected areas and in combination with ARTS and PQ as an alternative malaria therapy when other WHO recommended medications are either not available or are ineffective.

The electrochemical behaviour of PG was first studied using d. c. polarography in BR buffered media[115]. A reduction wave was observed which was attributed to the reduction of the two azomethine centers on the monoprotonated biguanide group. The detection limit was found to be 0.05-0.1 μg/mL. Gelatin, Triton X-100 and other substances having a half-wave potential within 100 mV of that of PG were found to interfere with the electrochemical response of the drug. Later, Smarzewska *et al* developed a renewable silver amalgam film electrode for determination of PG in tablets and spiked human urine[116]. Though it was observed that presence of atovaquone did not affect PG determination, the effect of other interferents (excipients commonly found in pharmaceutical preparations and endogenous substances present in biological fluid matrix) was not investigated.

3.3.2 Pyrimethamine (13)

Pyrimethamine (PYM) is a diamino-pyrimidine possessing the structure and activity similar to PG[117]. It inhibits dihydrofolate reductase thus adversely affecting the synthesis of folic acid by protozoa. This impedes cell replication by provoking lack of substrates for the formation of purines and pyrimidines. It is predominantly active against the later development stages of asexual malaria parasites and is also used to treat *Toxoplasma gondii* infections. It has been extensively employed in combination with sulfadoxine for prophylaxis and treatment of CQ-resistant malaria. Due to the incidence of side effects such as hypersensitivity reactions and hepatotoxicity, this combination has been relatively replaced by other approaches. However, it

is still used to treat malaria (predominantly in Africa) and for prophylaxis against CQ-resistant malaria in patients with contraindications to other drugs.

A PYM modified carbon graphite electrode surface was fabricated to investigate the electrochemical response of the drug in absence and presence of bentonite as the host matrix.[88] PYM was observed to undergo electro-oxidation in a $1e^-/1H^+$ pathway. The presence of bentonite as the host matrix did not significantly affect the redox potential of the drugs. This was attributed to the size of drug molecules which hindered isomorphous exchange or substitution within the tetrahedral and octahedral sites in the clay montmorillonite. The electrochemical interaction of the drug with amino acids (methionine, arginine, tyrosine and leucine) was also investigated. However, the work did not involve quantitative analysis of the drug. The electrochemical oxidation mechanism of PYM was examined at a screen printed carbon electrode (SPCE) in different aqueous supporting electrolytes[118]. Further, a dsDNA modified SPCE (dsDNA/SPCE) was fabricated and subsequently tested to determine the drug in 0.02 M phosphate buffer system. No interference towards the electrochemical response of PYM was observed from potential interfering substances present in biological fluids such as D-glucose, ascorbic acid, L-cysteine, uric acid and cysteine. The analytical applicability of the dsDNA/SPCE sensor was validated for the analysis of the drug in spiked human blood serum samples. SPCEs offer the advantage of being simple, economical, disposable, portable, versatile, and have mass production capability. Being disposable the problems associated with adsorption and fouling of the electrode surface by products of redox processes are also evaded. However, presence of organic solvents limits the use of SPCEs since these solvents may dissolve the insulate inks leading to decline in sensitivity and detection limit. Another drawback of the method employing SPCE is that the electrode had to be replaced after every measurement[119-121].

3.3.3 Sulfadoxine (14)

Sulfadoxine (SD) is a long-lasting sulfonamide that interferes with folate synthesis by competitively inhibiting dihydropteroate synthase[122]. It is generally used in combination with PYM to treat or prevent malaria[117]. However, due to possible side effects and availability of more effective ACTs, it is no longer recommended for routine use, but only advised in case of serious malaria infections or prophylaxis in areas where other drugs are not effective. A thorough literature search revealed only one study that used amperometric detection for the determination of sulfonamide residues including SD[123]. However, the method was employed in conjunction with ultra-performance liquid chromatography. The drawback of the method was that a solid-phase extraction step was required for clean-up, preconcentration and extraction of sulfonamide residues in shrimp samples prior to separation[123]. Yao *et al* reports the sole potentiometric study for the determination of the drug using SD and quaternary ammonium complex ion-pairs as membrane electrodes[124].

3.4 Antimicrobials and others

Some well-known antimicrobials and a hydroxynaphthaquinone drug were also found to exhibit activity on malaria parasites in their blood or mosquito stages, or both. The chemical structures of these drugs are displayed in **Fig. 4**.

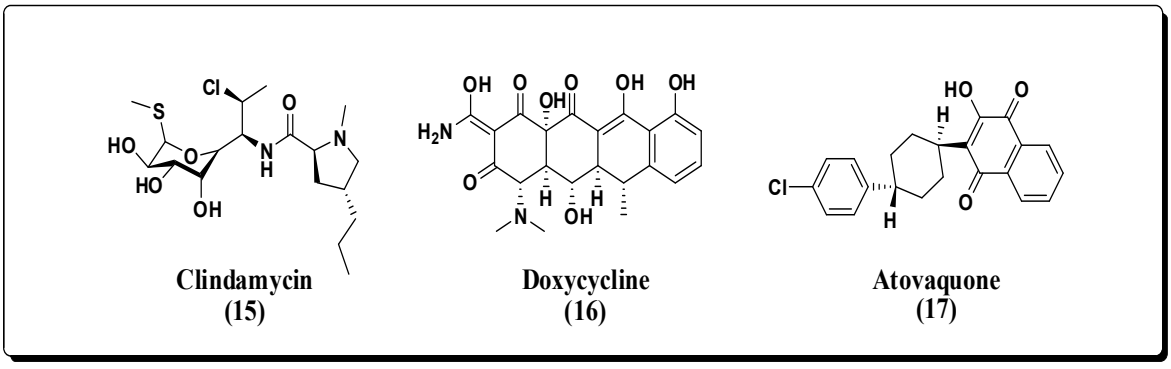

Fig. 4 Chemical structures of Clindamycin, Doxycycline and Atovaquone

3.4.1 Clindamycin (15)

An antibiotic belonging to lincosamide class of drugs, clindamycin (CM) is basically used to treat infections related to anaerobic bacteria, including infections of the skin, soft tissue, respiratory tract, peritonitis, and bone and joint infections[125]. It also shows antimalarial activities and is recommended in combination with Qn or ARTS for effective treatment of severe or uncomplicated *Plasmodium falciparum* malaria. Being a slow-acting drug, it is rarely advised as monotherapy. CM is well-tolerated having mild and transient side effects.

A fast fourier adsorptive stripping voltammetric method was developed using a gold ultramicroelectrode for the determination of CM in flow injection systems[126]. The method was accurate, precise, sensitive and successfully employed to analyse CM in capsules. Molecular imprinting is a process that creates selective binding sites in synthetic polymers. These molecular imprinted polymers are particularly beneficial for sensors since they selectively bind the analyte. The technique offers advantages such as low cost, ease of preparation, high chemical and mechanical stability. Zhang *et al* fabricated a molecularly imprinted electrochemical sensor by stepwise electrodeposition of a MWCNTs layer and a thin molecularly imprinted sol-gel film onto the surface of a gold electrode (MIP/sol-gel/MWCNTs/Au electrode) for detection of CM[127]. On comparing the response currents towards CM hydrochloride, erythromycin, oxacillin sodium monohydrate, benzylpenicillin potassium and streptomycin sulphate, the developed sensor displayed high selectivity towards CM demonstrating the highest response current. However, the effect of potential interferents (substances commonly present in biological matrix) was not assessed. The usability of the imprinted sensor for determination of the drug in human urine samples was successfully evaluated. The voltammetric behavior of CM hydrochloride and its phosphate salt was examined at a CPE using AdSV[128]. The method was accurate, precise and successfully applied for determining the drug in pharmaceutical preparations (capsules and lotion) and in

human urine samples. However, the effect of potential interferents on the voltammetric response of the drug was not reported.

3.4.2 Doxycycline (16)

Doxycycline (DC) is an antimicrobial of the tetracycline class used to treat a number of infections, including bacterial, protozoal and helminth[129-131]. It is generally prescribed in combination with other antimalarial agents, such as Qn or ARTS, for treatment of uncomplicated falciparum malaria.

A sensitive adsorptive stripping method was developed for trace analysis of DC at HMDE exhibiting a detection limit of 6×10^{-10} M[132]. The method involves potential risks of contamination, poisoning and disposal associated with the use of metallic mercury. A nickel-modified glassy carbon electrode (Ni/GCE) was fabricated for amperometric detection of DC in a flow injection system[133]. The electrode offered good reproducibility, stability, accuracy and was validated for analysis of DC in commercial pharmaceutical formulations (capsules). However, the effect of biologically common interferents was not investigated. The general electrocatalytic behaviour of Ni/GCE towards various compounds (amino acids, carbohydrates and hydroxylated compounds) was anticipated to interfere with detection of DC, thus limiting the selectivity of the modified electrode. It is implied that due to the same reason, Ni/GCE was not employed to quantify DC in biological fluid samples. More flow injection methods with amperometric detection were developed at anodized boron-doped diamond (BDD) thin film electrode and a gold rotating disk electrode (Au RDE) for the determination of DC in different pharmaceutical formulations[134,135]. Shaidarova *et al* fabricated a mixed-valence Ruthenium oxide-ruthenium cyanide (RuO-RuCN) film modified GCE for determining DC under BIA and FIA conditions[136]. The presence of adjuvants such as nystatin and hydrocortisone did not affect the determination of the drug. The analytical applicability of the method was successfully evaluated for analysis of DC in syrup. Though the modified electrode was stable for several

months, it required acidic conditions and the film was destroyed if the pH was increased towards alkalinity. Conzuelo *et al* developed the first disposable amperometric immunosensor for detection of DC in milk samples[137]. The immunosensor was fabricated by immobilizing DC antibody (Ab) on the surface of protein G-functionalized magnetic beads (ProtG-MBs) and depositing the suspension on SPCE. A horseradish peroxidase (HRP)-labelled specific tracer was used for direct competitive immunoassay of the drug. The presence of Ca^{2+} ions in milk and the non-target antibiotics (enrofloxacin, sulfapyridine, cefapirin, ampicillin, amoxicillin and penicillin G) did not affect the performance of the magneto-immunosensor. Pencil graphite electrode (PGE) modified with Ppy and imprinted with DC was used to investigate the voltammetric behaviour of the antibiotic in BR buffer solutions[138]. The MIP electrode was further employed to determine DC in pharmaceuticals. Presence of ciprofloxacin, a quinolone group antibiotic, did not affect the differential pulse voltammetric response of DC. The effect of additives commonly found in pharmaceutical formulations using MIP/PGE was not reported. Also, the observed detection limit was considerably high as compared to other reported voltammetric methods for DC quantification.

The first potentiometric study for determination of DC hydrochloride in pharmaceutical preparations was performed at a simple PVC membrane based ISE[139]. The electrode showed a linear response with Nernstian slope over the range of 7.9×10^{-5}- 1.9×10^{-3}M and exhibited appreciable selectivity for the drug over a large number of organic substances and inorganic cations of biological importance. Novak Pekli *et al* constructed DC-TPB ion pair containing PVC-based DC-sensitive electrodes for the analysis of the drug in pharmaceutical preparations (capsules)[140,141]. A conducting Ppy film based DC-selective sensor was prepared by immobilizing the polymer onto the surface of a DC ion-pair complex in PVC membrane coated GCE[142]. Among the developed GCEs modified with different DC ion-pairs, viz. DC-TPB, DC-phosphotungstate and DC-silicotungstate, as the electroactive substance in PVC membrane having dibutylphthalate (DBP) as the plasticizer agent, DC-TPB incorporated electrode

displayed the best response. The sensor was stable, reproducible, exhibited a near-Nernstian response and was successfully applied to determine the drug in pharmaceutical formulations. The selectivity of the sensor (GC/PPy/PVC) towards different inorganic cations (Na^+, K^+, NH_4^+, Ca^{2+}, Mg^{2+} and Al^{3+}) and citric acid was also investigated. Kamel *et al* developed a molecularly imprinted MAA based sensor for DC analysis in tablets and biological fluids[143]. The MIP was constructed using DC as a template molecule, MAA and/or AM as a functional monomer and EGDMA as a cross-linking agent. The MIP was then incorporated in a PVC matrix to develop the sensor. The sensor showed high selectivity, sensitivity, accuracy, precision and exhibited a near-Nernstian response. Issa *et al* demonstrated the potentiometric determination of DC in pharmaceutical preparations using DC-TPB ion-pair modified CPE with DBP as plasticizer[144]. Both BIA and FIA modes were employed. The sensor exhibited a Nernstian response over a wide concentration range, a fast response time and high selectivity over a wide variety of inorganic cations, sugars and amino-acids. Different carbon paste compositions were evaluated. The best performance was obtained with carbon paste composition of 3% DC-TPB, 48.5% DBP and 48.5% graphite. The sensor was successfully applied for determination of DC in pharmaceutical formulations. However, the electrode displayed limited long-term stability with a life span of only 5 days.

3.4.3 Atovaquone (17)

Atovaquone (ATQ) is a hydroxynaphthaquinone that exhibits antimalarial activity against all Plasmodium species. It is administered in combination with PG where both components work synergistically, inhibiting electron transport and collapsing mitochondrial membrane potential, thereby hindering the production of energy for use by the parasites[145]. ATQ functions by inhibiting the cytochrome bc1 complex of the mitochondrial respiratory chain and decreasing the mitochondrial membrane potential to a large extent. Despite the importance of the quantitative analysis of the drug, no substantial work has been reported with respect to quantification of ATQ using electroanalytical methods.

The important electrode characteristics and validation parameters associated with the significant electroanalytical methods (voltammetric and potentiometric) reported for the determination of various antimalarial drugs have been summarized in **Table 3** and **Table 4**. Comparing these parameters, it becomes easier to select the more sensitive and versatile method.

Table 3. Validation parameters of important voltammetric methods reported for determination of various antimalarial drugs.

Drug	Electrode	Method	LCR (M)	LOD (M)	LOQ (M)	Matrix	Ref
Chloroquine	dsDNA/CPE	DPV	1.0×10^{-7} to 1.0×10^{-5}	3.00×10^{-8}	-	Spiked human serum	46
	Cu-NW/CPE	DPV	2.1×10^{-7} to 2.1×10^{-5}	3.10×10^{-8}	-	Pharmaceutical formulations	47
Quinine	MWCNTs-RTIL/GCE	SWV	3.0×10^{-6} to 1.0×10^{-4}	0.44×10^{-6}	-	Pharmaceutical formulations	55
	Ppy-PCNFe/Pt	CV	1.0×10^{-3} to 9.0×10^{-3}	1.08×10^{-5}	-	-	56
	p-(AHNSA)/ GCE	SWV	0.1×10^{-6} to 1.0×10^{-5}	1.42×10^{-8}	-	Spiked human urine; Pharmaceutical formulations	57
	EGMRA-MIP/GCE	Amperometry	8.0×10^{-7} to 2.6×10^{-4}	2.00×10^{-8}	-	Tonic water	58
	HMDE in presence of 1% CTAB	DPV SWV	27.7×10^{-8} to 19.4×10^{-7} 9.2×10^{-8} to 64.7×10^{-8}	7.34×10^{-10} 4.07×10^{-10}	2.44×10^{-9} 1.36×10^{-9}	Spiked plant extract (bark of Cinchona officinalis); Spiked soft drink; Pharmaceutical formulations	59
Mefloquine	HMDE	SWV	6.0×10^{-6} to 6.0×10^{-5}	-	4.50×10^{-7}	Spiked human serum and urine; Pharmaceutical formulations	76

Amodiaquine	Hemin/GCE	CV	-	9.27×10^{-6}	3.09×10^{-5}	Breast milk	81
Primaquine	GCE	LSV DPV SWV	3.0×10^{-5} to 1.0×10^{-2} 3.0×10^{-5} to 1.0×10^{-4} 3.0×10^{-5} to 1.0×10^{-4}	3.62×10^{-5} 1.62×10^{-5} 6.94×10^{-6}	-	Pharmaceutical formulations	84
	Cu-NW/CPE	DPV	22.4×10^{-7} to 22.7×10^{-6}	9.64×10^{-7}	-	Pharmaceutical formulations	47
Artemisinin	DME	DPP	6.4×10^{-7} to 3.2×10^{-5}	2.05×10^{-7}	-	Plant extracts (*Artemisia annua L.*)	93
	Hemin modified carbon fat electrode	DPV	4.8×10^{-6} to 7.8×10^{-5}	1.40×10^{-6}	-	Plant extracts (*Artemisia annua*)	94
	cobalt phthalocyanine modified CPE	DPV	2.1×10^{-5} to 5.3×10^{-4}	6.50×10^{-6}	-	Plant extracts (*Artemisia annua*)	95
	DME	DPP	63.8×10^{-8} to 31.9×10^{-6}	-	-	Herbal tea preparation of *Artemisia annua*	96
	[FeT(*o*-glu)PPCl]/Au NPs/GCE	Amperometry	1.8×10^{-7} to1.7×10^{-9}	1.70×10^{-9}	-	-	97
	MWCNTs/DHP/GCE	LSV	14.2×10^{-7} to 14.2×10^{-5}	3.54×10^{-7}	-	Plant extracts (*Artemisia annua L.*)	98

	CPE/STH	Amperometry	5.0×10^{-8} to 1.0×10^{-6}	1.50×10^{-8}	5.20×10^{-8}	Plant extracts (*Artemisia vulgaris L.*)	99
	PHA/AuNPs/ HRP/ITO bio-electrode	DPV	35.4×10^{-9} to 28.3×10^{-8}	1.20×10^{-8}	3.90×10^{-8}	Spiked human serum	100
	ART-MIM/G/GCE	DPV	1.0×10^{-8} to 4.0×10^{-5}	2.00×10^{-9}	-	Plant extracts (*Artemisia annua L.*)	101
Artesunate	GCE in presence of CTAB	DPV SWV	10.4×10^{-6} to 10.4×10^{-5} 10.4×10^{-6} to 10.4×10^{-5}	1.28×10^{-6} to 1.03×10^{-5} 8.84×10^{-8} to 6.37×10^{-7}	-	Spiked human serum, plasma and urine; Pharmaceutical formulations	104
	MWCNTs/GCE	DPV SWV	5.2×10^{-6} to 5.2×10^{-5} 5.2×10^{-6} to 5.2×10^{-5}	1.40×10^{-7} 6.48×10^{-9}	4.73×10^{-7} 2.15×10^{-8}	Pharmaceutical formulations	105
	GrO/PANI/HRP/ITO	SWV	1.3×10^{-10} to 10.4×10^{-10}	3.12×10^{-11} to 8.11×10^{-11}	-	Spiked human urine, serum and plasma; Pharmaceutical formulations	106
Artemether	DME	DPP	3.4×10^{-7} to 3.0×10^{-5}	1.07×10^{-7}	-	Pharmaceutical formulations	109
Dihydroartemisinin	SWCNTs/GCE	LSV	5.0×10^{-7} to 5.0×10^{-4}	3.00×10^{-7}	-	-	110
Proguanil	Hg(Ag)FE	SWV	1.0×10^{-7} to 6.0×10^{-6}	2.90×10^{-8}	9.7×10^{-8}	Spiked human urine;	116

						Pharmaceutical formulations	
Pyrimethamine	DNA/SPCE	DPV	1.0×10^{-7} to 5.0×10^{-5}	1.00×10^{-8}	-	Spiked human serum	118
Sulfadoxine	G/PANI/SPCE	Amperometry	3.2×10^{-8} to 3.2×10^{-5}	9.65×10^{-9}	3.22×10^{-8}	Shrimp	123
Clindamycin	Au ultra-microelectrode	ASV	9.4×10^{-12} to 1.0×10^{-4}	3.06×10^{-12}	9.4×10^{-12}	Pharmaceutical formulations	126
	MIP/sol-gel/MWCNTs/Au	SWV	5.0×10^{-7} to 8.0×10^{-5}	2.44×10^{-8}	-	Spiked human urine	127
	CPE	DPAdSV	$2.02\times10^{-7}$to 10.1×10^{-7}	7.67×10^{-8}	2.55×10^{-7}	Spiked human urine; Pharmaceutical formulations	128
Doxycycline	Ni/GCE	FIA	5.62×10^{-6} to 22.5×10^{-5}	2.07×10^{-6}	-	-	133
	Anodized BDD	FIA	5.0×10^{-4} to 5.0×10^{-2}	1.00×10^{-8}	-	Pharmaceutical formulations	134
	Au RDE	FIA	$1.0\times10^{-6}$to 1.0×10^{-4}	1.00×10^{-6}	-	Pharmaceutical formulations	135
	RuO-RuCN/GCE	FIA	5.0×10^{-3} to 1.0×10^{-6}	-	-	Pharmaceutical formulations	136
	DC-HRP on antiDC-	Amperometry	$28.1\times10^{-9}$to 15.2×10^{-7}	8.77×10^{-9}	-	Spiked undiluted milk	137

	ProtG-MBs/SPCE						
	MIPpy/PGE	DPV	$5.0\times10^{-5}$to 5.0×10^{-4}	4.25×10^{-5}	1.41×10^{-4}	Pharmaceutical formulations	138

Table 4. A summary of response characteristics of some of the potentiometric sensors for the determination of antimalarial drugs.

Drug	Type of electrode/ sensor	Electrode Composition	LCR (M)	LOD (µM)	Slope (mV decade^{-1})	Working pH range	Response time (s)	Matrix	Ref
Chloroquine	[a]PVC membrane electrode	BEHA, KTCPB, THF	0.1×10^{-4} to 1.0×10^{-1}	20.0	28.3	-	-	Pharmaceutical formulations; Synthetic mixtures (tablet, serum electrolyte and biological fluids)	51
Quinine	PVC membrane electrode	PVC, NaTPB, DBP, THF	5.0×10^{-5} to 1.0×10^{-1}	-	56.3	5.3-7.3	-	-	66
	PVC membrane electrode	PVC, KTCPB, DDP, THF	0.1×10^{-4} to 1.0×10^{-2}	6.3	58.9 ± 1.0	4.4-8.0	10	Soft drinks	70
	[b]MIP membrane modified GCE	PVC, MAA, THF PVC, AA-EGMA, THF	4.0×10^{-6} to 1.0×10^{-2} 1.0×10^{-5} to 1.0×10^{-2}	1.2 8.2	61.3 to 55.7	-	-	Soft drinks	71
	[c]Solid state electrodes (Ag-CWEs Cu-CWEs)	QnRn, Qn_3PT, Qn_3PM, PVC, THF, DOP, Ag/Cu coated wire	1.0×10^{-6} to 1.7×10^{-2}	-	48.8 to 55.4	3.2-7.6	5	Pharmaceutical formulations	72

Amodiaquine	PVC membrane electrode	PVC, KTCPB, THF, DOP	1.0×10^{-2} to 1.6×10^{-5}	11.0	29.3	3.7-5.5	<30	Pharmaceutical formulations	82
Primaquine	PVC membrane electrode	PVC, KTCPB, DB24C8, DOPP	-	1.0	34.1	3.5-10	30	Pharmaceutical formulations	85
		PVC, KTCPB, DB30C10, DOPP		8.9	33.4	3.5-10	30		
Doxycycline	[d]Internal solid contact sensor (GC/PPy/PVC)	PVC, NaTPB, DBP, THF, PPy, GCE	1.0×10^{-2} to 1.0×10^{-5}	4.0	54.4	3.5-8.0	<15	Pharmaceutical formulations	142
	[e]DC-TPB ion pair modified CPE	NaTPB, graphite, DBP, CPE	19.9×10^{-6} to 31.9×10^{-6}	13.3	62.30	-	<8-10	Pharmaceutical formulations	144

[a]PVC membrane electrode: Poly(vinyl chloride) membrane based ion-selective electrode; [b]MIP membrane modified GCE: Quinine based molecularly imprinted polymer modified glassy carbon electrode; [c]Solid state electrodes (Ag-CWEs: Silver coated wire electrodes; Cu-CWEs: Copper coated wire electrodes); [d]Internal solid contact sensor (GC/PPy/PVC): Polypyrrole film immobilized glassy carbon electrode surface with a plasticized polyvinyl chloride membrane containing DC-TPB ion-pair; and [e]DC-TPB ion pair modified CPE: Doxycycline-tetraphenylborate ion-pair containing carbon paste electrode.

4. Recognition receptors based electrochemical analysis of antimalarial drugs

An electrochemical sensor is an analytical device that comprise of a chemical (molecular) recognition system (receptor) immobilized onto the potentiometric or voltammetric transducer. The analyte interacts selectively with the receptor molecules resulting in a change in its physical properties in such a way that the appending transducer generates an analytically useful signal. When the recognition receptor is of biological origin, the chemical sensor is referred to as a biosensor. Recognition receptors play a vital role in the development of sensors. The recognition process is governed primarily by the shape and size of the receptor pocket and the analyte of interest. The function of the receptor is usually achieved by fabricating a thin layer that responds to particular species or a group of substances.

In a biosensor, biological recognition elements such as antibodies, enzymes, DNA and aptamers have been used as specific receptors to a target molecule. Among these, enzymes are the most common recognition receptors. Enzyme based electrochemical sensors are characterized by the specific binding capabilities and catalytic activity of enzymes. The analyte is recognised *via* enzyme inhibition or conversion of the analyte into a product. Enzyme products or by-products may be electroactive, and thus the changes in their activity may be monitored amperometry. Other enzymes may produce or consume protons, and their activity can be studied through pH changes. Peroxidase is one of the most common enzyme labels for electrochemical biosensors. Horse radish peroxidase (HRP) was used to catalyze the oxidation of antimalarial drugs, ART and ARN, in presence of hydrogen peroxide[100,106]. Enzymes are also used as labels attached to antigens, antibodies and oligonucleotides with a specific sequence providing affinity-based sensors. A direct competitive immunoassay using a tracer with HRP for the enzymatic labeling was performed for amperometric detection of DC[134]. The drug was quantified by competitive binding between DC and a HRP-labeled specific tracer for binding sites of the captured antibodies immobilized on the surface of protein-functionalized magnetic beads. Aptamers are specific oligonucleic acid sequences (DNA or RNA) or peptide molecules that recognize

specific ligands and bind to various target molecules ranging from small metal ions and drugs to large proteins with high affinity and specificity. DNA strands have been used as receptors for antimalarial drug detection since they possess rich functional active groups such as amino groups and carbonyl groups, and could bind with drug molecules through electrostatic interactions, hydrogen bond and hydrophobic interactions[46,61,80,118]. Peptides are amino-acids sequences which hold possibility of being used as a receptor for antimalarial drug detection since it may, like DNA, form tertiary structures where the drug cations can bind. Similar to DNA, peptides can be synthesized and selected by automated routes in a combinatorial way, and hence, hold promise to function as effective recognition elements in electrochemical sensors for analysis of antimalarial drugs. Very few biological components have been employed as specific receptors to antimalarial drugs in electrochemical sensors. Lack of stability and reusability are the main drawbacks associated with their use. Also, biological receptors are labile, expensive and it is difficult to obtain and prepare them. Hence, there have been attempts to synthesize specific recognition elements as an alternative to bio-receptors.

Synthetic recognition layers are primarily developed using molecular imprinting technique, where specific recognition sites for a target molecule are easily molded in synthetic polymer networks. The technique is based on the formation of a complex between the template (analyte) and a functional monomer in presence of a cross-linker. After polymerization, when the template is removed it leaves behind specific recognition sites in the polymer matrix that are complementary in shape, size and chemical functionality to the template molecule. Thus, the molecularly imprinted polymers (MIPs) display high affinity to the template molecules and bind them selectively. MIPs have gained wide acceptance as new molecular recognition materials since they are less expensive, more stable, robust, temperature and pressure resistant, and can be easily tailored as compared to the biological receptors. Integration of MIP-based recognition elements with sensors is usually achieved by either in situ polymerization on the surface of transduction platform or by deposition onto the transducer surface as thin films. A number of

MIPs have been prepared to suit a variety of templates and used in immunoassays, chemical sensors and biosensors. The technology has been implemented to electrochemically detect and quantify few antimalarial drugs, as discussed above. A MIP film was created on GCE surface using free radical polymerization method for determination of Qn[58]. Kamel *et al* built MIPs based potentiometric sensors for flow injection analysis of Qn and DC[71,140]. A thin sol-gel film of MIPs was electrodeposited onto the surface of MWNT decorated gold electrode to fabricate an electrochemical sensor for selective determination of clindamycin[124]. DC imprinted polypyrrole modified electrodes were formed on PGE and successfully used to determine the drug[135]. ARN-imprinted membranes were polymerized on the surface of graphene modified GCE for sensitive analysis of ARN[140]. Owing to their compatibility to highly complex matrices, MIPs have gained an increasing interest in the analysis of drugs and for biological estimations.

5. Sample Preparation

The need for drug analysis in various biological fluids (serum, plasma and urine etc.) and pharmaceutical formulations is an important criteria for pharmacokinetic studies, investigation of therapeutic and toxic effects of the drug, and to determine the drug's physiological performance. Matrices of biological fluids and pharmaceutical products are complicated, containing a number of compounds such as proteins, acids, bases and organic compounds that may interfere in the analysis. Moreover, the analytes are usually present in low quantity in biological samples. Hence, sample preparation is of key importance in order to properly isolate the desired analyte from complex matrices since most of the analytical instruments cannot analyse the compound from the matrix with extreme specificity. The basic concept of sample-preparation methods is to convert a real matrix into a sample suitable for analysis. The procedure is expected to be fast, cheap, convenient, remove coexisting potential interfering components and able to recover a good amount of the analyte from the matrix with minimal sample loss. Various sample pre-treatments and extraction techniques have been employed for

the determination of antimalarial dugs using different techniques. Human blood serum and plasma were mainly found to be extracted by solid phase extraction or liquid-liquid extraction, directly. Majority of the analytical techniques reported for determination of antimalarials involve chromatography method, where sample preparation is a prerequisite step for effective analysis of the drug in real samples. The present review focusses on electroanalytical methods for determination of antimalarial drugs. These methods are simple and do not involve lengthy, tedious and time-consuming sample preparation and extraction processes. Pharmaceutical formulation samples were directly analysed after dissolving in water or any other solvent, which was sometimes followed by filtration[47,55,57,59]. Human serum and plasma samples were usually centrifuged to precipitate the proteins and then diluted with the buffer solution before carrying out the analysis[46,76,104,106]. For urine, a simple dilution is applied as a pre-extraction step, which is often be the only step performed[57,76,104]. Rarely, centrifugation of urine was done as a sample pretreatment step.[106] No pretreatment step was required for analysis of amodiaquine in breast milk using hemin based electrochemical sensor[81].

6. Current challenges and future perspectives

Last two decades witnessed a sharp rise in electroanalytical methods for antimalarial drug analysis, particularly for determination of CQ, Qn, ARN, ARTS, CM and DC. However, there were limited publications with respect to electrochemical analysis of MQ, PQ, DHA, PG, SD and PYM. PRQ and ATQ still remain unexplored electroanalytically. Thus, there is a need for substantial electrochemical study and determination of these drugs for effective analysis in various real samples. Though significant progress was observed in voltammetric determination of different antimalarial drugs with excellent sensitivity and selectivity, the analytical applicability of the developed sensors mainly remained restricted to their use in pharmaceutical formulations. Very few voltammetric methods and only one potentiometric method were evaluated to check their feasibility for analysis of the target drug in biological fluids. Thus, there is still a dearth of efficacious electroanalytical techniques that determine antimalarial drugs in

human body fluids, especially blood serum and plasma. Hence, the current challenge is to develop electrochemical sensors that determine the drugs in biological samples in order to enhance the utility of the technique for routine clinical analysis.

Considering the constant need for portable instruments for screening in a cost-effective and clinically pertinent manner, the construction of miniaturized small sensors would further extend their applicability. Thus, the possibility of commercialization suggests a promising future for development of commercially-available electrochemical sensors for analysis of antimalarial drugs for field use.

7. Conclusion

The present review investigates the electrochemical techniques for determination of antimalarial drugs revealing the current status and trends in their development. The prominent voltammetric and potentiometric methods used to quantify the drugs in complex matrices, such as biological fluids, pharmaceutical formulations, plant extracts and different kinds of drinks including milk, are discussed. Voltammetric techniques were observed to be more predominantly used as compared to the potentiometric ones. Various electrode materials, especially nano-dimensional, were employed to modify the electrode surface and improve the selectivity and sensitivity of the electrochemical sensor. Use of conducting polymers, nanomaterials and presence of surfactants significantly amplified the electrochemical signal achieving a lower limit of detection (upto as low as picomolar range) in antimalarial drug assays. It is expected that the information provided in the review would aid in development of improved electrochemical sensors for sensitive and selective determination of antimalarial drugs, particularly in real samples.

Acknowledgement

The author (N. T.) is thankful to the Nanotechnology Platform, University of KwaZulu-Natal (UKZN) and College of Health Sciences, UKZN, Durban, South Africa for providing financial support.

References

1 World Health Organization, Malaria Fact sheet N° 94, 2015, http://www.who.int/mediacentre/factsheets/fs094/en/ (Accessed on 4 December, 2015).

2 N. Tangpukdee, C. Duangdee, P. Wilairatana and S. Krudsood, *Korean. J. Parasitol*., 2009, **47,** 93-102.

3 S. Yeung, W. Pongtavornpinyo, I.M. Hastings, A.J. Mills and N.J. White, *Am. J. Trop. Med. Hyg.*, 2004, **71**, 179-186.

4 O.N. Adedeji, O.O. Bolaji, C.O. Falade, O.A. Osonuga and O.G. Ademowo, *Antimicrob. Agents Chemother*., 2015, **59**, 5114-5122.

5 V.F. Samanidou, E.N. Evaggelopoulou and I.N. Papadoyannis, *J. Pharm. Biomed. Anal.*, 2005, **38**, 21-28.

6 A. Lawal, R.A. Umar, M.G. Abubakar and U.Z. Faruk, *Int. J. Chem. Tech. Res*., 2012, **4**, 669-676.

7 P. Singhal, A. Gaur, A. Gautam, B. Varshney, J. Paliwal and V. Batra, *J. Chromatogr. B Analyt. Technol. Biomed. Life Sci.*, 2007, **859**, 24-29.

8 C.Z. Liu, H.Y. Zhou and Y. Zhao, *Anal. Chim. Acta*, 2007, **581**, 298-302.

9 U. Hellgren, T. Villen and O. Ericsson, *J. Chromatogr.*, 1990, **528**, 221-227.

10 K. Govender, L. Gibhard, L. Du Plessis and L. Wiesner, *J. Chromatogr. B Analyt. Technol. Biomed. Life Sci.*, 2015, **985**, 6-13.

11 M.T. Koesdjojo, Y. Wu, A. Boonloed, E.M. Dunfield and V.T. Remcho, *Talanta*, 2014, **130**, 122-127.

12 B.N. Divya, N. Shetty and S. Samshuddin, *J. Chem. Pharm. Res.*, 2012, **4**, 1647-1653.

13 D.J. Bell, S.K. Nyirongo, M.E. Molyneux, P.A. Winstanley and S.A. Ward, *J. Chromatogr. B Analyt. Technol. Biomed. Life Sci.*, 2007, **847**, 231-236.

14 O.A. Farghaly, R.S. Abdel Hameed and A.A.H. Abu-Nawwas, *Int. J. Electrochem. Sci.*, 2014, **9**, 3287-3318.

15 M.M. Ghoneim, M.K. Abdel-Azzem, H.S. El-Desoky, A.M. Ghoneim and A.E. Khattab, *J. Braz. Chem. Soc*., 2014, **25**, 1407-1418.

16 N. Thapliyal, R.V. Karpoormath and R.N. Goyal, *Anal. Chim Acta*, 2015, **853**, 59-76.

17 Y.W. Shaojun Dong, *Electroanalysis*, 1989, **1**, 99-106.

18 L. Yang, L. Zou, G. Li and B. Ye, *Talanta*, 2016, **147**, 634-640.

19 P.K. Brahman, N. Pandey, S. N. Topkaya and R. Singhai, *Talanta*, 2015, **134**, 554-559.

20 R.R. Chillawar, K.K. Tadi and R.V. Motghare, *J. Anal. Chem*., 2015, **70**, 399-418.

21 A. Lewenstam, *Electroanalysis*, 2014, **26**, 1171-1181.

22 E. Bakker and E. Pretsch, *Angew. Chemie*, 2007, **46**, 5660-5668.

23 J.S Rana, J. Jindal, V. Beniwal and V. Chhokar, *J. Am. Sci*., 2010, **6**, 353-375.

24 O. Walker, A.H. Dawodu, A.A. Adeyokunnu, L.A. Salako and G. Alvan, *Br. J. Clin. Pharmacol.*, 1983, **16**, 701-705.

25 L.L. Gustafsson, B. Lindstrom, A. Grahnen and G. Alvan, *Br. J. Clin. Pharmacol.*, 1987, **24**, 221-224.

26 C.B. Braga, A.C. Martins, A.D.E. Cayotopa, W.W. Klein, A.R. Schlosser, A.F. da Silva, M.N. de Souza, B.W. B. Andrade, J.A. Filgueira-Junior, W.deJ. Pinto and M. da Silva-Nunes, *Interdiscip. Perspect. Infect. Dis.*, 2015, **2015**, 346853/1-346853/7.

27 J. Achan, A.O. Talisuna, A. Erhart, A. Yeka, J.K. Tibenderana, F.N. Baliraine, P.J. Rosenthal and U. D'Alessandro, *Malar. J*., 2011, **10**, 144/1-144/12.

28 World Health Organization, Guidelines for the Treatment of Malaria, April 2015, http://apps.who.int/iris/bitstream/10665/162441/1/9789241549127_eng.pdf?ua=1&ua=1(Accessed on 4 December, 2015).

29 D.E. Schwartz, G. Eckert and J. M. Ekue, *Chemotherapy*, 1987, **33**, 305-308.

30 H. Jewell, J.L. Maggs, A.C. Harrison, P.M. O'Neill, J.E. Ruscoe and B.K. Park, *Xenobiotica*, 1995, **25**, 199-217.

31 G.W. Mihaly, S.A. Ward, G. Edwards, M.L. Orme and A.M. Breckenridge, *Br. J. Clin. Pharmacol*., 1984, **17**, 441-446.

32 J. Tarning, T. Singtoroj, A. Annerberg, M. Ashton, Y. Bergqvist, N.J. White, N.P. Day and N. Lindegardh, *J. Pharm. Biomed. Anal*., 2006, **41**, 213-218.

33 O.M. Minzi, I.A. Marealle, S. Shekalaghe, O. Juma, E. Ngaimisi, M. Chemba, M. Rutaihwa, S. Abdulla and P. Sasi, *Malar. J.*, 2013, **12**, 174/1-174/8.

34 A. Djimde and G. Lefevre, *Malar. J.*, 2009, **8**, S4/1-S4/8..

35 T.K. Dien, P.J. de Vries, N.X. Khanh, R. Koopmans, L.N. Binh, D.D. Duc, P.A. Kager and C.J. van Boxtel, *Antimicrob. Agents Chemother*., 1997, **41**, 1069-1072.

36 K.M. Matar, A.I. Awad and S.B. Elamin, *Am. J. Trop. Med. Hyg*., 2014, **90**, 1087-1093.

37 K. Na Bangchang, J. Karbwang, C.G. Thomas, A. Thanavibul, K. Sukontason, S.A. Ward and G. Edwards, *Br. J. Clin. Pharmacol*., 1994, **37**, 249-253.

38 P. Tan-ariya, K. Na-Bangchang, R. Ubalee, A. Thanavibul, P. Thipawangkosol and J. Karbwang, *Southeast Asian J. Trop. Med. Public Health*, 1998, **29**, 18-23.

39 A.A. Somogyi, H.A. Reinhard and F. Bochner, *Br. J. Clin. Pharmacol*., 1996, **41**, 175-179.

40 A. Le Liboux, H. Duquesne, G. Montay, D. Chassard, E. Pichard, J.J. Thebault, A. Frydman and J. Gaillot, *Eur. J. Drug Metab.Pharmacokinet.*,1991, **3**, 284-290.

41 H. Xie, H. Chen, Y. Hu, S. Xu, Q. He, J. Liu, W. Hu and Z. Liu, *Am. J. Nephrol.*, 2013, **38**, 179-183.

42 K.N. Agwuh and A. MacGowan, *J. Antimicrob. Chemother*., 2006,**58**, 256-265.

43 G.L. Nixon, D.M. Moss, A.E. Shone, D.G. Lalloo, N. Fisher, P.M. O'Neill, S.A. Ward and G.A. Biagini, *J. Antimicrob. Chemother*., 2013, **68**, 977-985.

44 L.W. Kitchen, D.W. Vaughn and D.R. Skillman, *Clin. Infect. Dis.*, 2006, **43**, 67-71.

45 V.R. Solomon and H. Lee, *Eur. J. Pharmacol*., 2009, **625**, 220-233.

46 A. Radi, *Talanta*, 2005,**65**, 271-275.

47 M.H. Mashhadizadeh and M. Akbarian, *Talanta*, 2009,**78**, 1440-1445.

48 V.V. Cosofret and R.P. Buck, *Anal. Chim. Acta*, 1985, **174**, 299-303.

49 S.S. Hassan and M.A. Ahmed, *J. Assoc. Off. Anal. Chem*., 1991, **74**, 900-905.

50 B. Saad, K. Kanapathy, M.N. Ahmad, A.H. Hussin and Z. Ismail, *Talanta*, 1991, **38**, 1399-1402.

51 B.Saad, M.Z. Zin, M. S. Jab, I.A. Rahman, M.I. Saleh and S. Mahsufi, *Anal. Sci*., 2005, **21**, 521-524.

52 P. Cettour-Rose, C. Bezençon,C. Darimont, J. le Coutre and S. Damak, *BMC Physiol.*, 2013, **13**, 1-11.

53 J. Thomas and H.P. Pietsch, *Lebensmittelindustrie*, 1990, **37**, 29-30.

54 C. Apetrei, M.L. Rodríguez-Méndez, V. Parra, F. Gutierrez and J.A. de Saja, *Sensors and Actuators B: Chem.*, 2004, **103**, 145-152.

55 X.M. Zhan, L.H. Liu and Z.N. Gao, *J. Solid State Electrochem*., 2011, **15**, 1185-1192.

56 S. Awasthi, A. Srivastava and M.L. Singla, *Synthetic Metals*, 2011, **161**, 1707-1712.

57 A. Geto, M. Amare, M. Tessema and S. Admassie, *Anal.Bioanal. Chem*., 2012, **404**, 525-530.

58 L. Liu, X. Tan, X. Fang, Y. Sun, F. Lei and Z. Huang, *Electroanalysis*, 2012, **24**, 1647-1654.

59 R.A. Dar, P.K. Brahman, S. Tiwari and K.S. Pitre, *Colloids Surf B Biointerfaces*, 2012, **98**, 72-79.

60 A.Alberich, N. Serrano, J.M. Díaz-Cruz, C. Ariño and M. Esteban, *J. Chem. Ed.*, 2013, **90**, 1681-1684.

61 Q. Zhang, Y. Huang, L. Guo, C. Chen, D. Guo, Y. Chen and Y. Fu, *New J. Chem*., 2014, **38**, 4600-4606.

62 D. Orata, Y. Amir, C. Nineza, D. Mbui and M. Mukabi, *IOSR J. Appl. Chem*., 2014, **7**, 81-89.

63 D. Orata, Y. Amir and C. Nineza, *IOSR J. Appl. Chem*., 2014, **7**, 56-72.

64 J. Kálmán, K. Toth and D. Küttel, *Acta Pharm. Hung.*, 1971, **41**, 267-272.

65 E.P. Diamandis and T.P. Hadjiioannou, *Anal. Chim. Acta*, 1981, **123**, 341-345.

66 J. Anzai, C. Isomura and T. Osa, *Chem. Pharm. Bull*., 1985, **33**, 236-241.

67 S.I. Obtemperanskaya, M.M. Buzlanova, I.V. Karandki, R. Shakhid and A.N. Kashin, *J. Anal. Chem*., 1996, **51**, 419-423.

68 B. Saad, Y. Bee-Leng and M.I. Saleh, *Lab. Robot.Autom*., 2000, **12**, 133-137.

69 B. Saad, Y. Bee-Leng, M.I. Saleh, I.A. Rahman and S.M. Mansor, *J. AOAC Int*., 2001, **84**, 1151-1157.

70 M.M. Zareh, E. Malinowska and K. Kasiura, *Anal. Chim. Acta*, 2001, **447**, 55-61.

71 A.H. Kamel and H.E. Sayour, *Electroanal*., 2009, **21**, 2701-2708.

72 L.A. Al Shatti, H.M. Marafie and A.F. Shoukry, *Am. J. App. Sci*., 2011, **8**, 116-123.

73 M. Cuartero, J.A. Ortuño, M.S. García and F. Martínez-Ortiz, *Electrochim. Acta*, 2012, **69**, 152-159.

74 R.L. Nevin*, Int. J. Parasitol.: Drugs Drug Resist*., 2014, **4**, 118-125.

75 P. Schlagenhauf, M. Adamcova, L. Regep, M.T. Schaerer and H.G. Rhein, *Malar. J.*, 2010, **9**, 357/1-357/15.

76 B. Uslu, B. Dogan, A. Sibel A., H.Y. Özkan and Y. Aboul-Enein, *Electroanal*., 2005, **17**, 1563-1570.

77 D.W. Mendenhall, T. Higuchi and L.A. Sternson, *J. Pharm. Sci*., 1979, **68**, 746-750.

78 C.C. Campbell, D. Payne, I.K. Schwartz and O.J. Khatib, *Am. J. Trop. Med. Hyg.*, 1983, **32**, 1216-1220.

79 L.N. Markham, E. Giostra, A. Hadengue, M. Rossier, M. Rebsamen and J. Desmeules, *Am. J. Trop. Med. Hyg.*, 2007, **77**, 14-15.

80 M.L.P.M. Arguelho, J.P.H. Alves, N.R. Stradiotto, V. Lacerda Jr., J.M. Pires and A. Beatriz, *Quim. Nova*, 2010, **33**, 1291-1296.

81 C.O. Valente, C.A.B. Garcia, J.P.H. Alves, M.V.B. Zanoni, N.R. Stradiotto and M.L.P. Arguelho, *ECS Transactions*, 2012, **43**, 297-304.

82 T.K. Malongo, B. Blankert, O. Kambu, K. Amighi, J. Nsangu and J.M. Kauffmann, *J. Pharm. Biomed. Anal.*, 2006, **41**, 70-76.

83 D. Fernando, C. Rodrigo and S. Rajapakse, *Malar. J.*, 2011, **10**, 351/1-351/12.

84 M.L.P.M. Arguelho, M.V. B. Zanoni and N.R. Stradiotto, *Anal. Lett.*, 2005, **38**, 1415-1425.

85 B.B. Saad, Z.A. Zahid, S.A. Rahman, M.N. Ahmad and A.H. Husin, *Analyst*, 1992, **117**, 1319-1321.

86 N. Gargano, F. Cenci and Q. Bassat, *Trop. Med. Int. Health*, 2011, **16**, 1466-1473.

87 Q. Bassat, *PLOS Negl. Trop. Dis*., 2011, **5**, e1325/1321-e1325/1310.

88 D. Orata, Y. Amir and C. Nineza, *J. Chem. Chem. Eng.* , 2014, **8**, 215-225.

89 F. Nosten and N.J. White, *Am. J. Trop. Med. Hyg.*, 2007,**77**, 181-192.

90 S. Krishna, A.C. Uhlemann and R.K. Haynes, *Drug Resist. Updat*., 2004, **7**, 233-244.

91 A. Fernandez-Martinez, P. Mula, P. Cravo, P. Charle, A. Amor, P. Ncogo, A. Benito and P. Berzosa, *Am. J. Trop. Med. Hyg.*, 2013, **88**, 43-47.

92 P.H. Yang, Z.J. Zhou and J.Y. Cai, *Coll. Surf. A: Physicochem. Eng. Aspects*, 2005, **257-258**, 467-472.

93 C. Debnath, E. Haslinger and A. Ortner, *Nat. Prod. Commun.*, 2006,**1**, 487-494.

94 C. Debnath, P. Saha and A. Ortner, *Electroanal.*, 2008, **20**, 1549-1555.

95 C. Debnath, P. Saha and A. Ortner, *Electroanal.*, 2009, **21**,657-661.

96 C. Debnath, A. Dobernig, P. Saha and A. Ortner, *J. Kor. Chem. Soc.*, 2011, **55**, 57-62.

97 F. C. Gong, Z. D. Xiao, Z. Cao and D. X. Wu, *Talanta*, 2007,**72**, 1453-1457.

98 X. Yang, T. Gan, X. Zheng, D. Zhu and K. Wu, *Bull. Kor. Chem. Soc.*, 2008, **29**, 1386-1390.

99 J.R.M. Reys, P.R. Lima, A.G. Cioletti, A.S. Ribeiro, F. Caxico de Abreu, M.O.F. Goulart, and L.T. Kubota, *Talanta*, 2008, **77**, 909-914.

100 P. Phukon, K. Radhapyari, B.K. Konwar and R. Khan, *Mater. Sci. Eng. C*, 2014, **37**, 314-320.

101 H.Bai, C. Wang, J. Chen, J. Peng and Q. Cao, *Biosens. Bioelectron.*,2015, **64**, 352-358.

102 Q. Li and P. Weina, *Pharmaceuticals*, 2010, **3**, 2322-2332.

103 A.K. Das, *Ann. Med. Health Sci. Res*., 2015, **5**, 93-102.

104 R. Jain and Vikas, *Coll. Surf. B: Biointerf*., 2011, **88**, 729-733.

105 R. Jain and Vikas, *Chem. Sens*., 2011, **1**, 15/11-15/18.

106 K. Radhapyari, P. Kotoky, M.R. Das and R. Khan, *Talanta*, 2013, **111**, 47-53.

107 L. Cui and X.Z. Su, *Expert Rev. Anti. Infect. Ther*., 2009, **7**, 999-1013.

108 Y. Chen, *J. Electrochem. Soc*., 1997, **144**, 1891-1894.

109 C. Debnath, E. Haslinger, W. Likussar and A. Michelitsch, *J. Pharm. Biomed. Anal*., 2006, **41**, 638-643.

110 H. Wang, P. Yang, S. Liang and J. Cai, *Yaowu Fenxi Zazhi*, 2010,**30**, 431-434.

111 A. Saifi, *Afr. J. Pharm. Pharmacol*., 2013, **7**, 148-156.

112 S. Waxman and V. Herbert, *New Eng. J. Med*., 1969, **280**, 1316-1319.

113 G.T. Strickland and J.E. Kostinas, *Am. J. Trop. Med. Hyg.*, 1970, **19**, 910-915.

114 J.E. Hyde, *Acta Tropica*, 2005, **94,** 191-206.

115 F. Vicente-Pedros, F. Tomas-Vert and J. Vera-Sanchez, *J. Pharm. Sci*., 1984, **73**, 1804-1806.

116 S. Smarzewska, S. Skrzypek and W. Ciesielski, *Electroanalysis*, 2012, **24**, 1966-1972.

117 A. Nzila, *J. Antimicrob. Chemother.*, 2006, **57**, 1043-1054.

118 A. E. Radi, H.M. Nassef and M.I. Attallah, *Anal. Methods*, 2015, **7**, 4159-4167.

119 J. Ddík, M. Janovcová, H. Dejmková, J.Barek and K.Pecková, *Sensing Electroanal.,* 2011, **6**, 129-138.

120 M.U. Ahmed, M.M. Hossain, M. Safavieh, Y.L. Wong, I.A. Rahman, M. Zourobd and E. Tamiya, *Crit Rev Biotechnol*., 2016, **36**, 495-505.

121 H.M. Mohamed, TrAC Trends Anal. Chem., 2016, DOI:10.1016/j.trac.2016.02.010.

122 S.U. Ambalkar, R.L. Bakal, A.P. Dewani and A.V. Chandewar, *Int. J. Drug Form. Res*., 2013, **4**, 26-44.

123 N. Thammasoontaree, P. Rattanarat, N. Ruecha, W. Siangproh, N. Rodthongkum, O. Chailapakul, *Talanta*, 2014, **123**, 115-121.

124 S. Yao, J. Shiao and L. Nie, *Talanta*, 1987, **34**, 977-982.

125 M. Smieja, *Can. J. Infect. Dis*., 1998, **9**, 22-28.

126 P. Norouzi, B. Larijani, M. Ezoddin and M.R. Ganjali, *Mater. Sci. Engg. C*, 2008, **28**, 87-93.

127 Z. Zhang, Y. Hu, H. Zhang and S. Yao, *J. Coll. Interfac. Sci*., 2010, **344**, 158-164.

128 I.H.I. Habib, M. S. Rizk and Th.R. El-Aryan, *Pharm. Chem. J*., 2011, **44**, 705-710.

129 K.R. Tan, A.J. Magill, M.E. Parise and P.M. Arguin, *Am. J. Trop. Med. Hyg*, 2011, **84**, 517-531.

130 E. van den Enden, *Expert Opin. Pharmacother*., 2009, **10**, 435-451.

131 S. Chodosh, J. Tuck and D. Pizzuto, *Scand. J. Infect. Dis. Suppl*., 1988, **53**, 22-28.

132 J. Wang, T. Peng and M. S. Lin, *Bioelectrochem. Bioenerg*., 1986, **15**, 147-156.

133 W. Oungpipat, P. Southwell-Keely and P. W. Alexander, *Analyst*, 1995, **120**, 1559-1565.

134 N. Wangfuengkanagul, W. Siangproh and O. Chailapakul, *Talanta*, 2004, **64**, 1183-1188.

135 T. Charoenraks, S. Palaharn, K. Grudpan, W. Siangproh and O. Chailapakul, *Talanta*, 2004, **64**, 1247-1252.

136 L.G. Shaidarova, A.V. Gedmina, I.A. Chelnokova and G.K. Budnikov, *Pharm. Chem. J.*, 2008,**42**, 545-549.

137 F. Conzuelo, M. Gamella, S. Campuzano, A.J. Reviejo and J.M. Pingarron, *Anal. Chim. Acta*, 2012, **737**, 29-36.

138 B. Gurler, S.P. Ozkorucuklu and E. Kir, *J. Pharm. Biomed. Anal*., 2013, **84**, 263-268.

139 A.F. Shoukry and S.S. Badawy, *Microchem. J*., 1987, **36**, 107-112.

140 M. Pekli-Novak, Anita Nagy and G. Nagy, *Bioelectroanal*., 1993, **2**, 411-416.

141 M. Pekli-Novak, Anita Nagy and G. Nagy, *Magyar Kemiai Folyoirat*, 1995, **101**, 12-16.

142 X.X. Sun and H.Y. Aboul-Enein, *Talanta*, 2002, **58**, 387-396.

143 A.H. Kamel, F.T.C. Moreira and M.G. F. Sales, *Sens. Lett*., 2011, **9**, 1654-1660.

144 Y.M. Issa, H.M. Abdel-Fattah and N.B. Abdel-Moniem, *Int. J. Electrochem. Sci*., 2013, **8**, 9578-9592.

145 R.J. Maude, C. Nguon, A.M. Dondorp, L.J. White and N.J. White, *Malar. J.*, 2014, **13**, 380/1-380/8.

CHAPTER 3

A Simple, Efficient and Ultrasensitive Gold Nanourchin Based Electrochemical Sensor for the Determination of an Antimalarial Drug: Mefloquine

Tirivashe Elton Chiwunze, Neeta Bachheti Thapliyal[#], Venkata Narayana Palakollu, Rajshekhar Karpoormath*

[a] Department of Pharmaceutical Chemistry, Discipline of Pharmaceutical Sciences, College of Health Sciences, University of KwaZulu-Natal (Westville), Durban-4000, South Africa.

Graphical Abstract

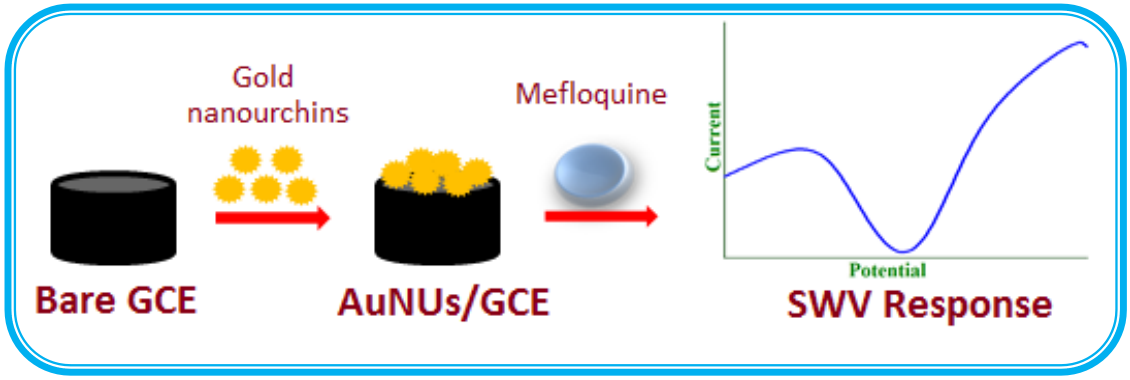

**Corresponding Author

Dr. Rajshekhar Karpoormath

Tel: + 27-312607179, Fax: + 27-312607792

Email: karpoormath@ukzn.ac.za

Full Paper Wiley Online Library ELECTROANALYSIS

DOI: 10.1002/elan.201700154

A Simple, Efficient and Ultrasensitive Gold Nanourchin Based Electrochemical Sensor for the Determination of an Antimalarial Drug: Mefloquine

Tirivashe Elton Chiwunze,[a] Neeta Bachheti Thapliyal+,[a] Venkata Narayana Palakollu,[a] and Rajshekhar Karpoormath*[a]

Abstract: Mefloquine (MQ) is a quinoline based antimalarial drug, which is potent against multiple drug-resistant *Plasmodium falciparum*. It is widely prescribed for the prophylactic treatment of malaria. Due to extensive usage of MQ, constant monitoring of the drug level in human body is of paramount importancein order to ensure that optimum drug exposure is achieved. The present work describes a gold nanourchins (AuNUs) based electrochemical sensor for the determination of MQ.AuNUs were synthesized via seed-mediated method and characterized using ultraviolet-visible spectroscopy, energy-dispersive X-ray spectroscopy, field emission scanning electron microscopy, zeta-sizer and electrochemical techniques (electrochemical impedance spectroscopy and cyclic voltammetry). Fabrication of the sensor was done by drop-coating the synthesized AuNUs onto a glassy carbon electrode. The fabricated sensor exhibited enhanced voltammetric response, which was attributed to the excellent conductivity and high surface area of AuNUs. Under optimum square wave voltammetric conditions, the sensor displayed two linear response ranges (from 2.0×10^{-9} to 1.0×10^{-6} M and from 1.0×10^{-6} to 1.0×10^{-3} M) with a detection limit of 1.4 nM. The electrode demonstrated good reproducibility, stability and selectivity over common interferents. The utility of the sensor was successfully assessed for quantification of the drug in pharmaceutical preparation and spiked human urine sample. Thus, the present study demonstrates a promising approach for determination of MQ with practical utility in quality control and clinical analysis.

Keywords: Mefloquine · Gold nanourchins · Square wave voltammetry · Pharmaceuticalpreparation · Human urine

Abstract

Mefloquine (*MQ*) is a quinoline based antimalarial drug, which is potent against multiple drug-resistant *Plasmodium falciparum.* It is widely prescribed for the prophylactic treatment of malaria. Due to extensive usage of MQ, constant monitoring of the drug level in human body is of paramount importance in order to ensure that optimum drug exposure is achieved. The present work describes a gold nanourchins (AuNUs) based electrochemical sensor for the determination of MQ. AuNUs were synthesized via seed-mediated method and characterized using ultraviolet-visible spectroscopy, energy-dispersive X-ray spectroscopy, field emission scanning electron microscopy, zeta-sizer and electrochemical techniques (electrochemical impedance spectroscopy and cyclic voltammetry). Fabrication of the sensor was done by drop-coating the synthesized AuNUs onto a glassy carbon electrode. The fabricated sensor exhibited enhanced voltammetric response, which was attributed to the excellent conductivity and high surface area of AuNUs. Under optimum square wave voltammetric conditions, the sensor displayed two linear response ranges (from 2.0 x 10^{-9} to 1.0 x 10^{-6} M and from 1.0 x 10^{-6} to 1.0 x 10^{-3} M) with a detection limit of 1.4 nM. The electrode demonstrated good reproducibility, stability and selectivity over common interferents. The utility of the sensor was successfully assessed for quantification of the drug in pharmaceutical preparation and spiked human urine sample. Thus, the present study demonstrates a promising approach for determination of MQ with practical utility in quality control and clinical analysis.

Keywords

Mefloquine; Gold nanourchins; Square wave voltammetry; pharmaceutical preparation; human urine.

1. Introduction

Malaria is a life-threatening parasitic infection, which is typically transmitted to humans through infected mosquitoes. According to World Health Organization (WHO), approximately 214 million cases of the disease resulting in 4,38,000 deaths were estimated in 2015, with most of the related deaths reported among children residing in Africa [1]. Pregnant women, older adults and immunocompromised individuals also show high probability of contracting the disease. Besides, travelers to the endemic area are also at higher risk since they lack the naturally acquired immunity present in indigenous people, rendering the need for prophylactic treatment imperative. Malaria is caused by a single-celled *Plasmodium* parasite with its five species (namely, *P. falciparum, P. ovale, P. vivax, P. knowlesi and P.malariae*) affecting the human race. Among these species, *P. falciparum* is the most common and responsible for maximum malaria-related deaths globally [2]. Prompt diagnosis and treatment remarkably lowers the morbidity and mortality rate associated with the disease. Antimalarial drugs play a crucial part in treating malaria, reducing transmission of the disease and controlling the proliferation of drug-resistant infecting species. Mefloquine (MQ; chemically known as [(2, 8-bis(trifluoromethyl)quinolin-4-yl]-(2-piperidyl)methanol; Figure 1) is a 4-methanol quinoline based antimalarial drug developed in the 1970s [3]. The drug possesses blood schizonticidal properties. It is a good prophylactic as well and can be safely consumed during all the three stages of pregnancy [4]. MQ is also effective against malaria parasites resistant to chloroquine. Though the mechanism of MQ action is not very clear, it seems to concentrate inside the acidic food vacuole of the parasite where it interferes with the digestion of haemoglobin. This inhibits the process of haem polymerization, thus facilitating an aggregation of cytotoxic haem which eventually kills the parasite. Though well tolerated, the drug is sometimes associated with

cardiovascular, gastrointestinal and neuropsychiatric disturbances [5-7]. Other side effects of the drug include muscle pain, dizziness headache, fever and skin rash [8-10]. When administered orally, the blood peak concentration is reached within 2-12 hours. The drug is metabolized in the liver and approximately 9% of the unchanged drug is excreted in urine.

In pharmaceutical research sector, the analytical study of bulk drug materials, intermediates, drug products and commercial formulations, as well as analysis of biological samples that contain the drugs and their metabolites is of extreme significance. Quantitative analysis of drugs in marketed formulations is also important to detect counterfeiting of medicines, especially in African countries where the markets are flooded with substandard and fake medicines. Owing to its therapeutic importance, determination of MQ in pharmaceutical preparations and human body fluids is of considerable significance in both quality control of preparations and clinical analysis. Thus, it is imperative to develop cheap, robust and accurate analytical methods for quantitative analysis of the antimalarial drug. Various methods have been developed for MQ determination, such as spectrophotometric, chromatographic, electrochemical and fluorometric methods [11-16]. Among these, the voltammetric methods are well known for detection of various organic and inorganic compounds on account of their high selectivity, sensitivity and reliability at a low cost with the instrumentation having a potential for miniaturization and automation [17, 18]. Additionally, the voltammetric techniques are characterized by extremely low detection limit and do not require tedious extraction or sample preparation processes for analysis of real samples. However, to date, only one voltammetric study has been reported for quantification of the drug where the electroreduction behavior and quantification of MQ was studied at a hanging mercury drop electrode [15]. Mercury electrodes are associated with several disadvantages such as contamination, risk of poisoning and disposal of metallic mercury.

Hence, the need to develop a more sensitive, selective, accurate and environment-friendly electroanalytical method for analysis of MQ is of great significance.

Nanotechnology has brought to the fore various nanomaterials and nanoparticles that can be utilized for the development of sensors and biosensors [19, 20]. Over the past decades, carbon and metallic nanoparticles have dominated the application of nanomaterials in electrochemistry. The modification of conventional electrodes with nanoparticles has attracted a great deal of interest among researchers since it conveys tunable physical, electronic and catalytic properties of the nanoparticles to the electrode surface [21]. Among various nanoparticles, gold nanoparticles (AuNPs) are one of the most frequently used with diverse applications, such as sensory probes, therapeutic agents, biomarkers and drug delivery. Gold AuNPs have also revealed great potential application in the field of electroanalysis due to their stable physical and chemical properties, high surface area, excellent conductivity, biocompatibility and catalytic activity. [22-27]. In particular, it is the small size of gold nanoparticles (AuNPs) that facilitate the conductive materials to come closer during an electrochemical process thus providing electrocatalytic activity that is used in sensor devices. They improve the electron transfer rate and increase the surface area of modified electrodes providing sensitive and selective systems for the electrochemical detection of various analytes [28, 29]. Thus, AuNPs are considered as ideal candidates for constructing electrochemical sensors. In recent years there have been a number of reports of new AuNPs variants that exhibit more and enhanced properties [30-32]. One such AuNP variant is the urchin-shaped gold nanoparticle, commonly known as gold nanourchins (AuNUs), that show higher electrocatalytic activity and sensitivity [33-35]. This is attributed to the urchin-like morphology of AuNUs having spikes coming out of their surface. Such kind of structure endows them with high surface to volume ratio resulting in more active surface area. These properties of urchins bestow them to have a wide range of applications in optics, catalysis, batteries, gas and biomolecules sensing [30, 36, 37].

The present work describes the first time use of AuNUs modified electrode for voltammetric determination of MQ, an antimalarial drug. Thus, the novelty of the work lies in the use of AuNUs as an electrode modifier for determination of MQ. The developed electrochemical sensor was found to exhibit significant electrocatalytic activity towards MQ oxidation and was successfully evaluated for determination of the drug in pharmaceutical formulations and human urine.

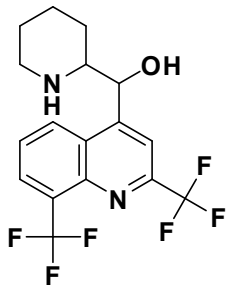

Fig. 1 Chemical structure of Mefloquine

2. Experimental

2.1 Materials

Mefloquine hydrochloride was provided by Cipla Ltd., Mumbai, India. Gold (III) chloride hydrate, silver nitrate, 3,4-dihydroxyphenylalanine (L-dopa) and trisodium citrate dihydrate were purchased from Sigma. Other chemicals employed were of analytical grade and used as received. The stock solution of MQ was freshly prepared in methanol daily prior to measurements to avoid any decomposition. Phosphate buffer solution (PBS) was prepared from 0.2 M Na_2HPO_4 and 0.2 M NaH_2PO_4, and employed as the supporting electrolyte. All aqueous solutions were prepared using double-distilled water.

2.2 Apparatus

The synthesis of AuNUs was confirmed by ultraviolet-visible (UV-Vis) spectral analysis. The absorbance spectrum of the suspension was monitored using UV-Vis spectroscopy (Varian spectrophotometer) in the wavelength range of 300-800 nm. The synthesized AuNUs were further characterized using field emission scanning electron microscopy (FE-SEM) (ZEISS FEGSEM Ultra Plus, Germany). The elemental composition of the nanourchins was assayed using the energy-dispersive X-ray spectroscopy (EDX) instrument connected to the FE-SEM microscope. The particle size distribution of AuNUs was determined using particle size analyzer (Zetasizer nano ZS, Malvern Instruments Ltd., U.K.). Cyclic voltammetry (CV), linear sweep voltammetry (LSV), square wave voltammetry (SWV) and electrochemical impedance spectroscopy (EIS) experiments were conducted using a CHI660E electrochemical workstation (CH Instruments, USA). A conventional three-electrode system was utilized throughout the experiments which comprised of a bare or modified glassy carbon electrode (GCE) as the working electrode, an Ag/AgCl reference electrode and a platinum counter electrode. All the three electrodes were purchased from CH Instruments, USA. The pH measurements were performed using EUTECH cyber scan pH 510 meter. The experiments were performed at room temperature (22 ± 3 °C).

The optimization of the SWV parameters was carried out in a 0.10 mM MQ solution by changing one parameter at a time while keeping the others constant. The influence of the experimental SWV parameters on the peak current value was investigated in the given corresponding ranges: square-wave frequency (f; 10 Hz to 50 Hz), square wave amplitude (a; 15 mV to 60 mV) and potential step (E; 3 mV to 6 mV). The observed optimum values for these parameters were: f=30 Hz, a=50 mV and E=4 mV.

2.3 Synthesis of AuNUs

AuNUs were synthesized according to the method reported by Xu et al [34]. Nanoseeds of silver were first prepared by adding 1% trisodium citrate dihydrate to rapidly boiling silver nitrate solution. 0.1 mL of the obtained silver nanoseeds were mixed to 1.0 mL of 12.0 mM DOPA solution, followed by addition of 1.0 mL of 5.0 mM $HAuCl_4$ solution. On gently shaking the mixture, a grey coloured homogenous solution is obtained which turned into a dark brown suspension after 5 minutes indicating the formation of AuNUs. The suspension was subjected to centrifugation at a speed of 5000 rpm for 5 min followed by washing with dil. HCl and double-distilled water thrice. The obtained AuNUs were then used to modify the electrode.

2.4 Fabrication of gold nanourchins modified electrode (AuNUs/GCE)

The GCE surface was carefully polished with 0.05 μm alumina on a microcloth pad to a mirror-like finish. It was then dipped in 0.2 M H_3PO_4 solution for two minutes followed by rinsing with double-distilled water to remove any adsorbed alumina particles from the electrode surface. 6.0 μL of the synthesized AuNUs suspension was dropped on the clean GCE surface and dried under an infrared lamp. The modified electrode (denoted as AuNUs/GCE) was then used for the electrochemical experiments.

For comparison studies, AuNPs modified electrode (AuNPs/GCE) was also fabricated. The AuNPs used were prepared by citrate reduction method, as reported in literature [38].

2.5 Sample preparation

A commercially available MQ tablet (Mefliam) containing 250 mg of Mefloquine hydrochloride was finely powdered using mortar and pestle. The powder was then transferred to a volumetric flask and dissolved in methanol. The proposed SWV

procedure was applied to determine MQ in the pharmaceutical formulation by taking a suitable diluted aliquot of the prepared solution (that falls within the linear concentration range) and conducting voltammetric analysis under similar conditions as used while conducting the concentration study.

Urine sample, collected from healthy laboratory personnel, was diluted 500 times with water in order to reduce the matrix effect. The sample was then spiked with a known amount of MQ solution for detection in the urine sample.

3. Results and discussion

3.1 Characterization of the synthesized AuNUs

The UV-vis absorption spectrum exhibited a single sharp absorption peak at 624 nm which confirmed the synthesis of AuNUs (Figure 2A) [39]. The surface morphology and elemental composition of the synthesized AuNUs were investigated using FE-SEM and EDX, respectively. Figure 2B depicts the presence of uniformly distributed spherical-shaped particles with “spikes” emerging out of their surface. The particles were found to possess an average size of 79.83 nm. The displayed urchin-like structure of the synthesized AuNUs is analogous to the surface texture of AuNUs reported in literature [34]. The EDX spectrum analysis exhibited a strong peak for gold atoms confirming the presence of gold (Figure 3C). The weaker signals indicate the presence of carbon, nitrogen, sodium, chlorine and silver atoms in extremely minute quantities. Figure 3D depicts the particle size analysis of AuNUs. The average particle size was found to be 83.09 nm, which is in accordance with the size of nanourchins observed using FE-SEM.

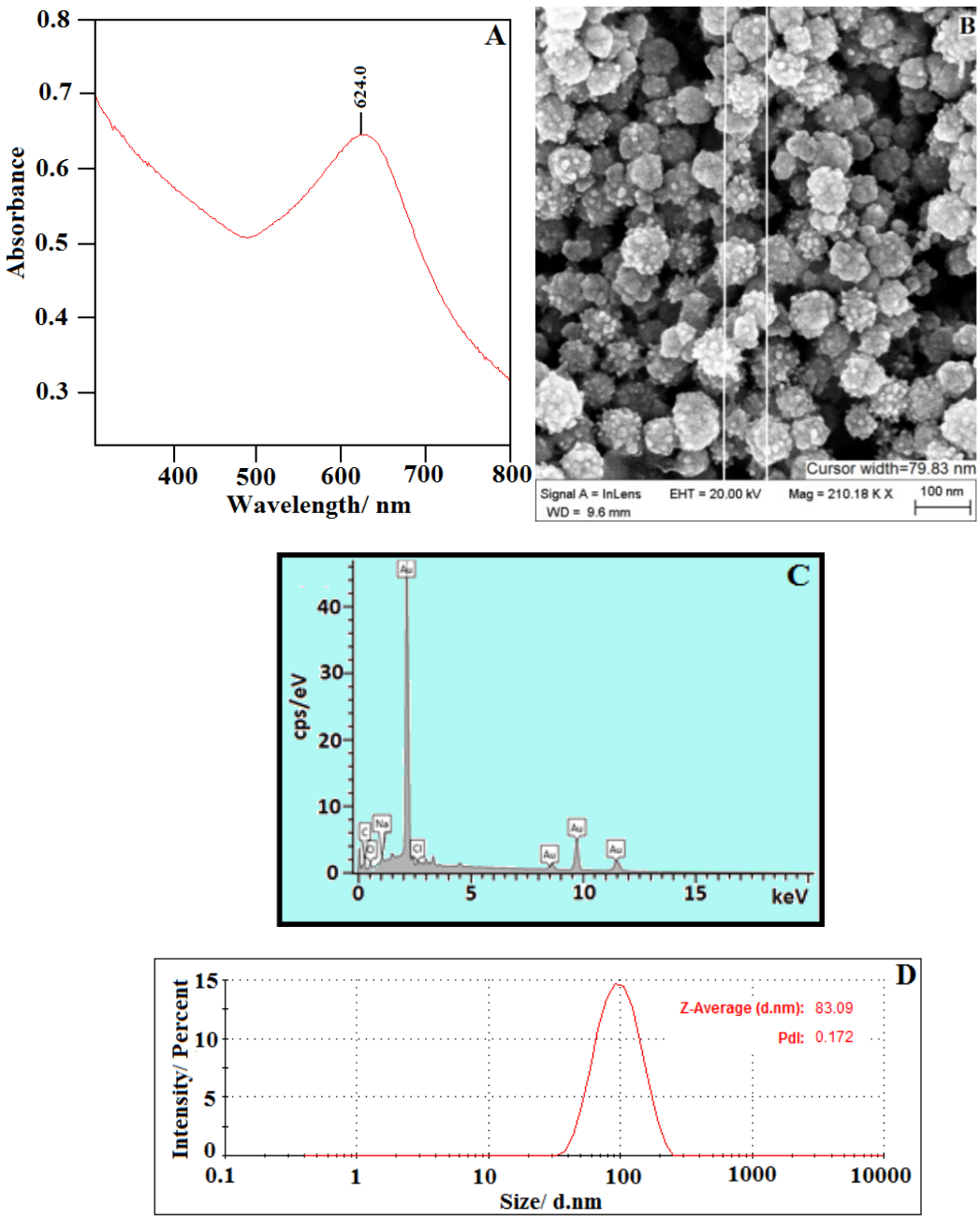

Fig. 2 (A) UV-visible spectra, (**B**) FE-SEM image at 100 nm magnification, (**C**) EDX image and (**D**) Particle size distribution of the synthesized gold nanourchins.

3.2 Electrochemical characterization

EIS technique was used for the electrochemical characterization of the electrodes (bare GCE, AuNPs/GCE and AuNUs/GCE) investigating their electron transfer properties. In EIS spectra, the Nyquist plot comprises of a semicircle at high frequency region. The diameter of the semicircle is equal to the interfacial charge transfer resistance (R_{ct}) [40,41]. Figure 3 depicts the EIS spectra recorded at bare GCE, AuNPs/GCE and AuNUs/GCE in the presence of 2.5 mM $[Fe(CN)_6]^{3-}/[Fe(CN)_6]^{4-}$ (1:1) in 0.1 M KCl. The measurements were taken in the frequency range of 1-10,000 Hz with an amplitude of 5 mV. The EIS data were fitted with a Randles equivalent circuit. A well-defined large semi-circle was observed at the bare electrode (R_{ct}=298.6 Ω). The semicircle was smaller at AuNPs/GCE (R_{ct}=102.1 Ω) and almost diminished when AuNUs/GCE was used (R_{ct}=39.83 Ω). This observation suggested that the R_{ct} values decreased and the diffusion of $[Fe(CN)_6]^{3-/4-}$ towards the electrode surface increased upon modification with nanosized gold particles. The good response of the modified electrodes is attributed to the excellent conductivity of gold. Further, since the R_{ct} value was the least at AuNUs/GCE, it is implied that AuNUs accelerate the electron transfer to a greater extent as compared to gold nanoparticles, which is anticipated to be due to higher surface area of AuNUs owing to its urchin-like morphology.

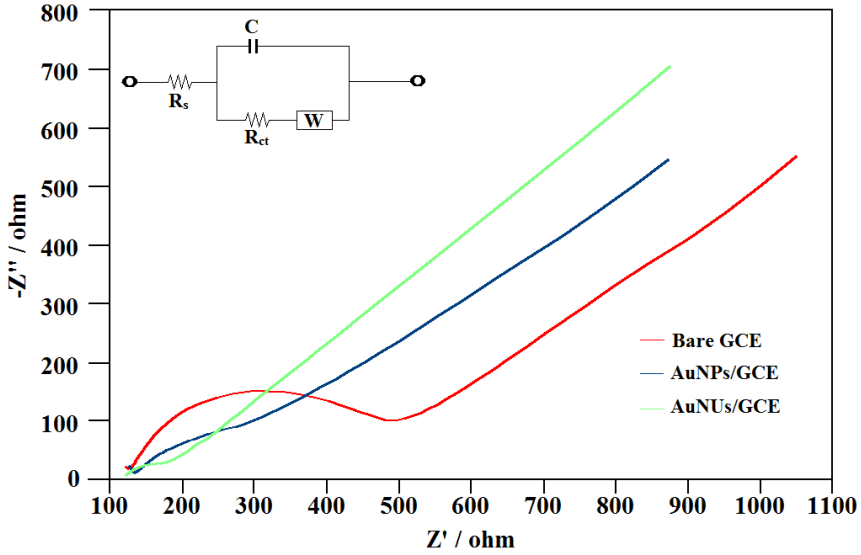

Fig. 3 Nyquist plot observed for the electrochemical impedance measurement in 2.5 mM $[Fe(CN)_6]^{3-/4-}$ at (a) bare GCE, (b) AuNPs/GCE and (c) AuNUs/GCE. The inset shows Randles equivalent circuit. (R_s, R_{ct}, C and W represents the resistance of the electrolyte solution, charge-transfer resistance, double layer capacitance and the Warburg impedance, respectively.).

The modified electrodes were further characterized by CV using $K_3[Fe(CN)_6]$ as the redox probe. Figure 4A shows the cyclic voltammograms of 5.0 mM $K_3Fe(CN)_6$ in 0.1 M KCl as the supporting electrolyte at bare GCE, AuNPs/GCE and AuNUs/GCE. Well-defined redox couple was observed at all the three electrodes. However, a significant increment in peak current (i_p) and a decrease in peak potential separation (ΔE_p) was noted for the modified electrodes in comparison to bare GCE. The best response was exhibited in presence of AuNUs/GCE. This superior electrocatalytic activity is ascribed to the higher surface area of AuNUs and hence more number of active sites for electron transfer. The effective surface area of the bare and modified electrodes was determined by measuring i_p observed for 5.0 mM $K_3[Fe(CN)_6]$ solution at various scan rates (Figure 4B) and using the Randles-Sevcik equation (Eq. 1).

$$Ip=2.68\text{x}10^5 n^{3/2} AD^{1/2} C\upsilon^{1/2} \qquad \text{(Eq.1)}$$

where i_p is defined as the peak current, n is the number of electrons involved in the charge transfer (n=1), A is the effective surface area of the electrode (in cm^2), D is the diffusion coefficient ($D=7.6\times10^{-6}$ cm^2s^{-1}), C in the concentration of $K_3[Fe(CN)_6]$ (mol cm^{-3}) and *v* is the scan rate (Vs^{-1}). The value of "A" was found to be 0.0265cm^2, 0.0339 cm^2 and 0.0536 cm^2 for bare GCE, AuNP/GCE and AuNUs/GCE, respectively. The results revealed that AuNUs/GCE exhibits the highest effective surface area, which was more than twice that of the bare GCE.

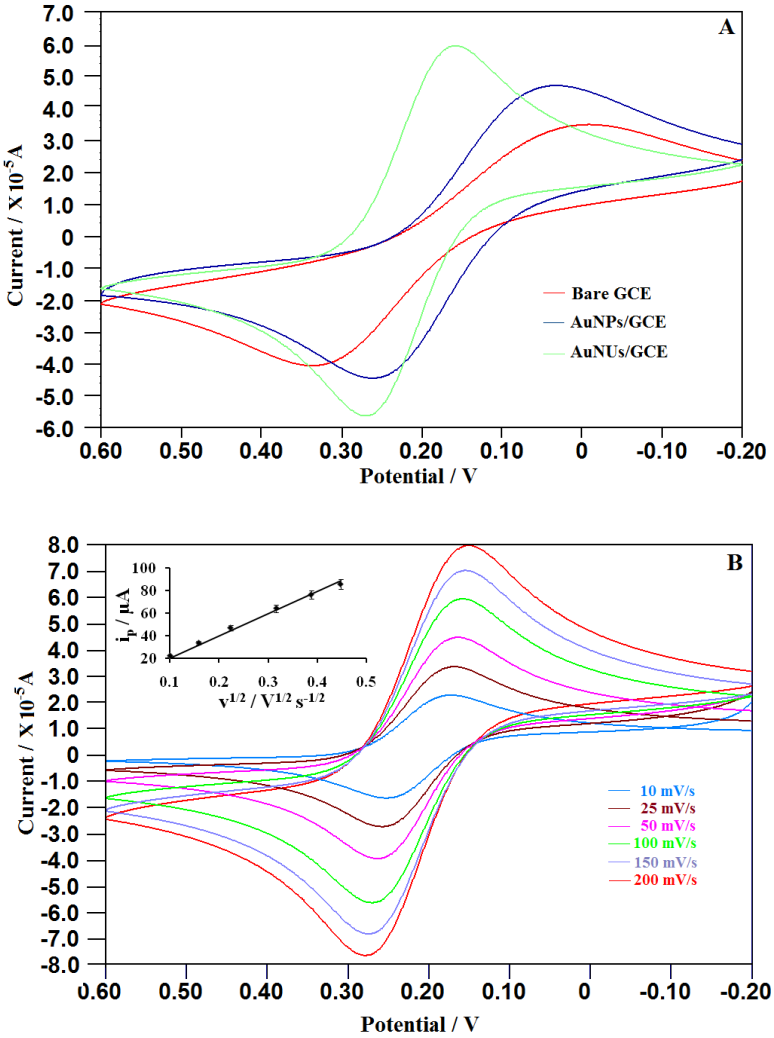

Fig. 4 (**A**) Cyclic voltammograms of 5.0 mM $K_3[Fe(CN)_6]$ in 0.1 M KCl solution at (a) bare GCE, (b) AuNPs/GCE and (c) AuNUs/GCE at 100 mV/s. (**B**) Cyclic voltammograms of 5.0 mM $K_3[Fe(CN)_6]$ in 0.1 M KCl solution at AuNUs/GCE at varying scan rates: (a) 10 (b) 25 (c) 50 (d) 100 (e) 150 (f) 200 mVs^{-1}. (Inset displays plot of peak current versus square root of scan rate.)

3.3 Electrochemical behavior of MQ at AuNUs/GCE

The electrochemical behavior of MQ was investigated at bare GCE, AuNPs/GCE and AuNUs/GCE using CV (Figure 5A). As can be seen from the figure, the bare electrode showed no response towards the antimalarial drug. However, under similar conditions, a small hump was observed at AuNPs/GCE at 1.10 V, which transformed to a well-defined oxidation peak at AuNUs/GCE. As expected, AuNUs/GCE gave a better response in comparison to AuNPs/GCE and hence, it was selected for further electrochemical studies. In order to examine the effect of scan rate on the voltammetric response of MQ, cyclic voltammograms were recorded with scan rates varying in the range 10-200 mVs^{-1}. As depicted in Figure 5B, the peak current (i_p) was found to have a linear correlation with the scan rate (v) suggesting that MQ electrooxidation process at AuNUs/GCE is adsorption-controlled [42]. This was further confirmed from the plot of log i_p versus log v (Figure 5C) where the slope was found to be 0.9249, which is close to the theoretical value of 1.0 for an ideal adsorption-controlled process [43].The peak potential (E_p) for an irreversible electrode process can be defined by the Laviron's equation as follows:

$$Ep = E° + \left(\frac{2.303RT}{\alpha nF}\right) Log \left(\frac{RTk°}{\alpha nF}\right) + \left(\frac{2.303RT}{\alpha nF}\right) Log\ \upsilon \qquad \text{(Eq. 2)}$$

where α is the electron transfer coefficient, k^0 is the standard rate constant of the surface reaction, $E^{0\prime}$ is the formal potential and the other symbols have their usual meanings [44]. A linear relationship was observed between E_p and log v (Figure 5D), which is represented by the equation E_p=0.0519log$v$ + 0.9717 (R^2=0.9889). Considering R=8.314 J/K mol, T=298 K and F=96480 C mol^{-1}, the value of αn was calculated. The Bard and Faulkner equation (Eq. 3) was then utilized to determine the value of α [45].

$$\alpha = \frac{47.7}{Ep - Ep_{1/2}} \qquad \text{(Eq. 3)}$$

where $E_{p1/2}$ is half of peak potential. The number of transferred electrons (n) was found to be ~ 2.0, suggesting that two electrons participate in the electrooxidation of MQ at AuNUs/GCE.

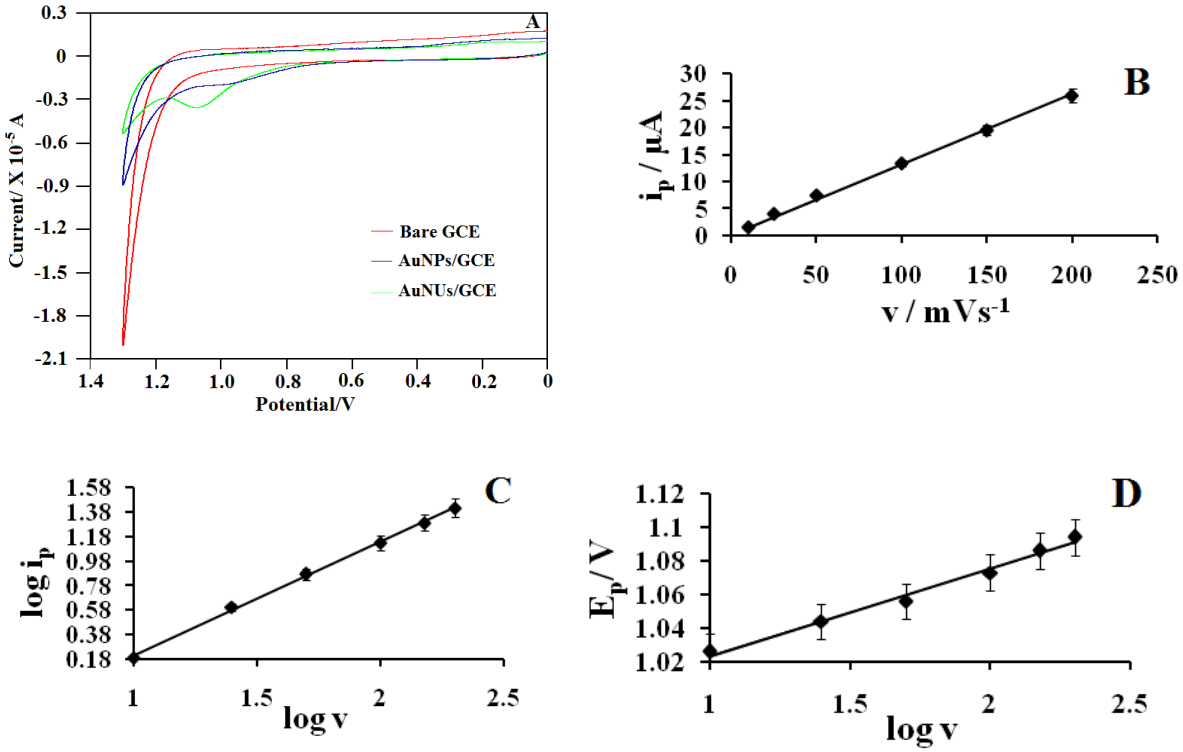

Fig. 5 (**A**) Cyclic voltammograms observed at (a) bare GCE (b) AuNPs/GCE and (c) AuNUs/GCE in 0.1 mM MQ (pH 2.0) at a scan rate of 100 mV s^{-1}; (**B**) Variation of peak current with scan rate for 0.1 mM MQ (pH 2.0) at AuNUs/GCE; (**C**) Relation between logarithm of peak current and logarithm of scan rate; (**D**) Observed dependence of E_p with logarithm of scan rate.

3.4 Influence of pH

The pH of the supporting electrolyte exerts a significant effect on the peak potential and current response of the analyte under study. The influence of pH on the electrooxidation of MQ was investigated from pH 2.0 to 5.5 (0.1M PBS) using linear sweep voltammetry (LSV). As illustrated in Figure 6, two defined breaks were observed in the linear

relationship between E_p and pH indicating the existence of two acid-base equilibria, the first at pH ≤2.9 and the other at pH≤4.7. The dependence of linear parts of the E_p-pH plot in the specified pH range is expressed by the following equations:

$E_p(V) = 1.1434 – 0.0210pH$ (2.0≤pH≤2.9)

$E_p(V) = 1.0697 + 0.0033pH$ (3.0≤pH≤4.7)

$E_p(V) = 1.6215 – 0.1156pH$ (4.8≤pH≤5.5)

In the region with pH≤ 2.9, E_p was observed to decrease with increase in pH with a slope of 0.021 which suggests that one proton was involved in the electrooxidation process. The results from the scan rate and pH study indicate the participation of two electrons and one proton in the electrooxidation process of MQ. In the pH range of 3 to 4.7, the peak potential was found to be independent of H^+ concentration. A linear decrease in the plot was again observed in the region of 4.8≤pH≤5.5. However, the voltammetric response disappeared beyond pH 5.5 indicating that the oxidation of MQ at the electrode surface becomes kinetically unfavourable. Since the best peak current response and a sharp peak was obtained at pH 2, it was chosen as the optimum pH for subsequent studies.

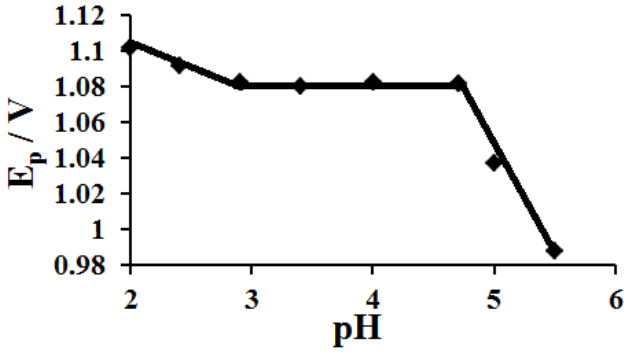

Fig. 6 Effect of pH on the oxidation peak response for 0.1 mM MQ at AuNUs/GCE.

3.5 Analytical performance

Being a highly sensitive electroanalytical technique, SWV was chosen for determination of MQ under optimized experimental conditions. The analyte concentration was observed to show a linear relationship with the peak current in two segments corresponding to the concentration range of 2.0 x 10^{-9} to 1.0 x 10^{-6} M for the first segment and 1.0 x 10^{-6} to 1.0 x 10^{-3} M for the second segment (Figure 7). The observed linear regression equations for the above-mentioned linear concentration ranges can be expressed as:

i_p (μA) = 2949.4C (μM) + 0.0584 (R^2=0.9967) (1.0×10^{-9} to 1.0×10^{-6} M)

i_p (μA) = 2.1566C (μM) + 3.1915 (R^2=0.9916) (1.0×10^{-6} to 1.0×10^{-3} M)

where C is the concentration of MQ. The limit of detection (LOD) and limit of quantification (LOQ) were calculated using the relation 3s/m and 10s/m, respectively, where s is the standard deviation of the blank solution and m is the slope of the calibration plot. The LOD and LOQ for MQ in the lower range region were found to be 1.4 x 10^{-9} M and 4.7 x 10^{-9} M, respectively. Table 1 compares the analytical performance for MQ quantification at AuNUs/GCE with the previously reported electroanalytical methods. As can be seen, the proposed method proved to be superior displaying a wider linear range with lower LOD and LOQ.

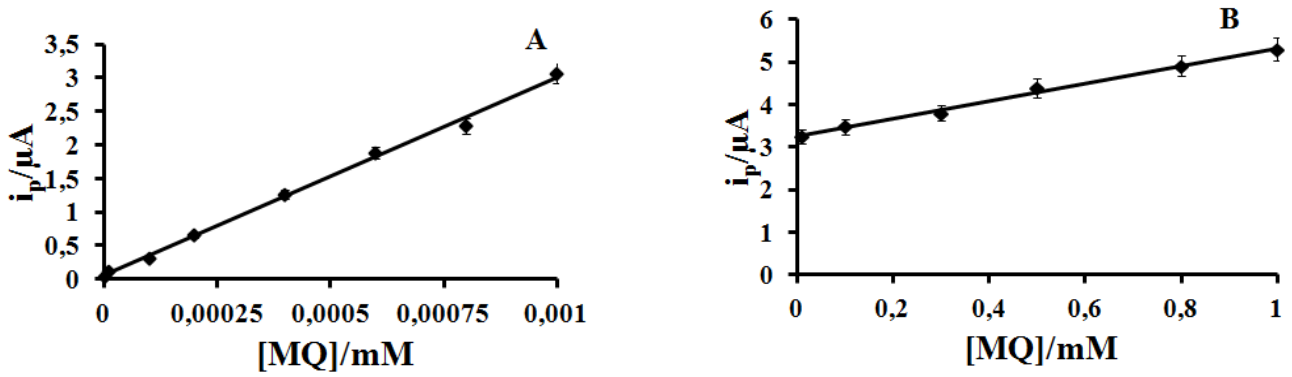

Fig. 7 The observed calibration plots for MQ in 0.1M PBS (pH 2.0) using SWV at AuNUs/GCE in linear ranges of (A) 2.0 x 10^{-9} to 1.0 x 10^{-6} M, and (B) 1.0 x 10^{-6} to 1.0 x 10^{-3} M.

Table 1. A comparison of validation parameters observed at AuNUs/GCE for determination of MQ with the reported electrochemical methods.

Electrode	Method	Linear range (M)	LOD (M)	LOQ (M)	Ref.
HMDE	DPV	6.00×10^{-6} to 8.00×10^{-5}	4.54×10^{-7}	1.51×10^{-6}	[15]
	SWV	6.00×10^{-6} to 8.00×10^{-5}	2.61×10^{-7}	8.70×10^{-7}	
AuNUs/GCE	SWV	2.00×10^{-9} to 1.00×10^{-6}	1.42×10^{-9}	4.75×10^{-9}	Present work
		1.00×10^{-6} to 1.00×10^{-3}			

MQ: Mefloquine; LOD: Limit of detection; LOD: Limit of quantification; HMDE: Hanging mercury drop electrode; DPV: Differential pulse voltammetry, SWV: Square wave voltammetry; AuNUs/GCE: Gold nanourchins modified glassy carbon electrode.

3.6 Effect of interferents

In order to evaluate the selectivity of the method, the effect of common interfering species (organic and inorganic) was investigated on the determination of 0.1 mM MQ (pH 2.0). The presence of 1000-fold concentration of Mg^{2+}, Na^{+}, K^{+}, NH_4^{+}, NO_3^{-}, Cl^{-}, glucose and citric acid was found to show no influence on the signals of MQ. Also, 500-fold concentrations of ascorbic acid and uric acid did not affect the peak current value of the drug with deviations below 5%. This suggests that AuNUs/GCE exhibits high selectivity towards MQ determination.

3.7 Reproducibility and stability

The reproducibility and stability of AuNUs/GCE were investigated by measuring the SWV peak current response for 0.1 mM MQ. The reproducibility for the modified sensor was determined by conducting consecutive determinations using three identically prepared modified sensors. The relative standard deviation (RSD) was found to be 2.1%

(n=3), suggesting that the sensor displays good reproducibility. To evaluate the long-term stability of the sensor, the electrode response for 0.1 mM MQ was measured over a period of 15 days. A slight decrease in the response was noted and the RSD was found to be 3.4%. Thus, the experimental results indicate that the modified sensor possesses good reproducibility and stability.

3.8 Real Sample Analysis

The utility of the proposed method was established by the quantification of MQ in commercial pharmaceutical formulations and biological samples. MQ content in a commercial tablet was determined at AuNUs/GCE using SWV under optimized conditions. The tablet analysis was processed as stated in experimental section and UV spectrophotometry was considered as the reference technique for comparison. The results were found to be in agreement with the declared amount and good recovery values were obtained (Table 2). Additionally, no interference was observed from the excipients present in the tablet. Thus, the proposed method is sensitive, accurate and practically applicable for the analysis of MQ pharmaceutical formulations in quality control laboratories.

Table 2. Assay results from MQ tablet (Mefliam) at AuNUs/GCE[a] and using UV-visible spectrophotometer[b]

Parameter	Results	
	Proposed Method[a]	**Reference Method[b]**
Labelled MQ (mg)	250	250
MQ content found (mg)	247.5	247.0
Bias (%)	0.25	0.30
RSD (%) (n=3)	0.28	1.25
Spiked (µM)	0.100	0.100
Found (µM)	0.098	0.097
Recovery (%)	98.0	97.0
Bias (%)	2.00	3.00
RSD (%) (n=3)	1.86	2.14

The analytical applicability of AuNUs/GCE in human urine sample was also explored. Prior to the analysis, the urine sample was diluted 100 fold with 0.1M PBS (pH 2.0). The sample was then spiked with known concentrations of MQ and recovery study was carried out. The calibration curve was used to determine the concentration of the spiked MQ in urine sample. As presented in Table 3, the recovery rates were found to be in the range of 97.0-97.3%. Thus, the method presents an excellent tool for the determination of MQ in human urine.

Table 3. Recovery results obtained for MQ in human urine sample at AuNUs/GCE.

Sr. No.	Added (M)	Found (M)	Recovery (%)
1	1.00×10^{-7}	9.71×10^{-8}	97.1
2	2.00×10^{-7}	1.94×10^{-7}	97.0
3	3.00×10^{-7}	2.92×10^{-7}	97.3

4. Conclusions

The present study reports the synthesis of urchin-shaped gold nanostructures by a seed-mediated approach and its use for the first time as sensing material for the square wave voltammetric determination of MQ. The electrooxidation and quantification of the antimalarial drug were investigated at AuNUs/GCE for the first time. AuNUs proved to be better electrode modifiers than AuNPs due to their spike-like morphology demonstrating excellent electrocatalytic activity. The proposed electrochemical sensor showed high sensitivity and selectivity, low LOD and a wide linear concentration range for the determination of MQ. Furthermore, the method was successfully applied for detection of the drug in pharmaceutical formulations and human urine with satisfactory recoveries, indicating that AuNUs is a promising candidate for the construction of a sensor for the electrochemical determination of MQ.

Acknowledgements

The authors are thankful to National Research Foundation (Pretoria, South Africa), the Nanotechnology Platform (University of KwaZulu-Natal, South Africa) and College of Health Sciences (University of KwaZulu-Natal, South Africa) for providing financial support.

References

1. World Health Organization, Fact Sheet: World Malaria Report 2015, http://www.who.int/malaria/media/world-malaria-report-2015/en/ (Accessed on 13/06/2016).
2. N. Tangpukdee, C. Duangdee, P. Wilairatana and S. Krudsood, *Korean J Parasitol.* **2009**, *47*, 93-102.
3. R.L. Nevin, Int. J. Parasitol.: Drugs Drug Resist, **2014**, *4*, 118-125.
4. P. Schlagenhauf, M. Adamcova, L. Regep, M.T. Schaerer and H.G. Rhein, *Malar. J.*, **2010**, *9*:357/1-357/15.
5. T.M.E. Davis, L.G. Dembo, S.A. Kaye-Eddie, B.J. Hewitt, R.G. Hislop and K.T. Batty, *Br. J. Clin. Pharmacol.*, **1996**, *42*, 415-421.
6. A.M. Ronn, J. Ronne-Rasmussen, P. Gotzsche and I.C. Bygbjerg, *Trop. Med. Int. Health*, **1998**, *3*, 83-8.
7. A.M. Croft and A. Herxheimer, *BMC Public Health*, **2002**, *2*, 6.
8. H.R. Smith, A.M. Croft and M. M. Black, *Clin. Exp. Dermatol.*, **1999**, *24*, 249-254.
9. P. Soentjens, M. Delanote and A. V. Gompel, *J. Travel Med.*, **2006**, *13*, 172-174.
10. F.O. ter Kuile, F. Nosten, C. Luxemburger, D. Kyle, P. Teja-Isavatharm, L. Phaipun, R. Price, T. Chongsuphajaisiddhi and N.J. White, *Bull. World Health Org.*, **1995**, *73*, 631-642.
11. A.B. Rao and R.S. Murthy, *J. Pharm. Biomed. Anal.*, **2002**, *27*, 959-65.
12. V. Arora, A. Bhandari, B. Kumar and R. Arora, Asian J. Chem., **2008**, *20*, 3319-3323.

13. G.O. Gbotosho, C.T. Happi, O. Lawal, A. Sijuade, A. Sowunmi and A. Oduola, *Malar J.* **2012**, 11:59.

14. Y. Bergqvist, U. Hellgren and F.C. Churchill, *J. Chromatogr.*, **1988**, *432*, 253-263.

15. B. Uslu, B. Dogan, A. Sibel A., H.Y. Özkan and Y. Aboul-Enein, *Electroanal.*, **2005**, *17*, 1563-1570.

16. J. Fidanza and J.J. Aaron, *Anal. Chim. Acta*, **1989**, *227*, 325-330.

17. N. Thapliyal, T.E. Chiwunze, R. Karpoormath, R.N. Goyal, H. Patel and S. Cherukupalli, *RSC Adv.*, **2016**, *6*, 57580-57602.

18. N. Thapliyal, R.V. Karpoormath and R.N. Goyal, *Anal. Chim Acta.*, **2015**, *853*, 59-76.

19. M.L. Yola, T. Eren, N. Atar, Saral, H. and İ. Ermiş, *Electroanalysis*, **2016**, *28*, 570 – 579.

20. M.L. Yola. and N. Atar, *J. Electrochem. Soc.*, **2016,** *163*, B718-B725.

21. M. Oyama, *Anal Sci.*, **2010**, *26*, 1-12.

22. K. Li, X. Zhu and Y. Liang, *Pharmacol. Pharm.*, **2012**, *3*, 275-280.

23. M.L. Yola, T. Eren and N. Atar, *Sens. Act. B: Chem.,* **2015**, *210*, 149-157.

24. M.L. Yola and N. Atar, *Electrochim. Acta.*, **2014.** *119*, 24-31.

25. M.L. Yola, T. Eren and N. Atar, *Biosens. Bioelectr.,* **2014**, *60*, 277-285.

26. M.L. Yola, N. Atar, T. Eren, H. Karimi-Maleh and S. Wang, *RSC Advances.*, **2015**, *5*, 65953-65962.

27. N. Atar, T. Eren, B. Demirdögen, M.L. Yola and M.O. Çağlayan, *Ionics*, **2015,** *21*, 2285-2293.

28. Q. Zhu, F. Cai, J. Zhang, K. Zhao, A. Deng and J. Li, *Biosens. Bioelectr.*, **2016**, *86*, 899-906.

29. N.S.K. Gowthaman, B. Sinduja and S.A. John, *RSC Advances*, **2016**, *6*, 63433-63444.

30. Y.M. Sabri, A.E. Kandjani, S.J. Ippolito and S.K. Bhargava, *Sci. Rep*. **2016**, *6*, 24625; doi: 10.1038/srep24625.

31. B.L. Sanchez-Gaytan, Z. Qian, S.P. Hastings, M.L. Reca,. Fakhraai, and S.J. Park, *J. Phys. Chem. C*, **2013,** *117*(17), 8916-8923.

32. L. Wang, T. Guo, Q. Lu, X. Yan, D. Zhong, Z. Zhang, Y. Ni, Y. Han, D. Cui, X. Li and L. Huang, *ACS Appl. Mater. Interfaces*, **2014**, *7*, 359-369.

33. W. Wang, Y. Pang, J. Yan, G. Wang, H. Suo, C. Zhao and S. Xing, *Gold Bull.*, **2012**, *45***,** 91-98.

34. F. Xu, K. Cui , Y. Sun, C. Guo, Z. Liu, Y. Zhang, Y. Shi and Z. Li, *Talanta*, **2010**, *82***,** 1845-1852.

35. N. Thapliyal, T.E. Chiwunze, R. Karpoormath and S. Cherukupalli, *Mater. Sc. Eng.: C*, **2017**, *74*, 27-35.

36. D.H. Kim, *Sol. Energ. Mat. Sol. Cells*, **2012**, *107*, 81-86.

37. Z. Yang, X. Huang, J. Li, Y. Zhang, S. Yu, Q. Xu and X. Hu, *Microchimica Acta*, **2012**, *177*, 381-387.

38. C. R. Raj, T. Okajima and T. Ohsaka, *J. Electroanal. Chem.*, **2003**, *543*, 127-133.

39. G.A. Lopez-Munoz, J.A. Balderas-Lopez, J. Ortega-Lopez, J.A. Pescador-Rojas and J. S. Salazar, *Nanoscale Res Lett,* **2012**, 7, 667.

40. V.N. Palakollu, N. Thapliyal, T.E. Chiwunze, R. Karpoormath, S. Karunanidhi, and S. Cherukupalli, *Mater. Sci. Eng. C*, **2017,** *77*, 394-404.

41. P. Gopal, T. M. Reddy, V. N. Palakollu, *ChemistrySelect* **2017**, *2*, 3804-3811.

42. H.M. Elqudaby, G.G. Mohamed, F.A. Ali and Sh.M. Eid, *Arab. J. Chem*, **2013**, *6*, 327-333.

43. E. Bicer and C. Arat, *Croat. Chem. Acta*, **2009**, *82***,** 583-593.

44. E. Laviron, *J. Electroanal, Chem.*, **1979**, *101***,** 19-28.

45. A.J. Bard, L.R. Faulkner, Electrochemical methods: Fundamentals and applications (2nd ed.), Wiley, New York, **2004**, pp. 236.

CHAPTER 4

Fabrication of Highly Sensitive Gold Nanourchins Based Electrochemical Sensor for Nanomolar Determination of Primaquine

Neeta Thapliyal, Tirivashe E. Chiwunze, Rajshekhar Karpoormath*, Srinivasulu Cherukupalli

[a] Department of Pharmaceutical Chemistry, Discipline of Pharmaceutical Sciences, College of Health Sciences, University of KwaZulu-Natal (Westville), Durban-4000, South Africa.

*Corresponding author

E-mail: karpoormath@ukzn.ac.za, rvk2006@gmail.com

Tel no.: +27(0)312607179, +27721107207; Fax No.:+27(0)312607792

Contents lists available at ScienceDirect

Materials Science and Engineering C

journal homepage: www.elsevier.com/locate/msec

Fabrication of highly sensitive gold nanourchins based electrochemical sensor for nanomolar determination of primaquine

Neeta Bachheti Thapliyal *, Tirivashe Elton Chiwunze, Rajshekhar Karpoormath *, Srinivasulu Cherukupalli

Department of Pharmaceutical Chemistry, College of Health Sciences, University of KwaZulu-Natal, Durban 4000, South Africa

ARTICLE INFO

Article history:
Received 15 August 2016
Received in revised form 1 November 2016
Accepted 16 December 2016
Available online 7 January 2017

Keywords:
Gold nanourchins
Glassy carbon electrode
Voltammetry
Primaquine
Pharmaceutical formulations
Human urine

ABSTRACT

A gold nanourchins modified glassy carbon electrode (AuNu/GCE) was developed for the determination of antimalarial drug, primaquine (PQ). The surface of AuNu/GCE was characterized by electrochemical impedance spectroscopy (EIS), scanning electron microscopy (SEM), transmission electron microscopy (TEM) and cyclic voltammetry (CV). EIS results indicated that the electron transfer process at AuNu/GCE was faster as compared to the bare electrode. The SEM and TEM image confirmed the presence and uniform dispersion of gold nanourchins on the GCE surface. Upon investigating the electrochemical behavior of PQ at AuNu/GCE, the developed sensor was found to exhibit high electrocatalytic activity towards the oxidation of PQ. Under optimal experimental conditions, the sensor showed fast and sensitive current response to PQ over a linear concentration range of 0.01–1 μM and 0.001–1 μM with a detection limit of 3.5 nM and 0.9 nM using differential pulse voltammetry (DPV) and square wave voltammetry (SWV), respectively. The AuNu/GCE showed good selectivity, reproducibility and stability. Further, the developed sensor was successfully applied to determine the drug in human urine samples and pharmaceutical formulations demonstrating its analytical applicability in clinical analysis as well as quality control. The proposed method thus provides a promising alternative in routine sensing of PQ as well as promotes the application of gold nanourchins in electrochemical sensors.

Abstract

A gold nanourchins modified glassy carbon electrode (AuNu/GCE) was developed for the determination of antimalarial drug, primaquine (PQ). The surface of AuNu/GCE was characterized by electrochemical impedance spectroscopy (EIS), scanning electron microscopy (SEM), transmission electron microscopy (TEM) and cyclic voltammetry (CV). EIS results indicated that the electron transfer process at AuNu/GCE was faster as compared to the bare electrode. The SEM and TEM image confirmed the presence and uniform dispersion of gold nanourchins on the GCE surface. Upon investigating the electrochemical behavior of PQ at AuNu/GCE, the developed sensor was found to exhibit high electrocatalytic activity towards the oxidation of PQ. Under optimal experimental conditions, the sensor showed fast and sensitive current response to PQ over a linear concentration range of 0.01-1 μM and 0.001-1 μM with a detection limit of 3.5 nM and 0.9 nM using differential pulse voltammetry (DPV) and square wave voltammetry (SWV), respectively. The AuNu/GCE showed good selectivity, reproducibility and stability. Further, the developed sensor was successfully applied to determine the drug in human urine samples and pharmaceutical formulations demonstrating its analytical applicability in clinical analysis as well as quality control. The proposed method thus provides a promising alternative in routine sensing of PQ as well as promotes the application of gold nanourchins in electrochemical sensors.

Keywords

Gold nanourchins; glassy carbon electrode; voltammetry; primaquine; pharmaceutical formulations; human urine.

1. Introduction

Primaquine (PQ; chemically known as N-(6-methoxyquinolin-8-yl)pentane-1,4-diamine; Fig. 1) is an 8-aminoquinoline commonly used as an antimalarial drug. First synthesized in 1940s by Robert Elderfield, PQ is the only FDA approved drug that can eliminate the intra-hepatic forms (schizonts and hypnozoites) of P. vivax and P. ovale [1]. It exhibits significant gametocytocidal activity in P. falciparum malaria substantially lowering the risk of transmission [2]. PQ is also suggested for causal and terminal prophylaxis in vivax malaria [3]. In addition, the drug is used for the treatment of mild to moderate cases of pneumocystis pneumonia in AIDS patients [4]. Though PQ is highly effective and largely recommended for management of falciparum and vivax malaria, there have been reports about potential haemolytic toxic effects associated with its use in patients with G6PD deficiency [5]. Other common side effects of the drug are gastrointestinal disorders, headache, cardiac arrhythmia, leucopenia, hypertension and methemoglobinemia [6-9]. Considering the importance of drug analysis in quality control and therapeutic drug monitoring, it is imperative to develop cheap, robust and accurate analytical methods to determine PQ in pharmaceutical samples and human body fluids.

Various methods have been developed for PQ determination, such as spectrophotometry, mass spectrometry, chromatography, electrochemical methods, colorimetry and fluorimetry [10-18]. Among these, the voltammetric methods have proved efficacious for detection of several organic and inorganic compounds on account of their selectivity, sensitivity and reliability at a low cost, with the instrumentation having potential for miniaturization and automation [19, 20]. So far, only two voltammetric methods have been reported in literature for quantification of PQ exhibiting detection limits in micromolar range [15, 21]. Hence, the need to develop a more sensitive, selective and accurate electroanalytical method for trace analysis of PQ is significant.

Last few decades have witnessed significant progress in the development of electrochemical sensors based on the use of a range of nanoparticles modified electrodes. Various metallic

nanomaterials with enhanced electrical properties have been synthesized [22-30]. Gold nanoparticles (AuNPs) have revealed great potential application in the field of electroanalysis due to their unique properties, such as excellent conductivity, chemical stability, resistance to corrosion, high surface area and catalytic activity [31]. When immobilized onto an electrode surface, AuNPs increase the surface area of the modified electrode and improve the electron transfer rate providing sensitive and selective systems for the detection of various analytes. Since AuNPs are considered as ideal candidates for constructing electrochemical sensors, these were chosen over other metallic particles for the proposed work. Among them, gold nanourchins that are endowed with a rough surface and urchin-like morphology are worth investigating. Normal AuNPs are spherical in shape. However, the gold nanourchins have urchin-like shape i.e., spherical shaped structure with spikes or needles coming out of the surface. This provides the nanourchins with more active surface area and hence the gold nanourchins modified electrode shows higher electrocatalytic activity as compared to simple gold nanoparticles modified electrode. Thus, using gold nanourchins as electrode modifier improves the sensitivity of the electrode to a greater extent and hence, a much lower concentration of the analyte can be detected. These nanostructures are suggested to have high surface to volume ratio thus making them an exceptional candidate for electrode modification [32, 33]. The presence of spike shaped protrusions in nanourchins increases the effective surface area of the electrode resulting in improved electrochemical response as compared to spherical shaped gold nanoparticles modified electrode. The concept of employing urchin-shaped gold nanoparticles as an electrode modifier in voltammetry is very new. Literature survey reveals extremely few reports on the use of gold nanourchins based electrode for detection of an organic or inorganic compound. The present study describes the first-time use of a gold nanourchins modified glassy carbon electrode for voltammetric determination of PQ, an antimalarial drug. The novelty of the work thus lies in the use of gold nanourchins as an electrode modifier for determination of primaquine. The developed electrochemical sensor was found to exhibit

significant electrocatalytic activity towards PQ oxidation and was successfully evaluated for determination of PQ in real samples.

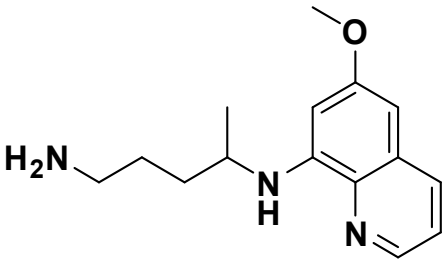

Fig. 1. Chemical structure of Primaquine.

2. Experimental

2.1. Materials

Primaquine bisphosphate and gold nanourchins were purchased from Aldrich. Other chemicals employed were of analytical grade and used as received (without further purification). Phosphate buffer solution (PBS) was prepared from 0.2 M Na_2HPO_4 and 0.2 M NaH_2PO_4 and employed as the supporting electrolyte. Stock solution of PQ (2.0 mM) was freshly prepared in water prior to measurements to avoid any decomposition. All aqueous solutions were prepared using double-distilled water.

2.2. Apparatus

The morphology of the modified electrode was observed using transmission electron microscopy (TEM) (JEOL 1010, USA) and scanning electron microscopy (SEM) (LEO 1450 Ultra Plus, Zeiss, Germany). The electrochemical impedance spectroscopy (EIS), cyclic voltammetry (CV), differential pulse voltammetry (DPV) and square wave voltammetry (SWV) experiments were carried out using a CHI660E electrochemical workstation (CH Instruments, USA). A conventional three electrode system was utilized throughout the experiments which comprised of a bare or modified GCE (3.0 mm in diameter) as the working electrode, a platinum counter electrode and an Ag/AgCl reference electrode. All the three electrodes were

provided by CH Instruments, USA. The pH measurements were performed using EUTECH cyber scan pH 510 meter. All the electroanalytical measurements were performed at room temperature (25 ± 2 °C). Instrumental conditions for DPV were: scan rate 100 mVs^{-1}, pulse amplitude 0.05 V, sample width 0.02 s, pulse width 0.05 s and pulse period 0.5 s. The operating conditions to record square wave voltammograms were: square wave frequency (f): 15 Hz, square wave amplitude: 0.05 V and potential step (E): 0.004 V. All DPV and SWV measurements were carried out in pH 7.2 PBS.

2.3. Electrode preparation

Before electrode modification, the GCE was carefully polished to a mirror-like surface with 0.05 μm alumina on a microcloth pad. It was then dipped in a beaker containing 0.2 M H_3PO_4 solution followed by rinsing with double distilled water to remove any adsorbed alumina particles from the electrode surface. 15 μL of gold nanourchins solution was then cast onto the cleaned GCE surface and dried under an infrared lamp. The resultant electrode was used for electrochemical studies and denoted as AuNu/GCE.

2.4. Sample preparation

A commercially available PQ tablet (Malirid, Ipca Laboratories Ltd., India) containing 7.5 mg of primaquine phosphate was finely powdered using mortar and pestle. The powder was then transferred to a volumetric flask and dissolved in double distilled water. Square-wave voltammograms were recorded (as described for the standard PQ solution) at AuNu/GCE to determine PQ in the pharmaceutical formulation by taking suitably diluted aliquot of the prepared solution (that falls within the linear concentration range) and conducting SWV analysis under similar conditions as used while conducting the concentration study. The content of PQ in the sample was calculated from the related calibration equation.

Urine samples were collected from laboratory personnel and diluted 500 times with 0.1 M PBS (pH 7.2). The dilution process helps in reducing the matrix effect. The samples were then spiked with appropriate amounts of PQ solution for volumetric analysis. The standard addition method was used to determine spiked PQ in the samples.

3. Results and discussion

3.1. Characterization of AuNu/GCE

The surface morphology of the modified electrode was explored using SEM and TEM. As shown in Fig. 2A, uniformly dispersed spherical structures with "nanothorns" emerging on their surface and having an average size of 73 nm were observed on the electrode surface. The urchin-like structure of gold nanoparticles is in accordance with the morphology of gold nanourchins reported in literature [33], which was further confirmed from the TEM image (Fig. 2B). Thus, the images indicate that gold nanourchins were successfully assembled on the surface of the electrode. Furthermore, the presence of gold (Au) on the electrode surface was confirmed by energy-dispersive X-ray spectroscopy (EDX) spectra, as depicted in Fig. 2C. A strong Au peak in the figure shows that gold nanourchins were successfully coated onto the electrode surface. Trace amounts of sodium and chlorine were also found to be present in addition to carbon and oxygen.

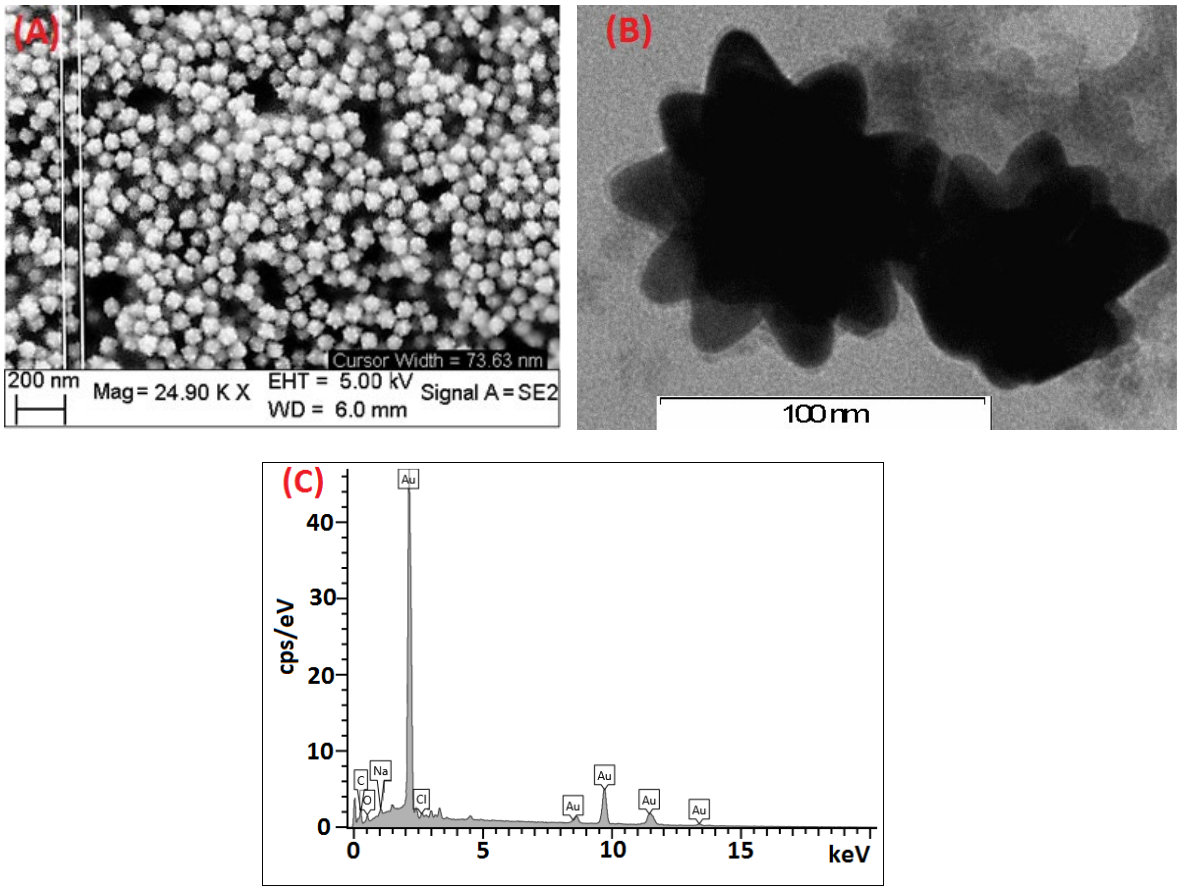

Fig. 2. (A) SEM image, **(B)** TEM image, and **(C)** EDX spectra of the gold nanourchins modified GCE.

EIS records the impedance changes of the electrode surface prior and after modification, and is used to characterize the interface properties of the electrode surfaces. Fig. 3 gives the Nyquist plots of bare GCE and AuNu/GCE observed in a solution containing 2.0 mM $K_3[Fe(CN)_6]$. The diameter of the semicircle, which corresponds to the charge transfer resistance, was found to decrease remarkably at AuNu/GCE as compared to the bare electrode indicating a reduction in the resistance towards the redox reaction. This suggests improved electrical conductivity of the modified electrode. AuNu/GCE was further characterized by CV. Fig. 4A shows the voltammetric response observed at bare GCE and AuNu/GCE in the presence of 2.0 mM $K_3[Fe(CN)_6]$ in 0.1 M KCl solution. An increase in the peak current along with a slight negative shift in the peak potential was observed at the modified electrode as compared to the bare

electrode, which suggests that the gold nanourchins effectively electrocatalyze the redox process of $K_3[Fe(CN)_6]$ and promote the electron transfer rate. This is attributed to high surface area and excellent electrical conductivity of the gold nanostructures.

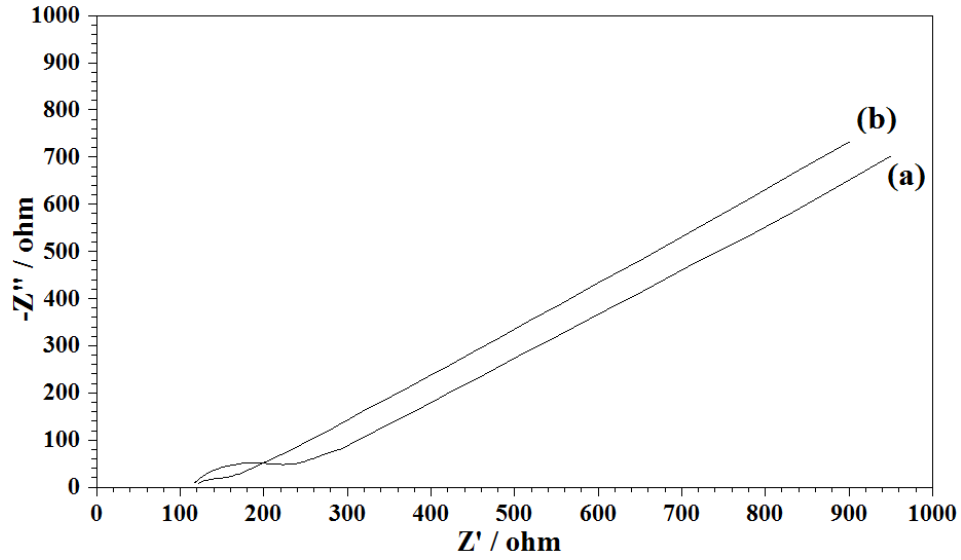

Fig. 3. EIS response of 2.0 mM $K_3[Fe(CN)_6]$ in 0.1 M KCl solution at (a) bare GCE and (b) AuNu/GCE.

The effective surface area of bare GCE and AuNu/GCE was determined by recording cyclic voltammograms in 2.0 mM $K_3[Fe(CN)_6]$ solution in 0.1 M KCl at different scan rates (Fig. 4B). The Randles-Sevcik equation (Eq. (1)) indicates the peak current (i_p) as a function of square root of scan rate ($v^{1/2}$) in the voltammetric experiment.

$$Ip=2.68\text{x}10^5 n^{3/2} AD^{1/2} C\upsilon^{1/2} \qquad \text{Eq.(1)}$$

where n stands for the number of electrons transferred in the electrochemical process (n=1 in the present case), A is the effective surface area of the electrode, D (in $cm^2\ s^{-1}$) is the diffusion coefficient ($D=7.6\times10^{-6}\ cm^2\ s^{-1}$ for $[Fe(CN)_6]^{3-}$) and C (in mol cm^{-3}) is the concentration of the electroactive species. Using the slope of i_p versus $v^{1/2}$ plot (inset of Fig. 4B), A was calculated to be 0.070 cm^2 and 0.1404 cm^2 for bare GCE and AuNu/GCE, respectively. The effective surface

area of the modified electrode was almost twice as that of the bare GCE leading to high electrical conductivity and electrocatalytic activity.

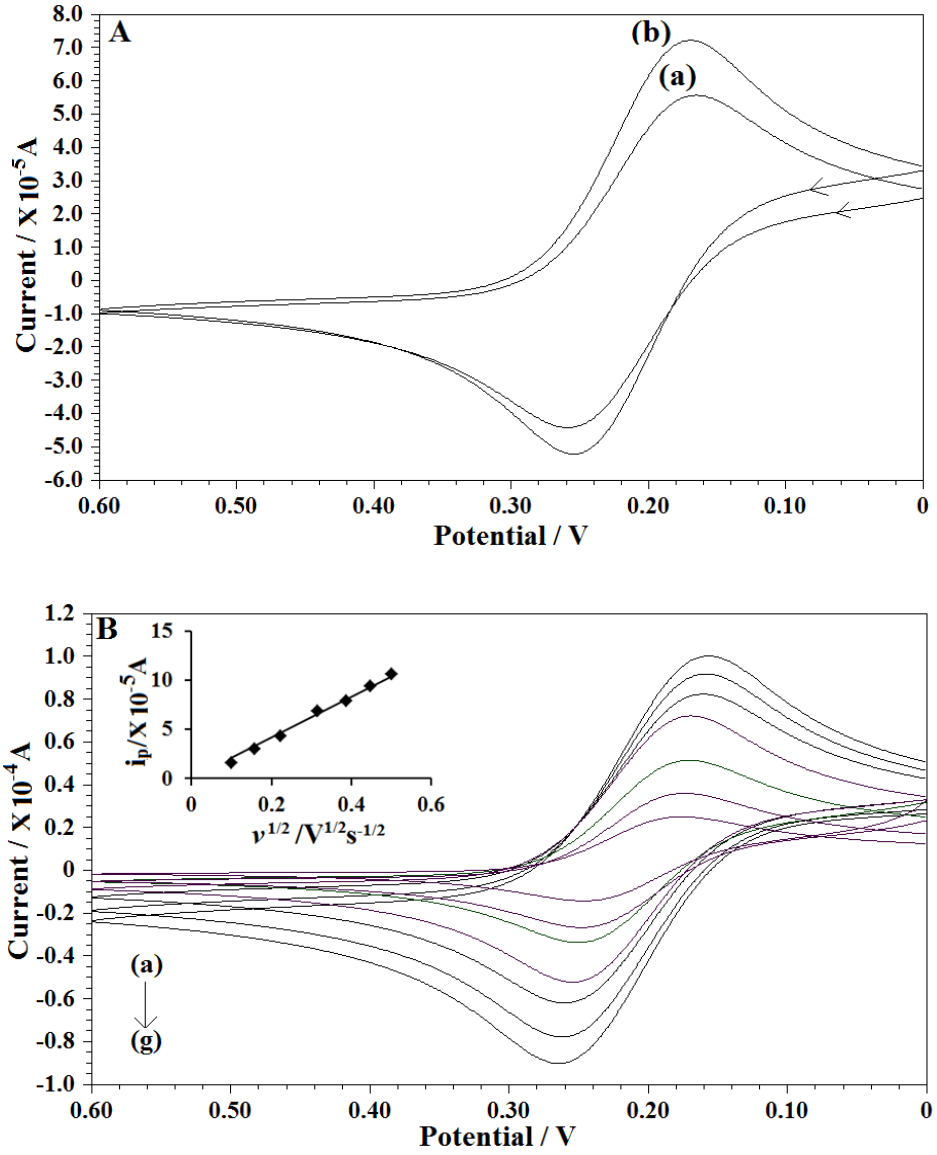

Fig. 4. (A) Cyclic voltammograms of 2.0 mM $K_3[Fe(CN)_6]$ in 0.1 M KCl solution at (a) bare GCE and (b) AuNu/GCE at 100 mV/s. (B) Cyclic voltammograms of 2.0 mM $K_3[Fe(CN)_6]$ in 0.1 M KCl solution at AuNu/GCE at sweep rates: (a) 10 (b) 25 (c) 50 (d) 100 (e) 150 (f) 200 and (g) 250 mV s^{-1} (Inset displays plot of peak current versus square root of sweep rate).

3.2. Electrochemical behavior of PQ at AuNu/GCE

The electrochemical behaviour of PQ on bare GCE and AuNu/GCE was studied by CV in 0.10 M PBS (pH 5.0) containing 0.1 mM PQ at a scan rate of 100 mVs^{-1}, as illustrated in Fig. 5A. A

small oxidation curve was observed at ~ 0.6 V on the bare electrode. No reverse peak was observed showing that PQ undergoes irreversible oxidation. Compared with the bare GCE, a higher current signal was obtained at 0.57 V on AuNu/GCE indicating that the modified electrode greatly facilitated the electrooxidation of PQ. The electrocatalytic activity was appraised to be due to the large surface area and excellent conductivity of the urchin-like gold nanostructures which provided more active sites and thus enhanced the transfer of electrons at the electrode surface.

In order to investigate the electrochemical reaction mechanism, the effect of scan rate (v) on the voltammetric signal of PQ was studied using model solution of 0.1 mM PQ 0.10 M PBS (pH 5.0). The peak current response was found to increase with increasing v in the range from 10 to 250 mV s^{-1} (Fig. 5B). Linear dependence was obtained between the peak height and the square root of the scan rate ($v^{1/2}$), and the linear regression equation can be expressed as (^{R2}=0.9929) signifying that the anodic process is diffusion-controlled [34]. The relationship between log i_p and log v (Fig. 5C) was linear displaying a slope of 0.47, which is close to the theoretical value of 0.5 for an ideal diffusion-controlled electrochemical process [35]. This further confirmed that the PQ oxidation process at AuNu/GCE is under diffusion control. In addition, the peak potentials shifted to more positive potentials with an increase in v suggesting that the electrooxidation process is irreversible in nature.

According to Laviron's equation, the peak potential (E_p) for an irreversible electrode process can be described as follows:

$$Ep = E° + \left(\frac{2.303RT}{\alpha nF}\right) Log \left(\frac{RTk°}{\alpha nF}\right) + \left(\frac{2.303RT}{\alpha nF}\right) Log\ \upsilon \qquad \text{Eq. (2)}$$

where α is the electron transfer coefficient, k^0 is the standard rate constant of the surface reaction and $E^{0\prime}$ is the formal potential [36]. The other symbols stated in the equation have their standard meanings. The value of αn was deduced from the slope of E_p versus log v (Fig. 5D) by considering R= 8.314 J/K mol, T = 298 K and F = 96480 C mol^{-1}. The α was determined from the equation given by Bard and Faulkner as follows:

$$\alpha = \frac{47.7}{Ep - Ep_{1/2}} \qquad \text{Eq. (3)}$$

where $E_{p1/2}$ is the potential at which the current is half the peak value [37]. The value of n was then calculated to be one which indicated that one electron was involved in the oxidation of PQ at AuNu/GCE. The value of k^0 was obtained from the intercept of the linear plot of E_p versus log v and it was calculated to be 3.689 s^{-1}.

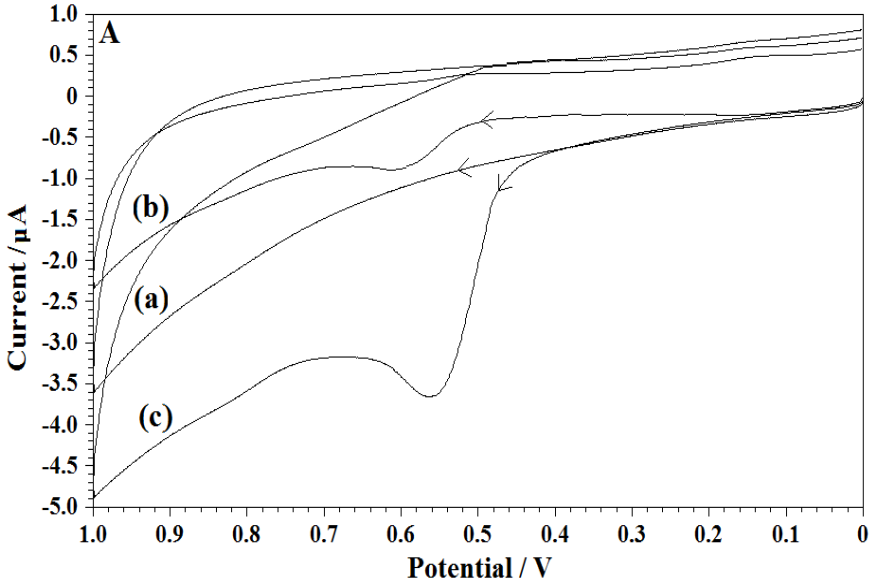

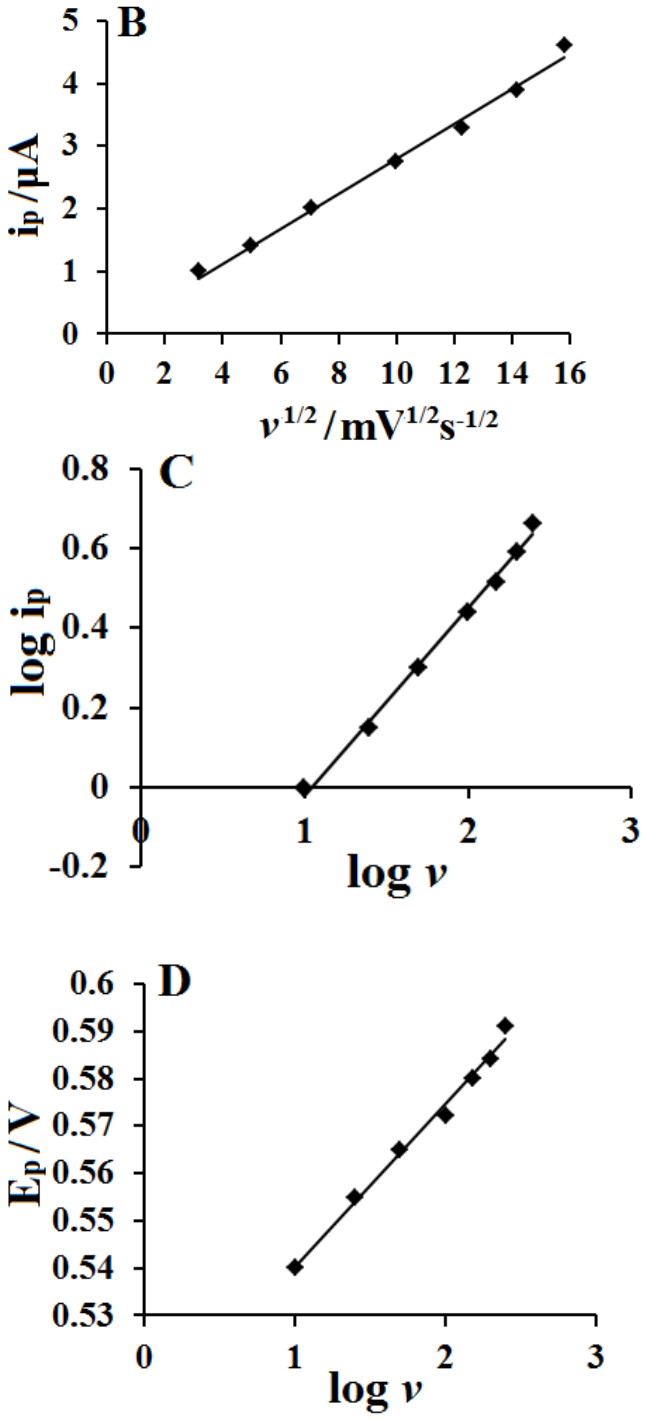

Fig. 5. (A) A comparison of cyclic voltammograms (a) in absence of PQ at AuNu/GCE, and in presence of 0.1 mM PQ at (b) bare GCE and (c) AuNu/GCE in 0.1 M PBS (pH 5.0) at a scan rate of 100 mV/s; (B) Variation of peak current (i_p) with square root of sweep rate ($v^{1/2}$) observed for 0.1 mM PQ (pH 5.0) at AuNu/GCE; (C) Plot of logarithm of peak current vs. logarithm of scan rate; (D) Variation of E_p with the logarithm of scan rate for 0.1 mM PQ at AuNu/GCE.

The pH exerted tremendous influence on the electrooxidation of PQ. The electrooxidation of 0.1 mM PQ was studied over the pH range of 2.1 to 10.7 in 0.1 M PBS by cyclic voltammetry. The anodic signal was found to shift towards less positive potentials with increasing pH of the solution indicating the presence of a proton coupled electron transfer reaction [38]. Two defined breaks were observed in the linear relationship between E_p and pH (Fig. 6) which corresponds to two known acid-base equilibria, one between the diprotonated (PQH_2^{2+}) and the monoprotonated (PQH^+) forms at pH ≤5.0, and the other between PQH^+ and the molecular form (PQ) at pH ≥8.7.

$PQH_2^{2+} \rightleftharpoons PQH^+ + H^+$

$PQH^+ \rightleftharpoons PQ + H^+$

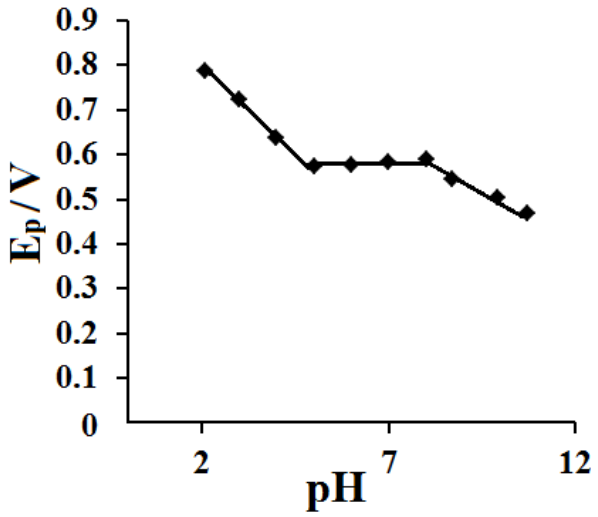

Fig. 6. Effect of pH on the oxidation peak for 0.1 mM PQ (pH 5.0) at AuNu/GCE.

The dependence of linear parts of the E_p-pH plot in the specified pH range is expressed by the following equations:

Ep(V) = 0.9467 - 0.0757pH (2.1≤pH≤5.0)

Ep(V) = 0.5451 - 0.0053pH (6.0≤pH≤8.0)

Ep(V) = 0.8635 - 0.0366pH (8.7≤pH≤10.7)

The electrochemical oxidation of PQ is envisaged to involve the quinoline ring nitrogen. The equations suggest that the acidic medium (2.1≤pH≤5.0) facilitates PQ oxidation process where the quinoline ring nitrogen is anticipated to oxidize in the protonated form and involves an electron transfer and a proton. The peak potential was found to be independent of H^+ concentration in the pH range 6.0 to 8.0. A linear decrease in the plot was again observed in the basic medium (pH≥8.7), which indicates that the electrode reaction involved hydrogen ions. This behavior is in agreement with similar studies reported in literature for electrooxidation of PQ. Since the best results with respect to a sharp response and sensitivity was obtained with pH=5.0, it was selected for further experiments.

3.3. Calibration curve and validation

Quantitative analysis is based on the linear relationship between the concentration of the analyte and the observed peak current. In order to develop a voltammetric method for PQ determination, DPV and SWV pulse techniques were selected since they display better defined peaks with improved sensitivity and lower detection limits as compared to those attained using LSV and CV. The voltammetric response at bare GCE and AuNu/GCE in presence of 1.0 μM PQ (pH 5.0) was compared using both the techniques, DPV and SWV (Fig. 7). Differential pulse and square wave voltammograms were further recorded under optimum conditions in the presence of various concentrations of PQ in 0.1 M PBS (pH 5.0), as displayed in Fig. 8. The results showed a linear response between the peak current and the drug concentration (C) in the range of 0.01-1 μM and 0.001-1 μM using DPV and SWV, respectively. The linear regression equations over the mentioned concentration range are given below:

$i_p(\mu A) = 368.12\ C + 0.0549$ (R^2=0.994) (using DPV technique)

$i_p(\mu A) = 1105.1\ C + 0.0713$ (R^2=0.999) (using SWV technique)

The analytical parameters are summarized in Table 1. Since SWV displayed better sensitivity as compared to DPV, it was chosen for further voltammetric studies.

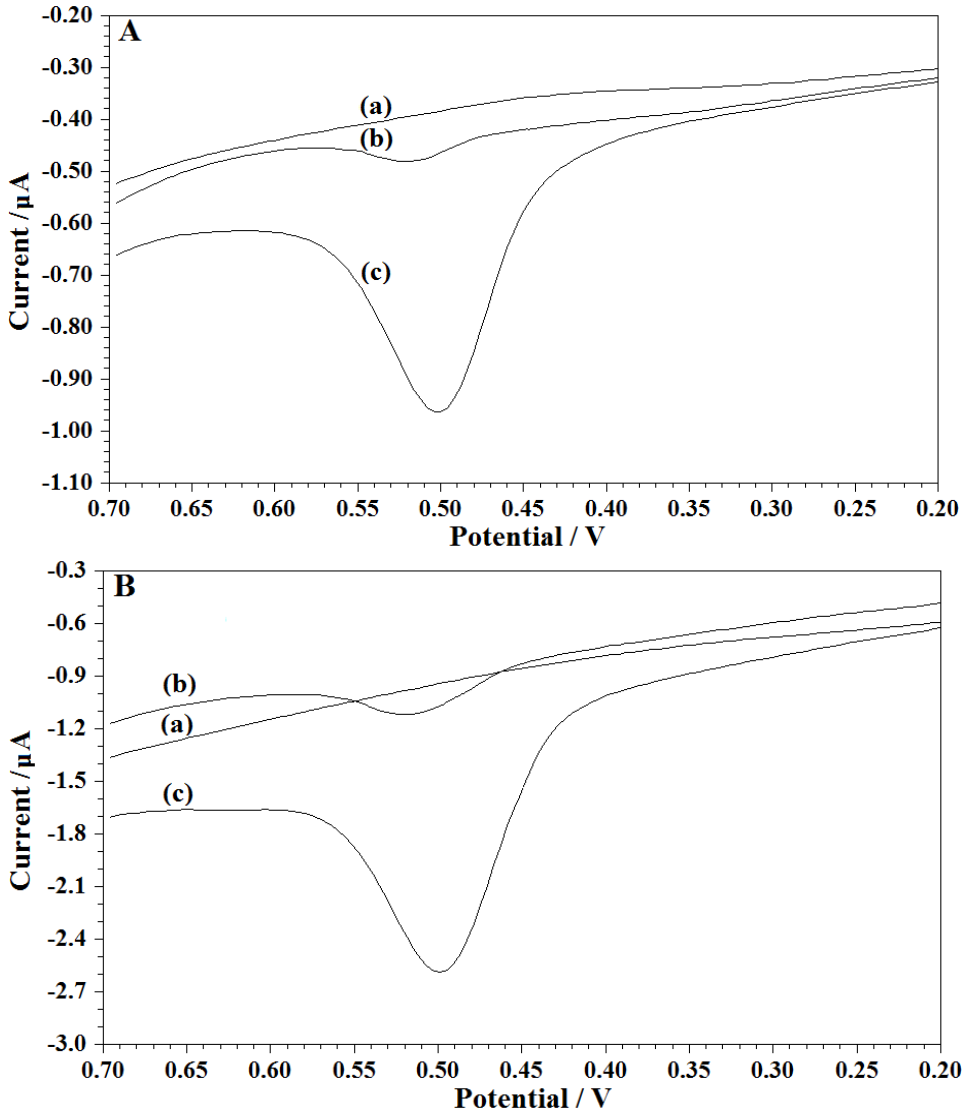

Fig. 7. Voltammograms observed (a) in absence of PQ at AuNu/GCE, and in presence of 0.1 mM PQ at (b) bare GCE and (c) AuNu/GCE in 0.1 M PBS (pH 5.0) using (A) differential pulse voltammetry and (B) square wave voltammetry.

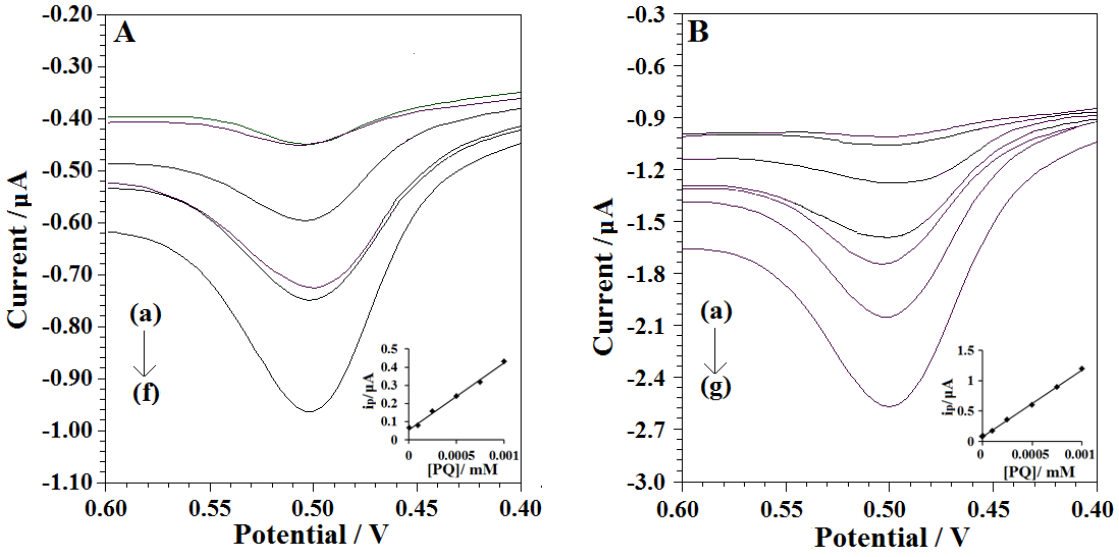

Fig. 8. (A) Differential pulse voltammograms for various concentrations of PQ: (a) 0.01, (b) 0.1, (c) 0.25, (d) 0.5, (e) 0.75 and (f) 1.0 µM in 0.1 M PBS (pH 5.0) using AuNu/GCE (The inset shows the calibration plot); (B) Square wave voltammograms for various concentrations of PQ: (a) 0.001 (b) 0.01, (c) 0.1, (d) 0.25, (e) 0.5, (f) 0.75 and (g) 1.0 µM in 0.1 M PBS (pH 5.0) using AuNu/GCE (The inset shows the calibration plot).

Table 1 Analytical parameters observed for determination of PQ in 0.1M PBS (pH 5.0) at AuNu/GCE.

Technique	**Linear range (M)**	**Sensitivity (µA/µM)**	**LOD (M)**	**LOQ (M)**	**Response Time (s)**
DPV	1.0×10^{-8} to 1.0×10^{-6}	0.368	3.52×10^{-9}	11.74×10^{-9}	120
SWV	1.0×10^{-9} to 1.0×10^{-6}	1.105	9.91×10^{-10}	3.30×10^{-9}	17

DPV, Differential pulse voltammetry; SWV, Square wave voltammetry; LOD, Limit of detection; LOQ, Limit of quantification

The response characteristics of AuNu/GCE were compared with those of other electrodes reported in the literature for the voltammetric determination of PQ (Table 2). As can be seen, the proposed method exhibited much improved analytical characteristics (such as wide linear concentration range and low detection limit) and additional analytical applicability for the electrochemical determination of the drug.

Table 2 A comparison of the performance of different electrodes reported for voltammetric determination of PQ.

Electrode	Method	Linear concentration range (M)	LOD (M)	LOQ (nM)	Matrix	Ref.
GCE	LSV	3.0×10^{-5} to 1.0×10^{-2}	3.62×10^{-5}	-	Pharmaceutical formulations	15
	DPV	3.0×10^{-5} to 1.0×10^{-4}	1.62×10^{-5}			
	SWV	3.0×10^{-5} to 1.0×10^{-4}	6.94×10^{-6}			
Cu-NW/CPE	DPV	22.4×10^{-7} to 22.7×10^{-6}	0.96×10^{-6}	-	Pharmaceutical formulations	21
AuNu/GCE	DPV	1.0×10^{-8} to 1.0×10^{-6}	3.52×10^{-9}	11.74	Pharmaceutical formulations Human urine	This work
	SWV	1.0×10^{-9} to 1.0×10^{-6}	9.91×10^{-10}	3.30		

GCE, glassy carbon electrode; LSV, linear sweep voltammetry; DPV, differential pulse voltammetry; SWV, square wave voltammetry; Cu-NW/CPE, $Cu(OH)_2$ nano-wire modified carbon paste electrode; AuNu/GCE, gold nanourchins modified glassy carbon electrode LOD, limit of detection and LOQ, limit of quantification.

3.4. Repeatability, reproducibility and stability of the electrode

The repeatability, reproducibility and stability of the voltammetric response are significant parameters for assessing the performance of an electrode. The repeatability of AuNu/GCE was evaluated by assaying freshly prepared 1.0 µM PQ solution in 0.1 M PBS (pH 5.0) four times repeatedly using the same electrode on the same day using the proposed SWV procedure. The relative standard deviation (RSD) value for the peak current measurements was 1.96 %, indicating excellent repeatability of the response of the developed sensor. The sensor also displayed good reproducibility. For four identically prepared electrodes, the RSD of the current response was 2.45%. In order to evaluate its stability, the sensor was stored at 4°C for 15 days. No obvious change in the current response for the same sample concentration was noted, indicating that the sensor possessed good stability.

3.5. Effect of interferents

The effect of various potential interfering compounds (commonly present in biological media as well as additives in pharmaceutical formulations) on the determination of 1.0 μM PQ was investigated using SWV at AuNu/GCE. Addition of 200-fold concentration of Na^{+}, K^{+}, Ca^{2+}, Mg^{2+}, Fe^{3+}, Cl^{-}, SO_4^{2-}, starch, glucose, sucrose, caffeine, citric acid and oxalic acid, and 50-fold concentration of uric acid, dopamine and ascorbic acid did not show any significant influence on the PQ current signal with deviations below the tolerance limit of 5.0 %. Thus, the developed sensor was considered highly selective towards the determination of PQ in the presence of various possible interferents.

3.6. Real Sample Analysis

The proposed method was applied to the determination of PQ in a commercial dosage form (tablet). The tablet was processed as mentioned in the experimental section and optimized SWV conditions were employed for the quantification. No interference from the excipients present in the formulations of the tablets was observed. The amount of PQ in the tablet was found to be 7.47 mg which is in good agreement with the drug content stated in the label. The analytical applicability of the developed SWV method was further assessed for the determination of PQ in human urine using standard addition method. No complex pretreatment was involved for the analysis. The urine samples were spiked with specific concentrations of the drug and measured three times (n=3) to determine drug content. Fig. 9 exhibits the square wave voltammograms of blank and spiked urine (sample 1). Two peaks were observed in the voltammogram of spiked sample. The peak at 0.5 V is assigned to the presence of PQ, while the peak at ~ 0.38 V (also observed in voltammogram of blank sample) indicates the existence of uric acid. This demonstrates that the biological compounds present in urine do not interfere in the determination of PQ using the proposed method. The recovery of PQ ranged from 96.8 to 103.4 %, confirming accuracy of the modified electrode for detecting the drug in urine samples. The

obtained results are summarized in Table 3 and 4. These results indicate that the sensor has high sensitivity and selectivity for determining PQ in commercial tablets and human urine. However, the method was not evaluated for quantification of the drug in blood samples.

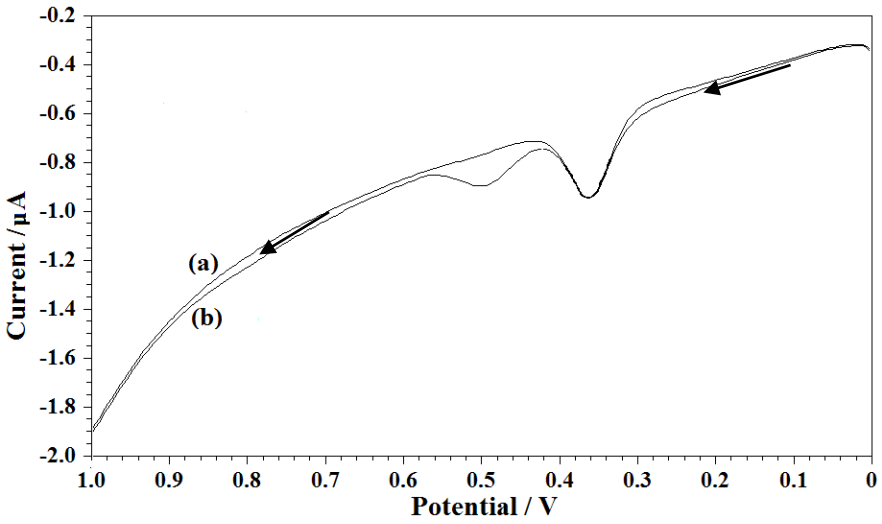

Fig. 9. Square wave voltammograms of (a) blank urine sample 1 and (b) urine sample 1 spiked with 0.01 µM PQ.

Table 3 Determination of PQ in commercial tablet using proposed SWV method.

Parameters	Results
Labelled PQ (mg)	7.50
PQ content found (mg)	7.47
Bias (%)	0.40
RSD (%) (n=3)	1.07
Spiked (µM)	0.100
Found (µM)	0.099
Recovery (%)	99.0
Bias (%)	1.00
RSD (%) (n=3)	1.41

RSD, relative standard deviation

Table 4 Application of the proposed SWV method to determine PQ in human urine using standard addition method.

Sample	Spiked ($\times10^{-8}$ M)	Found ($\times10^{-8}$ M)	Bias (%)	Recovery (%)	RSD (%)
Urine Sample 1	1.00	0.989	1.10	98.9	1.84
	5.00	4.838	3.24	96.8	1.53
	10.00	10.14	1.40	101.4	1.81
Urine Sample 2	1.00	0.998	0.20	99.8	1.02
	5.00	5.172	3.44	103.4	1.15
	10.00	10.26	2.60	102.6	2.63

RSD, relative standard deviation

4. Conclusion

A simple, sensitive and reliable square wave voltammetric method for quantitative analysis of PQ in real samples using gold nanourchins as the electrode modifier is proposed. AuNu/GCE was fabricated and utilized as an electrochemical sensor for determination of PQ. The electrocatalytic behavior of the proposed sensor was studied using CV, DPV and SWV. The developed gold nanourchins based electrochemical sensor exhibited low detection limit, wide linear concentration range, high sensitivity and appreciable stability for the determination of PQ. The feasibility of the method for quantification of PQ in pharmaceutical formulations and human urine samples was validated with satisfactory results. The method is superior to earlier reported electrochemical methods and could even quantify PQ in the nanomolar range in bulk as well as real samples. Thus, the proposed sensor assures a reliable quantitative analysis of PQ in pharmaceutical formulations and human urine samples, without any interference or matrix

complications, offering a novel and promising tool for quality control purpose and clinical analyses.

Acknowledgement

The authors gratefully acknowledge the Nanotechnology Platform (University of KwaZulu-Natal, South Africa), College of Health Sciences (University of KwaZulu-Natal, Durban, South Africa) and National Research Foundation (NRF), Pretoria, South Africa for providing financial support.

References

[1] D.R. Hill, J.K. Baird, M.E. Parise, L.S. Lewis, E.T. Ryan, A.J. Magill, Primaquine: report from CDC expert meeting on malaria chemoprophylaxis I., Am. J. Trop. Med. Hyg. 75 (2006) 402-415.

[2] D. F. Clyde, Clinical problems associated with the use of primaquine as a tissue schizontocidal and gametocytocidal drug, Bull. World Health Organ. 59 (1981) 391-395.

[3] D. Fernando, C. Rodrigo, S. Rajapakse, Primaquine in vivax malaria: an update and review on management issues, Malar J. 10 (2011) 351/1-351/12.

[4] J.A. Fishman, Treatment of infection due to pneumocystis carinii, Antimicrob. Agents Chemother. 42 (1998) 1309-1314.

[5] E. Beutler, S. Duparc, G6PD Deficiency Working Group, Glucose-6-phosphate dehydrogenase deficiency and antimalarial drug development, Am. J. Trop. Med. Hyg., 77 (2007) 779-789.

[6] C.B. e Braga, A.C. Martins, A.D.E. Cayotopa, W.W. Klein, A.R. Schlosser, A.F. da Silva, M.N. de Souza, B.W.B. Andrade, J.A. Filgueira Jr, W. de Jesus Pinto, M. da Silva-Nunes, Side Effects of Chloroquine and Primaquine and Symptom Reduction in Malaria Endemic Area (Mâncio Lima, Acre, Brazil), Interdisc. Persp. Infect. Dis. 2015 (2015) 346853/1-346853/7.

[7] J.K. Baird, M.D. Lacy, H. Basri, M.J. Barcus, J.D. Maguire, M.J. Bangs, R. Gramzinski, P. Sismadi, L.J. Krisin, I. Wiady, M. Kusumaningsih, T.R. Jones, D.J. Fryauff, S.L. Hoffman, United States Naval Medical Research Unit 2 Clinical Trials Team, Randomized, parallel placebo-controlled trial of primaquine for malaria prophylaxis in Papua, Indonesia. Clin. Infect. Dis. 33 (2001) 1990-1997.

[8] G.N.L. Galappaththy, P. Tharyan, R. Kirubakaran, Primaquine for preventing relapse in people with Plasmodium vivax malaria treated with chloroquine, Cochrane database Syst. Rev. 10 (2013) CD004389/1- CD004389/34.

[9] J. Carmona-Fonseca, G. Alvarez, A. Maestre, Methemoglobinemia and adverse events in Plasmodium vivax malaria patients associated with high doses of primaquine treatment, Am. J. Trop. Med. Hyg. 80 (2009) 188-193.

[10] M.D. Karad, V.D. Barhate, Spectrophotometric determination of an antimalarial drug primaquine in bulk and pharmaceutical formulations, World J. Pharm. Res. 4 (2015) 2370-2377.

[11] M. Page-Sharp, K.F. Ilett, I. Betuela, T.M.E. Davis, K.T. Batty, Simultaneous determination of primaquine and carboxyprimaquine in plasma using solid phase extraction and LC-MS assay, J. Chromatogr. B 902 (2012) 142-146.

[12] J.J.A. van Kampen, P.C. Burgers, R. de Groot, T.M. Luider, Qualitative and quantitative analysis of pharmaceutical compounds by MALDI-TOF mass spectrometry, Anal. Chem. 78 (2006) 5403-5411.

[13] L. Zuluaga-Idarraga, N. Yepes-Jimenez, C. Lopez-Cordoba, S. Blair-Trujillo, Validation of a method for the simultaneous quantification of chloroquine, desethylchloroquine and primaquine in plasma by HPLC-DAD, J. Pharm. Biomed. Anal. 95 (2014) 200-206.

[14] K. Na-Bangchang, E.A. Guirou, A. Cheomung, J. Karbwang, Determination of Primaquine in Whole Blood and Finger-Pricked Capillary Blood Dried on Filter Paper Using HPLC and LCMS/MS, Chromatographia 77 (2014) 561-569.

[15] M.L.P.M. Arguelho, M.V.B. Zanoni, N.R. Stradiotto, Electrochemical oxidation and voltammetric determination of the antimalaria drug primaquine, Anal. Lett. 38 (2005) 1415-1425.

[16] B.B. Saad, Z.A. Zahid, S.A. Rahman, M.N. Ahmad, A.H. Husin, Primaquine-selective electrodes based on macrocyclic crown ethers, Analyst, 117 (1992) 1319-1321.

[17] T. John, S. Rani, R. Hiremath, Colorimetric method for the estimation of primaquine phosphate, Indian Drugs 33 (1996) 293.

[18] M. Tsuchiya, E. Torres, J.J. Aaron, J.D. Winefordner, Photochemical fluorimetric determination of primaquine in a flowing solvent with application to blood serum, Anal. Lett. 17 (1984) 1831-1841.

[19] O.A. Farghaly , R.S.A. Hameed, A.A.H. Abu-Nawwas, Analytical application using modern electrochemical techniques, Int. J. Electrochem. Sc. 9 (2014) 3287-3318.

[20] N. Thapliyal, R.V. Karpoormath, R.N. Goyal, Electroanalysis of antitubercular drugs in pharmaceutical dosage forms and biological fluids: a review, Anal Chim Acta, 853 (2015) 59-76.

[21] M.H. Mashhadizadeh, M. Akbarian, Voltammetric determination of some anti-malarial drugs using a carbon paste electrode modified with $Cu(OH)_2$ nano-wire, Talanta, 78 (2009) 1440-1445.

[22] C. Li, S. Liu, T.S. Luk, J. J. Figiel, I. Brener, S.R.J. Brueck, G.T. Wang, Intrinsic polarization control in rectangular GaN nanowire lasers, Nanoscale, 8 (2016) 5682-5687.

[23] K.R. Reddy, B.C. Sin, C.H. Yoo, W. Park, K.S. Ryu, J.S. Lee, D. Sohn, Y. Lee, A new one-step synthesis method for coating multi-walled carbon nanotubes with cuprous oxide nanoparticles, Scripta Materialia, 58 (2008) 1010-1013.

[24] A.M. Showkat, Y.P. Zhang, M.S. Kim, A.I. Gopalan, K.R. Reddy, K.P. Lee, Analysis of heavy metal toxic ions by adsorption onto amino-functionalized ordered mesoporous silica, Bulletin of the Korean Chemical Society, 28 (2007) 1985-1992.

[25] K.R. Reddy, K.P. Lee, A.I. Gopalan, M.S. Kim, A.M. Showkat, Y.C. Nho, Synthesis of metal (Fe or Pd)/alloy (Fe-Pd)-nanoparticles-embedded multiwall carbon nanotube/sulfonated polyaniline composites by γ irradiation, Journal of Polymer Science, Part A: Polymer Chemistry, 44 (2006) 3355-3364.

[26] K.R. Reddy, K.P. Lee, A.I. Gopalan, Novel electrically conductive and ferromagnetic composites of poly(aniline-co-aminonaphthalenesulfonic acid) with iron oxide nanoparticles: synthesis and characterization, Journal of Applied Polymer Science, 106 (2007) 1181-1191.

[27] K.R. Reddy, M. Hassan, V.G. Gomes, Hybrid nanostructures based on titanium dioxide for enhanced photocatalysis, Applied Catalysis, A: General, 489 (2015) 1-16.

[28] K.R. Reddy, B.C. Sin, K.S. Ryu, J.C. Kim, H. Chung, Y. Lee, Conducting polymer functionalized multi-walled carbon nanotubes with noble metal nanoparticles: Synthesis, morphological characteristics and electrical properties, Synthetic Metals, 159 (2009) 595-603.

[29] M. Hassan, E. Haque, K.R. Reddy, A.I. Minett, J. Chen, V.G. Gomes, Edge-enriched graphene quantum dots for enhanced photo-luminescence and supercapacitance, Nanoscale, 6 (2014) 11988-11994.

[30] K.R. Reddy, K. Nakata, T. Ochiai, T. Murakami, D.A. Tryk, A. Fujishima, Facile fabrication and photocatalytic application of Ag nanoparticles-TiO2 nanofiber composites, Journal of Nanoscience and Nanotechnology, 11 (2011) 3692-3695.

[31] J. Zhang, M. Oyama, Gold nanoparticle arrays directly grown on nanostructured indium tin oxide electrodes: Characterization and electroanalytical application, Anal. Chim. Acta 540 (2005) 299-306.

[32] W. Wang, Y. Pang, J. Yan, G. Wang, H. Suo, C. Zhao, S. Xing, Facile synthesis of hollow urchin-like gold nanoparticles and their catalytic activity, Gold Bull. 45 (2012) 91-98.

[33] F. Xu, K. Cui , Y. Sun, C. Guo, Z. Liu, Y. Zhang, Y. Shi , Z. Li, Facile synthesis of urchin-like gold submicrostructures for nonenzymatic glucose sensing, Talanta 82 (2010) 1845-1852.

[34] S.N. Prashanth, K.C. Ramesh, J. Seetharamappa, Electrochemical oxidation of an immunosuppressant, mycophenolate mofetil, and its assay in pharmaceutical formulations, Int. J. Electrochem. 2011 (2011) 1-7.

[35] D.K. Gosser, Cyclic Voltammetry: Simulation and Analysis of Reaction Mechanisms, VHS, New York, 1993.

[36] E. Laviron, General expression of the linear potential sweep voltammogram in the case of diffusionless electrochemical systems, J. Electroanal. Chem. 101 (1979) 19-28.

[37] A.J. Bard, L.R. Faulkner, Electrochemical methods: Fundamentals and applications (2nd ed.), Wiley, New York, 2004, pp. 236.

[38] A. Ullah, A. Rauf, U.A. Rana, R. Qureshi, M.N. Ashiq, H. Hussain, H.B. Kraatz, A. Badshah, A. Shah, pH dependent electrochemistry of anthracenediones at a glassy carbon electrode, J. Electrochem. Soc. 162 (2015) H157-H163.

CHAPTER 5

A Highly Dispersed Multi-walled Carbon Nanotubes and Poly(methyl orange) Based Electrochemical Sensor for the Determination of an Anti-Malarial Drug: Amodiaquine

Tirivashe Elton Chiwunze[a], Venkata Narayana Palakollu[a], Atal A.S. Gill[a], Francis Kayamba[a], Neeta Bachheti Thapliyal[a,b], Rajshekhar Karpoormath[a]*

[a]Department of Pharmaceutical Chemistry, College of Health Sciences, University of KwaZulu-Natal, Durban 4000, South Africa.

[b]Department of Applied Sciences, Women Institute of Technology, Dehradun 248007, India.

***Corresponding Author**

Dr. Rajshekhar Karpoormath

Tel: +27-312607179, Fax: +27-312607792

Email: karpoormath@ukzn.ac.za

Materials Science & Engineering C 97 (2019) 285–292

Contents lists available at ScienceDirect

Materials Science & Engineering C

journal homepage: www.elsevier.com/locate/msec

A highly dispersed multi-walled carbon nanotubes and poly(methyl orange) based electrochemical sensor for the determination of an anti-malarial drug: Amodiaquine

Tirivashe Elton Chiwunze[a], Venkata Narayana Palakollu[a], Atal A.S. Gill[a], Francis Kayamba[a], Neeta Bachheti Thapliyal[a,b], Rajshekhar Karpoormath[a,*]

[a] Department of Pharmaceutical Chemistry, College of Health Sciences, University of KwaZulu-Natal, Durban 4000, South Africa
[b] Department of Applied Sciences, Women Institute of Technology, Dehradun 248007, India

ARTICLE INFO

Keywords:
Amodiaquine
Multi-walled carbon nanotubes
Poly(methyl orange)
Electrochemical determination
Voltammetry

ABSTRACT

A glassy carbon electrode modified with electrochemically polymerized methyl orange (PMO) and multi-walled carbon nanotubes (MWCNT) was developed. The morphologies of the fabricating materials (PMO and MWCNT) were investigated by field-emission scanning electron microscopy (FE-SEM). The designed sensor was used for the sensitive determination of amodiaquine (AQ), an anti-malaria drug. AQ was developed as an alternative to chloroquine because of its activity against chloroquine-resistant *Plasmodium falciparum* (*P. falciparum*) parasites. The modified electrode was employed to study the electrochemical oxidation of AQ using cyclic voltammetry (CV) and differential pulse voltammetry (DPV) techniques. Under optimal experimental conditions, DPV exhibited a linear response in the concentration range from 1.0×10^{-7} to 3.5×10^{-6} mol L^{-1} with a limit of detection (LOD) of 8.9×10^{-8} mol L^{-1}. Furthermore, the number of electrons and protons involved in the electrochemical study of AQ was also calculated and a plausible mechanism for the electro-oxidation of AQ was deduced. The developed sensor demonstrated analytical applicability as it was successfully employed to determine the drug AQ in pharmaceutical formulations and human urine samples.

Abstract

A glassy carbon electrode modified with electrochemically polymerised methyl orange (PMO) and multi-walled carbon nanotubes (MWCNT) was developed. The morphologies of the fabricating materials (PMO and MWCNT) were investigated by field-emission scanning electron microscopy (FE-SEM). The designed sensor was used for the sensitive determination of amodiaquine (AQ), an anti-malaria drug. AQ was developed as an alternative to chloroquine because of its activity against chloroquine-resistant *Plasmodium falciparum (P. falciparum)* parasites. The modified electrode was employed to study the electrochemical oxidation of AQ using cyclic voltammetry (CV) and differential pulse voltammetry (DPV) techniques. Under optimal experimental conditions, DPV exhibited a linear response in the concentration range from 1.0×10^{-7} to 3.5×10^{-6} mol L^{-1} with a limit of detection (LOD) of 8.9×10^{-8} mol L^{-1}. Furthermore, the number of electrons and protons involved in the electrochemical study of AQ was also calculated and a plausible mechanism for the electro-oxidation of AQ was deduced. The developed sensor demonstrated analytical applicability as it was successfully employed to determine the drug AQ in pharmaceutical formulations and human urine samples.

Keywords: Amodiaquine; Multi-walled carbon nanotubes; Poly(methyl orange); Electrochemical determination; Voltammetry

1. Introduction

Amodiaquine (AQ) is an anti-malarial drug that belongs to the group of 4-aminoquinolines (Figure 1). It is a Mannich base which has a similar mode of action as that of chloroquine [1]. AQ was developed as an alternative to chloroquine because of its activity against chloroquine-resistant *Plasmodium falciparum (P. falciparum)* parasites [2]. Initially, it was used as a malaria prophylaxis, however, it was dropped from the essential drugs list due to its severe adverse effects that include agranulocytosis and hepatitis [3, 4]. Recently, the drug has been re-introduced in an Artesunate based combination therapy against drug resistance in *P. falciparum* [5-7]. The increase in usage of Amodiaquine-Artesunate combination therapy makes it paramount to develop an accurate and easy to use analytical method for quality control and clinical analysis. Due to the flooding of counterfeit and substandard medicines on the market, quality control of marketed medicines is very crucial, especially in third world countries.

There are many analytical techniques described in the literature for the quantification of AQ. The commonly used methods are high-performance liquid chromatography (HPLC), fluorimetry, spectrophotometry and capillary electrophoresis [8-14]; electrochemical methods provide a better alternative because of its practical advantages that includes high sensitivity, high selectivity, and above all its reliability at a low cost [15-18]. Additionally, electroanalytical methods have attracted more attention in recent years for environmental and biological compound analysis due to their simple preparation by modifying the electrodes with different types of materials to achieve suitable chemical selectivity without any complicated alterations to the instrument [19-25]. To the best of our knowledge, only two studies on electroanalytical techniques for quantitative analysis of AQ have been reported [26, 27]. Hence, there is a high demand for developing new and more efficient electrochemical methods for detection and quantification of AQ.

In the past few decades, many different transducers have been utilized in fabricating electrodes for chemical sensing over the past few decades. Recently, conducting polymers and nanomaterials have widely been utilized in the application as fabricating material in electrochemistry because of their enhanced conductivity [20, 28-35]. Various methodologies for the preparation of polymers have been reported over the years. Electrochemical polymerisation is increasingly becoming the preferred method over the conventional synthetic route for making polymers. Electrochemical polymerisation enables the deposition of a homogeneous layer of polymer that is stable and strongly adheres to the electrode surface [36]. Methyl orange (MO) is an organic dye that can form polymers and has the ability to facilitate proton and electron transfer. Methyl orange polymers (PMOs) have not been exploited enough as electrode modifiers with only three papers reported to date, Reddaiah *et al*., Giribabu *et al* and most recently Bairagi *et al* [37-39].

Over the decades, nanostructured carbon materials have attracted considerable attention, especially multi-walled carbon nanotubes (MWCNT) due to their extraordinary structural, mechanical, electrochemical and electrical properties. They have shown great promise in the field of material science with wide application in various fields of research such as optics[40], field-emission [41], nanoscale electronics [42], sensors [43] and electrochemistry [44, 45]. The ability of MWCNT to promote redox reactions has qualified them to be excellent candidates for electrode modifying material for electrochemical sensors [46-50]. One of the major challenges of working with MWCNT is their inability to properly disperse in solvents. They tend to coagulate due to the strong Van der Waals interactions between the nanotubes. However, acid yellow 9 (AY) can be used as an effective dispersing agent and stabiliser for MWCNT as reported by S. A. Kumar *et al* in 2010 [51].

Based on all of the above-mentioned facts, this work was aimed at developing a facile strategy based electrochemical sensor with electrochemically polymerized methyl orange and uniformly dispersed MWCNT with the aid of acid yellow 9 solution. Thus, the novelty of the work lies in

the use of PMO and MWCNT as a combination for development of electrochemical sensor for determination of AQ. The developed sensor exhibited improved performances such as enormous enhancement in the peak current, sensitivity, low detection limit. Moreover, the developed electrochemical sensor was also successfully applied for the determination of AQ content in pharmaceutical formulations and human urine.

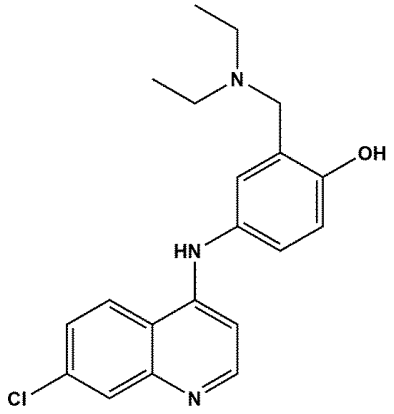

Fig. 1 Structure of Amodiaquine

2. Experimental

2.1. Apparatus and chemical reagents

All the electrochemical measurements were carried out using a CHI660E electrochemical workstation (CH Instrument, USA). A conventional three-electrode system purchased from CH Instrument, USA, was employed at 25 ± 1 °C. All three electrodes, an Ag/AgCl/NaCl (3.0 mol L^{-1}) electrode, a platinum wire and a glassy carbon electrode (3.0 mm in diameter) were used as the reference, auxiliary and working electrodes, respectively. An EXTECH PH60 (China) pH meter was used to perform all pH measurements. FE-SEM (ZEISS Ultra Plus, Germany) was used to study the surface morphology of materials.

Amodiaquine hydrochloride and Primaquine bisphosphate were acquired from Sigma-Aldrich. Buffer solutions were prepared using sodium phosphate dibasic and monosodium dihydrogen orthophosphate from Merck. MWCNT, methyl orange, acid yellow 9 and all other chemicals

utilized in the experiments were procured from Sigma-Aldrich and were of analytical grade. Deionized water was used for the preparation of all aqueous solutions.

2.2. Preparation of homogeneous MWCNT dispersion

Uniformly dispersed MWCNT were prepared by suspending 10 mg of MWCNT in 10 mL of 2.5 mmol L^{-1} AY solution. Thereafter, the solution was sonicated for about an hour to achieve a homogenous mixture. The MWCNT/AY solution remained stable and no coagulation was observed for over a month.

2.3. Preparation of MWCNT/PMO/GCE

Prior to modification, the GCE surface was polished to a mirror shine using 0.3 and 0.05 μm of alumina slurry on a microcloth pad and then followed by a thorough rinsing with deionized water to remove any adsorbed alumina. The cleaned GCE was then placed into an electrochemical cell with 1.25 mmol L^{-1} of methyl orange in 0.1 mol L^{-1} PBS (pH 7.0) and was scanned for 20 successive CV cycles, between the window range from -0.6 to 1.4 V at a scan rate of 0.05 V s^{-1} [39]. Figure 2 shows the development of PMO coat onto the glassy carbon electrode in 0.1 mol L^{-1} PBS (pH 7.0) as supporting electrolyte. As the polymerization progresses the CV cycles start to condense which is an indication that the PMO film is depositing on the electrode surface. After completion of the cycles, the excess methyl orange was washed off with deionized water and a thin layer of conductive layer of PMO remained. This modified electrode was annotated as PMO/GCE.

A suspension of MWCNT/AY was further used to modify the PMO/GCE by casting 6μL onto the surface and dried it under an IR lamp for 30 min. Then, the electrode was dipped into PBS buffer for two minutes to wash off the acid yellow dye and was further dried for 10 more minutes. The electrode was denoted as MWCNT/PMO/GCE and was used for all electrochemical experiments.

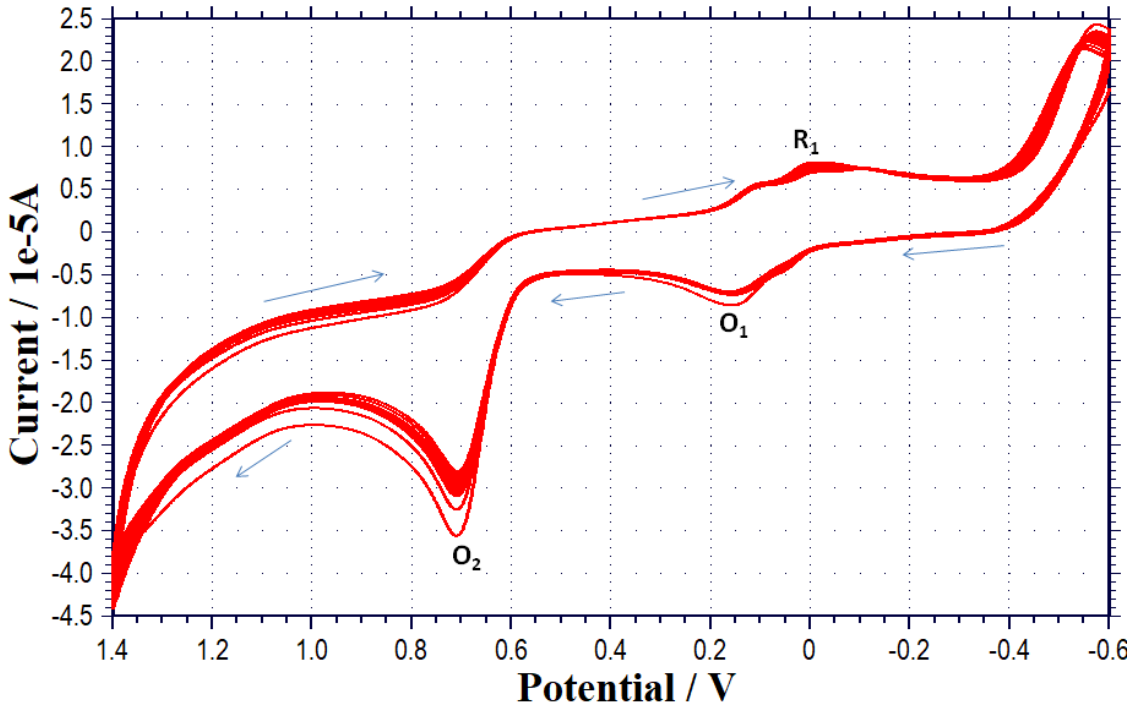

Fig. 2 Cyclic voltammograms for the electrochemical polymerization of methyl orange at GCE.

2.4. Preparation of tablet and urine sample

Two commercially available AQ tablets weighing an average of 715 mg (ASAQ-Denk containing 270 mg of AQ per tablet) were ground into fine particles. 250 mg of the fine powder was then dissolved in 200 ml of de-ionized water and filtered off the residues. The amount in the AQ in the pharmaceutical formulation was then determined by taking suitable dilutions that fall within the linear concentration range and conducting voltammetric analysis using the proposed DPV procedure. Also, the recovery study was carried out by the standard addition of known concentrations of AQ into the solution used in the tablet analysis and measuring the increase in the current peak. For the biological matrix, urine sample was provided by a middle aged male volunteer for analysis and diluted 100 fold with 0.1 mol L^{-1} PBS (pH 6.5). A range of known amounts of AQ solution were spiked into the urine sample for the practical applicability for detection of AQ.

3. Results and discussion

3.1. FE-SEM characterization

Figure 3 shows the surface morphologies of PMO and MWCNT/PMO acquired using field emission scanning electron microscopy (FE-SEM) at low (Figure 3A and 3C) and high (Figure 3B and 3D) magnification. The low magnification image of PMO (Figure 3A) displayed a dense growth of a dendrite-like structure, while at high magnification (Figure 3B) it showed a uniformly arranged structure with porous-like features. The micrographs (Figure 3C and 3D) show a good dispersion of MWCNT that form a spaghetti-like distribution with PMO on the surface of a GCE.

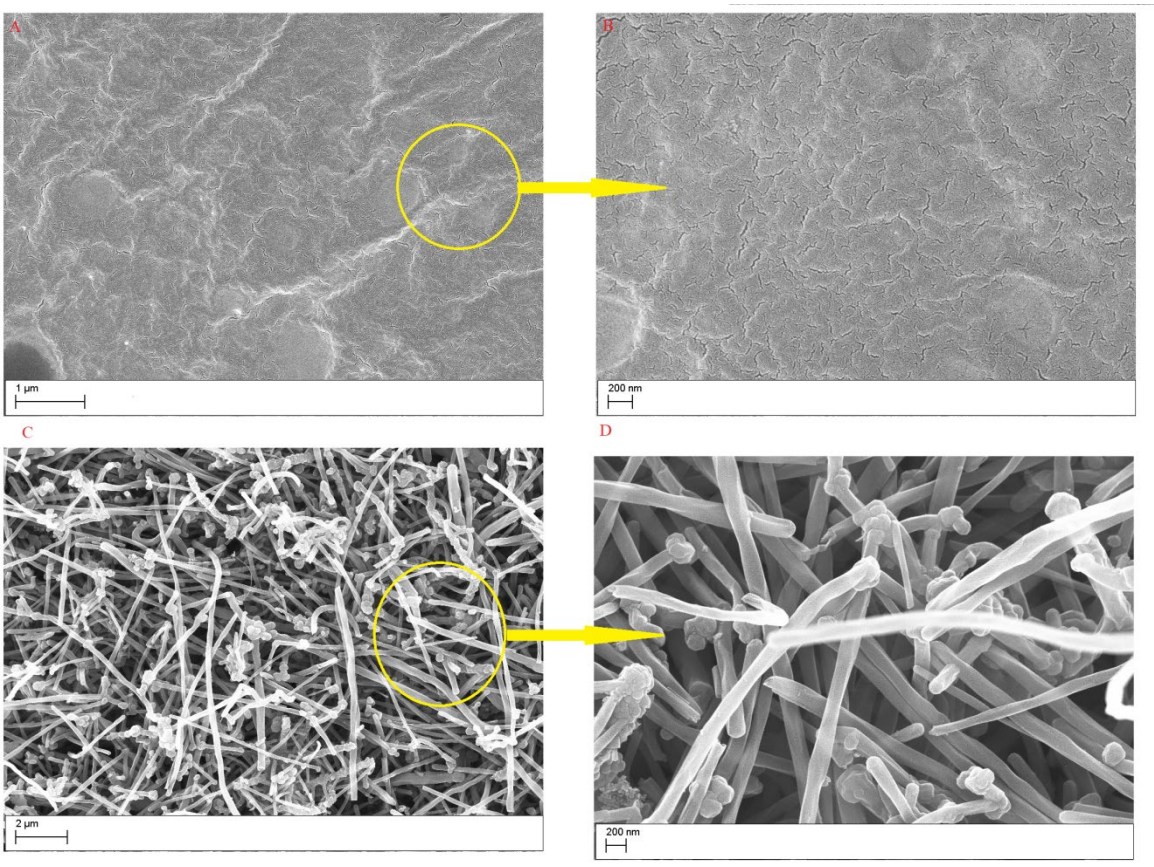

Fig. 3 SEM images PMO (A, B) and MWCNT/PMO (C, D) at low (A, C) and high (B, D) magnifications.

3.2. Electrochemical behaviour of AQ

The electrochemical behaviour of AQ was initially investigated at bare GCE using CV (Figure 4A) from the window of -0.4 to 1.4 V in 0.1 mol L^{-1} PBS of pH 6.5. Three distinctive peaks were observed with two oxidative peaks (O_1 and O_2) and one reduction peak (R_1) indicating the presence of two oxidizable groups in the structure of AQ. For this study, we used the aforementioned window of -0.4 to 1.4 V to investigate the electrochemical behaviour of AQ at GCE, MWCNT/GCE, PMO/GCE and MWCNT/PMO/GCE (Figure 4).

As can be observed from the Figure 4, the bare GCE (blue) displayed poor sensitivity towards the detection of AQ. However, the modified electrodes; PMO/GCE (pink) and MWCNT/GCE (green) proved to have better sensitivity as they significantly increased the current peaks with a positive shift in the peak potentials. PMO/GCE exhibited poorly defined redox peaks and a greater ΔE_p (between peak O_1 and R_1) as compared to MWCNT/GCE which is an indication that electron-transfer kinetics is slower at the electrode. As expected, the combination of the two materials yielded a better response than the individual entities. Thus, a notable enhancement in the peak currents of AQ was observed at the surface of MWCNT/PMO/GCE (orange). This behaviour reveals that the combination of PMO and MWCNT onto a GCE holds a great potential as an electrochemical sensor for AQ. The ΔE_p between the oxidation peak O_1 and reduction peak R_1 was observed to be greater than 100 mV which is an indication that the MWCNT/PMO/GCE electrode process is quasi-reversible [52].

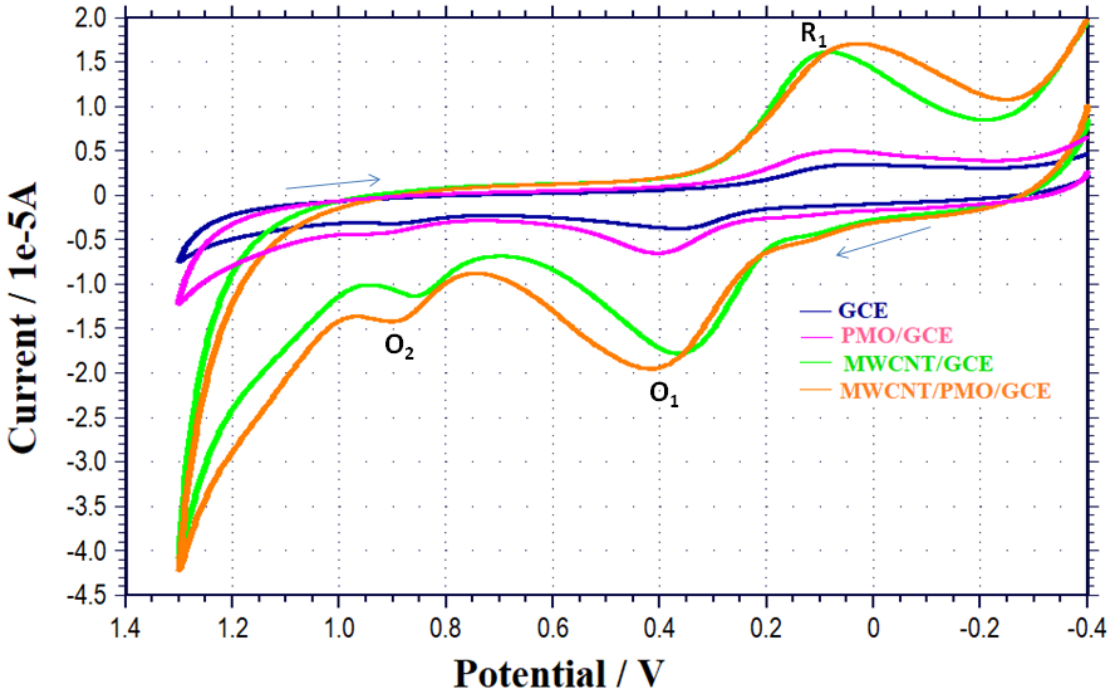

Fig. 4 A Cyclic voltammograms for the electrochemical response of 0.05 mmol L^{-1} AQ in 0.1 mol L^{-1} PBS (pH 6.5) at (a) bare GCE, (b) PMO/GCE, (c) MWCNT/GCE and (d) MWCNT/PMO/GCE at scan rate of 100 mV s^{-1}.

3.3. Effect of solution pH

The pH exerted a tremendous influence on the electrochemical response of AQ at MWCNT/PMO/GCE. For optimization of electrolyte solution pH, the voltammetric responses of AQ were recorded over the pH range of 3.0 to 11.0. It was observed that as the pH of the system gets more basic, all the three peak potentials of AQ shifted towards the negative potential direction which suggests a proton-coupled electron transfer [53]. Figure 5A demonstrates the pH dependence of AQ at MWCNT/PMO/GCE and all three peaks exhibited a linear relationship between the pH and E_p (Figure B, C and D). The linear regression equations can be expressed as follows:

$$E_p\,(V) = 0.7798 - 0.0607pH; \quad R^2 = 0.9759, \text{(peak } O_1\text{)} \qquad (1)$$

$$E_p\,(V) = 1.2782 - 0.0598pH; \quad R^2 = 0.9746, \text{(peak } O_2\text{)} \qquad (2)$$

$$E_p\,(V) = 0.3411 - 0.0437pH; \quad R^2 = 0.9756, \text{(peak } R_1\text{)} \qquad (3)$$

From the graphs, the values of the slopes were close to the theoretical value of 0.059 V/pH indicating that equal number of protons and electrons are involved in the electro-oxidation and reduction processes of AQ at MWCNT/PMO/GCE [54]. Moreover, the best pH was selected to be 6.5, as it exhibited optimum peak currents for all the three peaks. This pH was then utilized for all the subsequent electrochemical experiments.

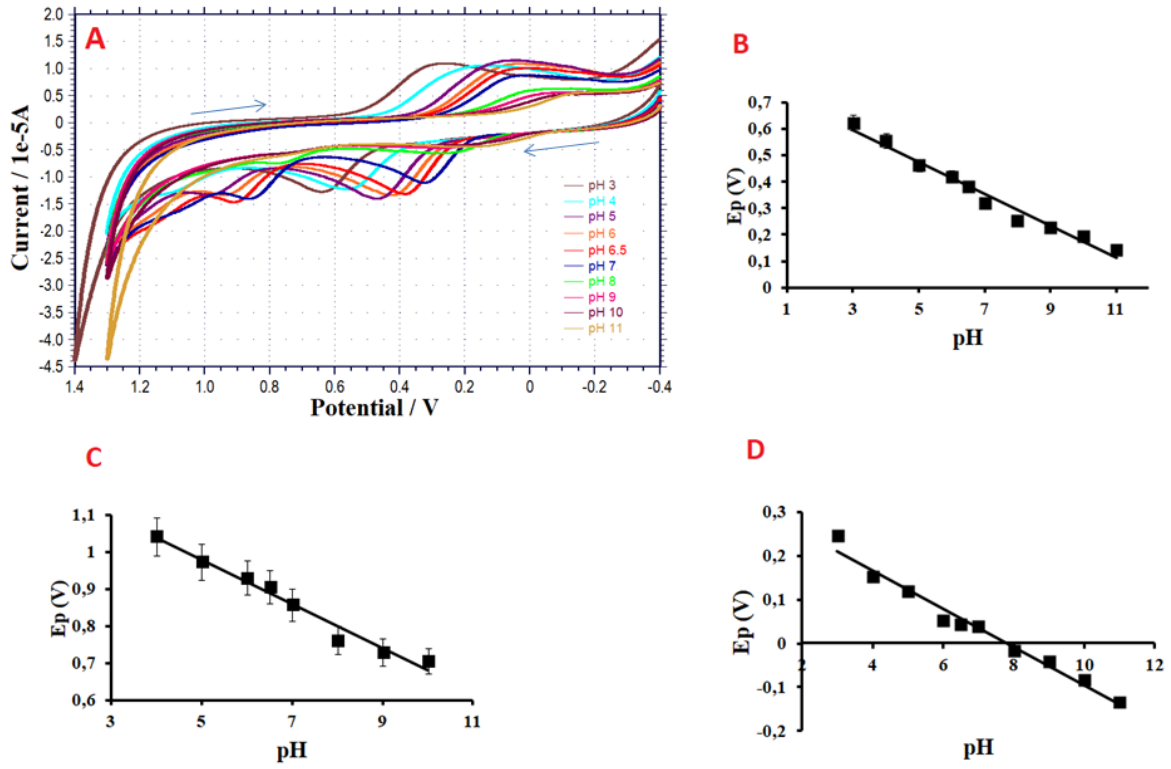

Fig. 5 (A) Cyclic voltammograms displaying the effect of pH on the oxidation and reduction peaks response for 0.05 mmol L^{-1} AQ at MWCNT/PMO/GCE from pH 3.0 to 11.0. (B, C and D) show the linear relationships between the pH and the E_p values of peaks O_1, O_2 and R_1 respectively.

3.4. Effect of scan rate

The effect of different scan rates on the voltammetric response of 0.05 mmol L^{-1} AQ in 0.1 molL^{-1} PBS (pH 6.5) was analysed (Figure.6A). The peak currents were found to display a linear dependence with the square root of scan rates (Figure 6B, 6C and 6D) which indicates that both the electro-oxidation and reduction of AQ at MWCNT/PMO/GCE are diffusion-controlled processes [55]. The corresponding linear regression equations can be expressed as,

$$I_{pa}\,(\mu A) = 1.3407v^{1/2}\,(V\,s^{-1})^{1/2} - 2.1040; \quad R^2 = 0.9883 \text{ (peak } O_1) \qquad (4)$$

$$I_{pa}\,(\mu A) = 1.8917v^{1/2}\,(V\,s^{-1})^{1/2} - 3.3788; \quad R^2 = 0.9780 \text{ (peak } O_2) \qquad (5)$$

$$I_{pa}\,(\mu A) = 2.0166v^{1/2}\,(V\,s^{-1})^{1/2} - 3.3807; \quad R^2 = 0.9860 \text{ (peak } R_1) \qquad (6)$$

The plots of log I_{pa} vs log v further confirmed that the processes are indeed diffusion- controlled. The linear plots gave slopes close to the theoretical value 0.5 for an ideally diffusion-controlled process [56]. The plots are represented by the equations below,

$$\log I_{pa}\,(\mu A) = 0.6652 \log v\,(V\,s^{-1}) - 0.2859; \qquad R^2 = 0.9976 \text{ (peak } O_1) \qquad (7)$$

$$\log I_{pa}\,(\mu A) = 0.6922 \log v\,(V\,s^{-1}) - 0.2109; \qquad R^2 = 0.9845 \text{ (peak } O_2) \qquad (8)$$

$$\log I_{pa}\,(\mu A) = 0.6978 \log v\,(V\,s^{-1}) - 0.1802; \qquad R^2 = 0.9846 \text{ (peak } R_1) \qquad (9)$$

In addition, the E_p exhibited dependence towards the scan rate; for the oxidation peaks O_1 and O_2 the E_p shifted to the more positive potentials with an increase in v while the Ep for the reduction peak R_1 shifted to a more negative potential. The Linear relationships between the E_p and the logarithm of v were observed with the following linear equations.

$$E_p\,(V) = 0.088\log v\,(Vs^{-1}) + 0.237; \qquad R^2 = 0.9821 \text{ (peak } O_1) \qquad (10)$$

$$E_p\,(V) = 0.0689\log v\,(Vs^{-1}) + 0.7506; \; R^2 = 0.9747 \text{ (peak } O_2) \qquad (11)$$

$$E_p\ (V) = -0.0908 \log v\ (Vs^{-1}) + 0.2192;\ R^2 = 0.9953\ (\text{peak } R_1) \qquad (12)$$

According to Laviron the relationship of E_p and log □ can be defined by the following equation [57],

$$Ep = E° + \left(\frac{2.303RT}{\alpha nF}\right) Log \left(\frac{RTk°}{\alpha nF}\right) + \left(\frac{2.303RT}{\alpha nF}\right) Log\ \upsilon \qquad (13)$$

where $E^{0'}$ is the formal redox potential, α is the electron transfer coefficient, n is the number of electrons involved and k^0 is the standard rate constant of the surface reaction. The other symbols have their standard meanings. The slope of the plot E_p vs log v was used to deduce the value of αn by considering the following constants as R=8.314 J/K mol, T = 298 K and F = 96480 C mol^{-1}. The value of α can be calculated using the Bard and Faulkner equation below [58],

$$\alpha = \frac{47.7}{Ep - Ep_{1/2}} \qquad (14)$$

where $E_{p1/2}$ is defined as the potential that corresponds to half the peak current. From the above formulae, the number of electrons involved in the electro-oxidation of AQ at MWCNT/PMO/GCE was calculated to be two; with each peak O_1 and O_2 involving one electron each. The reduction process was also found to involve two electrons and two protons

Based on the data extrapolated from both the pH and scan rate studies a plausible mechanism for the electro-oxidation of AQ that involves two electrons and two protons has been proposed in scheme 1.

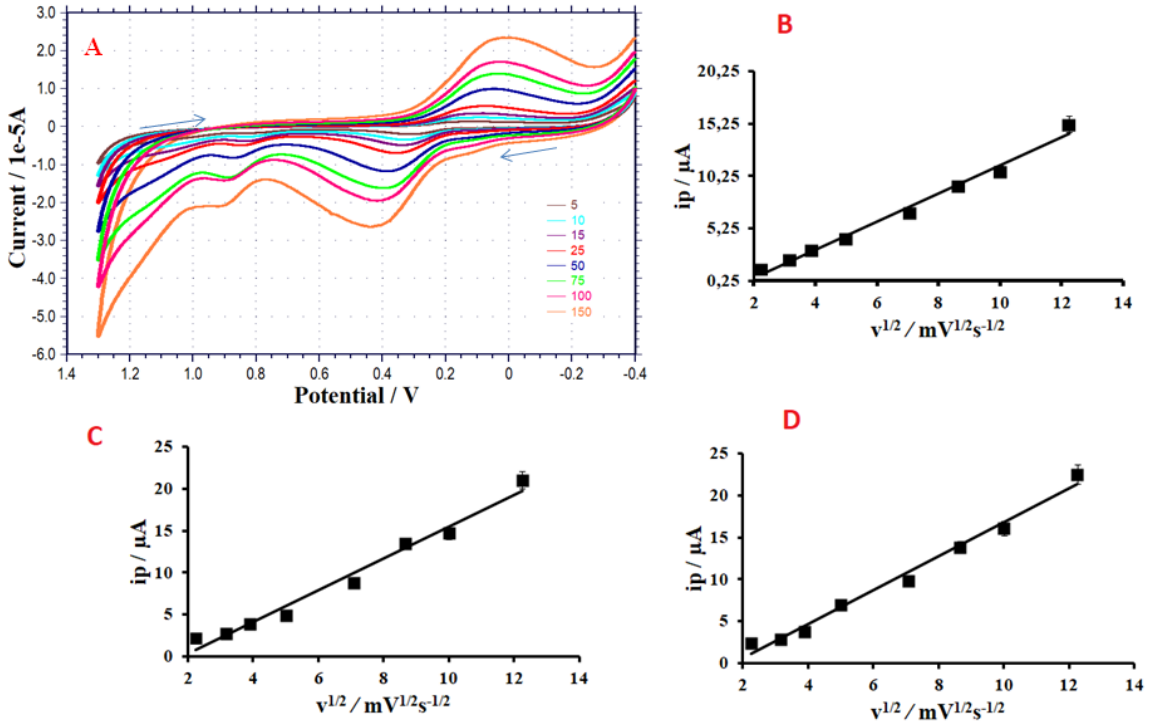

Fig. 6 (A) Cyclic voltammograms observed at varying scan rates: 5-150 mVs. (B,C and D) Variation of peak currents (O_1, O_2 and R_1 respectively) with the square root of scan rate observed for 0.05 mmol L^{-1} AQ (pH 6.5) at MWCNT/PMO/GCE.

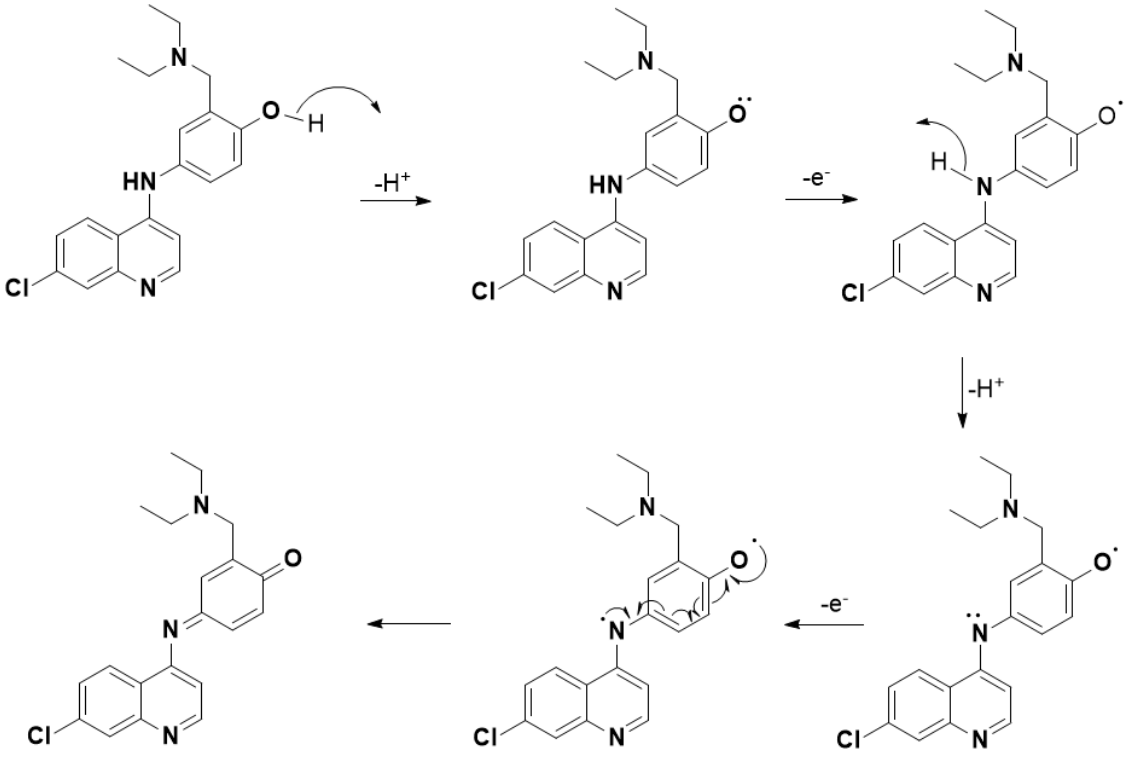

Scheme 1. Plausible electrochemical oxidation mechanism of AQ

3.5. Electrochemical determination of AQ

The main objective of this work was to develop a modified electrode capable of facilitating electrocatalytic oxidation of AQ. From here onwards we only focused on the oxidation peak O_1 as it showed better sensitivity and reproducibility than the other oxidation peak O_2. In order to evaluate the catalytic ability of the developed MWCNT/PMO/GCE electrode, DPV was selected as the electroanalytical technique to be used. DPV voltammograms were obtained under optimized experimental conditions in 0.1 mol L^{-1} PBS with varying concentrations of AQ (Figure 7A). A linear relationship was observed between the current peak and the concentration of AQ within the range of 1.0 x 10^{-7} to 3.5 x 10^{-6} mol L^{-1}. The linear regression observed (Figure 7B) in the aforementioned concentration range was expressed as below:

$$I_p\ (\mu A) = 7.8635C\ (\mu\ mol\ L^{-1}) + 2.1913;\ (R^2 = 0.9983) \qquad (15)$$

where I_p represents the peak current and C is the concentration of AQ. The detection limit was found to be 8.9×10^{-8} mol L^{-1} using the relation 3S/N where S is the standard deviation of the blank response and N is the slope of the calibration curve. Table 1 shows the comparison of the analytical performance of MWCNT/PMO/GCE for quantification of AQ with previously reported literature. It is evident that the proposed method proved to be superior by exhibiting much improved analytical characteristics such as the lowest limit of detection (LOD), wide linear concentration range and analytical applicability for the quantification of AQ in both the drug formulations and human urine samples.

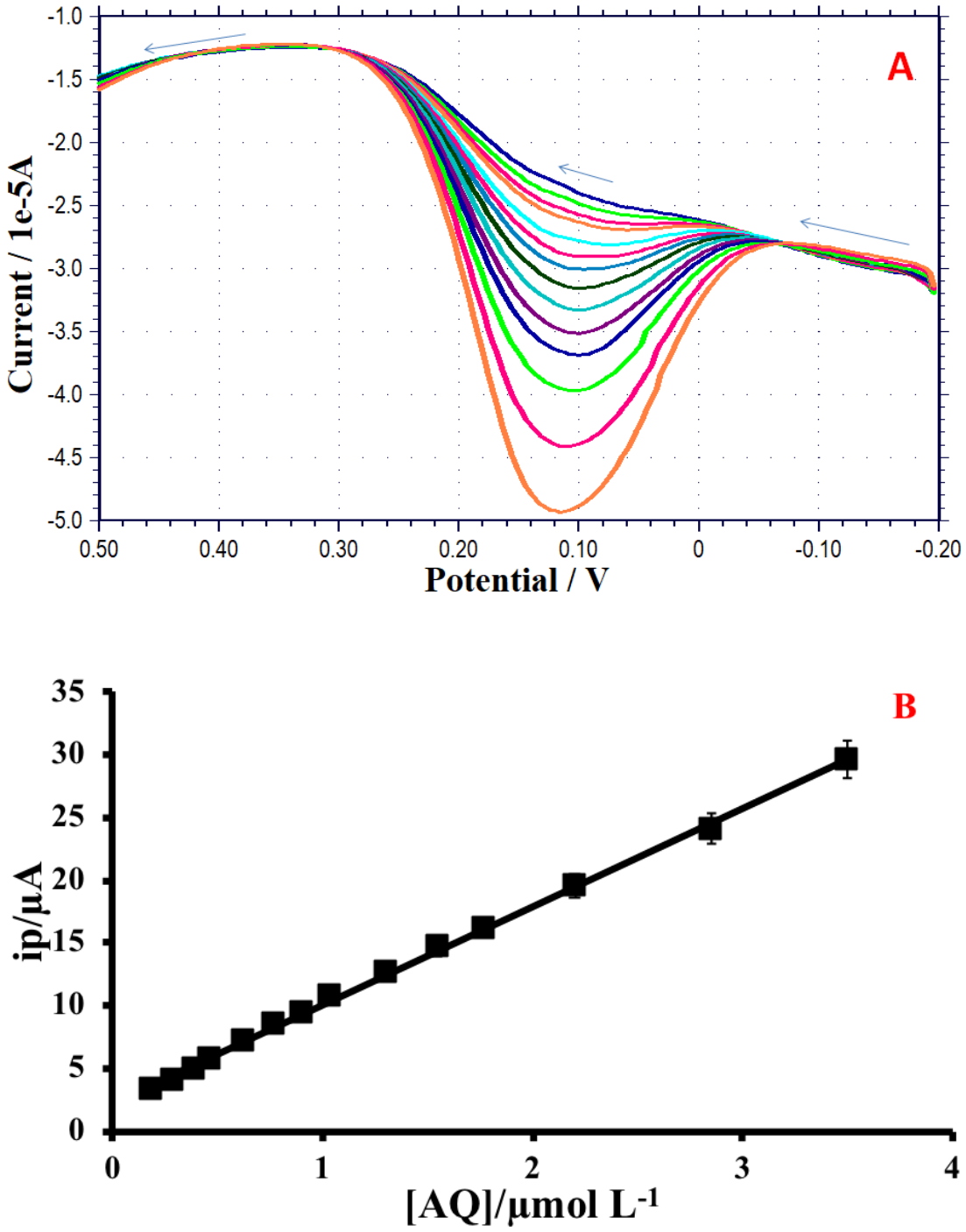

Fig. 7 (A) DP voltammograms of AQ with the different concentrations in 0.1 mol L^{-1} PBS (pH 6.5). **(B)**. Calibration plot of concentration of AQ vs I_p.

Table 1. A comparison of electrochemical methods reported for the determination of AQ.

Electrode	Concentration range (in mol L^{-1})	LOD (in mol L^{-1})	Matrix	Ref
Hemin-Based Electrode	1.9×10^{-5} to 1.0×10^{-4}	7.04×10^{-6}	Maternal milk	[26]
PVC membrane sensors *	3.2×10^{-6} to 2.0×10^{-2}	NR	Pharmaceutical formulations	[27]
MWCNT/PMO/GCE	1.0×10^{-7} to 3.5×10^{-6}	8.90×10^{-8}	Pharmaceutical formulations Human urine	This work

*PVC: Poly vinyl chloride; NR: not recorded.

3.6. Interference study

The effect of various common interfering substances in the determination of AQ using MWCNT/PMO/GCE was investigated by using 1000 fold concentration of glucose, starch, citric acid uric acid, ascorbic acid and a range of ionic salts (Mg^{2+}, K^{+}, Na^{+}, SO_4^{2-}, Cl^{-}). The results revealed that the interfering substances did not cause an error greater than 5% for determination of AQ. The interference effect of quinolines was also assessed by using Primaquine as a representative of the quinolines class of drugs. It was found that Primaquine did not interfere in the electrochemical determination of AQ up to 5-fold excess. Thus the proposed method was able to quantify AQ even in the presence of the excipients, suggesting that MWCNT/PMO/GCE is highly selective towards AQ.

3.7. Real sample analysis

In order to evaluate the practical utility of the proposed method, we used it to quantify the content of AQ in commercially available pharmaceutical tablets. The tablet analysis was carried

out under optimal DPV conditions and using the procedure outlined in the experimental section. The results were found to be in-line with the claim on the drug label and a low bias percentage of 1.6% as shown in Table 2.

The recovery studies of the real sample were calculated using the standard addition method and are reported in Table 2. The standard addition curve Figure 8 showed a similar linear relationship as that obtained in the concentration study; both graphs illustrated almost similar slopes. This proves that the excipients found in the tablets do not interfere with our proposed method which makes it an efficient and reliable tool for the analysis of AQ in pharmaceutical formulations. Below is the linear regression of the standard addition curve:

$$i_p\ (\mu A) = 7.99\ C\ (\mu mol\ L^{-1}) + 2.42; \qquad (R^2 = 0.9795) \tag{16}$$

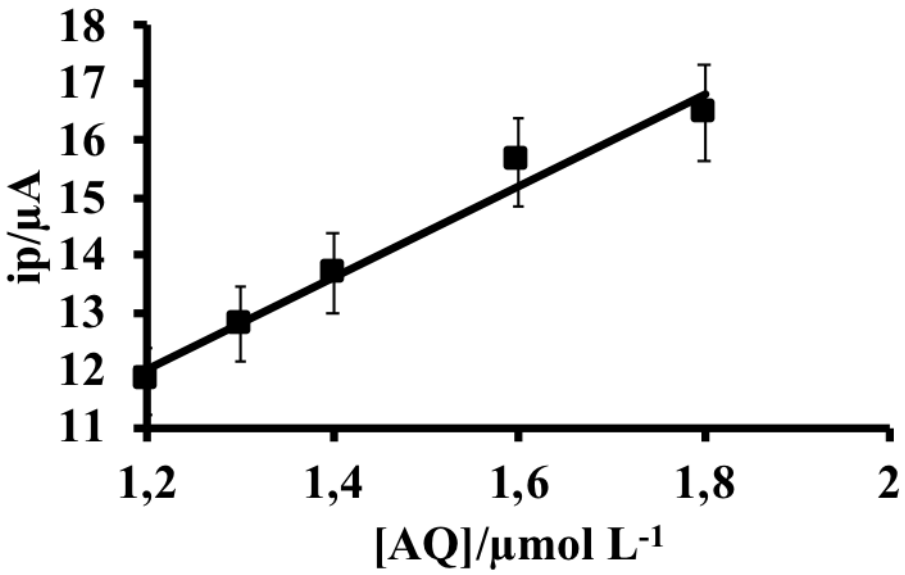

Fig. 8 Standard addition curve of AQ in the pharmaceutical sample.

Table 2. Assay results from AQ tablet at MWCNT/PMO/GCE.

Sample	Add (µmol L^{-1})	Expected (µmol L^{-1})	Detected (µmol L^{-1})	Recovery (%)	Bias (%)
Tablet	0.0	1.0	1.016	101.6	1.6
Spike 1	0.2	1.2	1.223	101.9	1.9
Spike 2	0.3	1.3	1.349	103.8	3.8
Spike 3	0.4	1.4	1.462	104.4	4.4
Spike 4	0.6	1.6	1.651	103.2	3.2
Spike 5	0.8	1.8	1.821	101.1	1.1

Additionally, the developed DPV method was assessed for the analytical applicability to determine AQ in a human urine sample. Urine samples were collected from a healthy volunteer and prior analysis the sample was diluted a 100 fold with 0.1 mol L^{-1} PBS (pH 6.5). Different concentrations of AQ were spiked into the sample using the standard addition method. The calculated recovery results are presented in Table 3 and were found to be in the range of 102.0 to 104.0%. Thus this method can be utilised in the determination of AQ in human samples.

Table 3. Recovery results obtained for AQ in a human urine sample at MWCNT/PMO/GCE.

S. No	Added (mol L^{-1})	Found (mol L^{-1})	Recovery (%)
1	2.00×10^{-7}	2.04×10^{-7}	102.0
2	3.00×10^{-7}	3.12×10^{-7}	104.0
3	4.00×10^{-7}	4.08×10^{-7}	102.3

4. Conclusions

In summary, this work presents a simple and highly sensitive electrochemical determination of AQ in real samples using a GCE modified with PMO and MWCNT. The electrochemical behaviour of the AQ at MWCNT/PMO/GCE was studied using CV and it was observed that the oxidation process was diffusion-controlled and involved two electrons and two protons at the electro-oxidation step. A plausible oxidation mechanism of AQ was presented. The proposed method was successfully utilized as an electrochemical sensor for determination of AQ with a very low detection limit of 8.9×10^{-8} mol L^{-1}. The obtained detection limit was lower than those reported in the literature. The practical applicability of the modified electrode was evaluated by studying the recovery (101.1 to 104.4%) of AQ in pharmaceutical products as well as in urine samples. Thus, the proposed sensor is reliable and a suitable tool for quantitative analysis of AQ in pharmaceutical formulations and clinical analysis.

Acknowledgements

The authors are thankful to National Research Foundation (Pretoria, South Africa), UKZN-Nanotechnology Platform and College of Health Sciences (University of KwaZulu-Natal, South Africa) for providing financial support

.**References**

[1] J.P. Daily, The Journal of Clinical Pharmacology 46 (2006) 1487-1497.

[2] S. Misra, J. Nandi, S. Lal, The Indian journal of medical research 102 (1995) 119-123.

[3] C.I. Fanello, C. Karema, W. Van Doren, C.E. Rwagacondo, U. D'alessandro, Tropical medicine & international health 11 (2006) 589-596.

[4] F.T. Aweeka, P.I. German, Clinical pharmacokinetics 47 (2008) 91-102.

[5] K. Koram, L. Quaye, B. Abuaku, Ghana medical journal 42 (2008) 55.

[6] M. Adjuik, P. Agnamey, A. Babiker, S. Borrmann, P. Brasseur, M. Cisse, F. Cobelens, S. Diallo, J. Faucher, P. Garner, The Lancet 359 (2002) 1365-1372.

[7] J.L. Ndiaye, M. Randrianarivelojosia, I. Sagara, P. Brasseur, I. Ndiaye, B. Faye, L. Randrianasolo, A. Ratsimbasoa, D. Forlemu, V.A. Moor, Malaria journal 8 (2009) 125.

[8] G.R. Rao, Y.P. Rao, I. Raju, Analyst 107 (1982) 776-780.

[9] M.T. Ansari, T.M. Ansari, A. Raza, M. Ashraf, M. Yar, Chemia Analityczna 53 (2008) 305.

[10] O. Minzi, M. Rais, J. Svensson, L. Gustafsson, Ö. Ericsson, Journal of Chromatography B 783 (2003) 473-480.

[11] S.K. Sanghi, A. Verma, K.K. Verma, Analyst 115 (1990) 333-335.

[12] F. Ibrahim, F. Belal, A. El-Brashy, Microchemical journal 39 (1989) 65-70.

[13] G. Trenholme, R. Williams, E. Patterson, H. Frischer, P. Carson, K. Rieckmann, Bulletin of the World Health Organization 51 (1974) 431.

[14] J.P. Mufusama, L. Hoellein, D. Feineis, U. Holzgrabe, G. Bringmann, Electrophoresis (2018).

[15] H. Beitollahi, H. Karimi-Maleh, H. Khabazzadeh, Analytical Chemistry 80 (2008) 9848-9851.

[16] H. Beitollahi, S. Nekooei, Electroanalysis 28 (2016) 645-653.

[17] S. Jahani, H. Beitollahi, Electroanalysis 28 (2016) 2022-2028.

[18] S. Tajik, M.A. Taher, H. Beitollahi, Electroanalysis 26 (2014) 796-806.

[19] T.E. Chiwunze, N.B. Thapliyal, V.N. Palakollu, R. Karpoormath, Electroanalysis 29 (2017) 2138-2146.

[20] V.N. Palakollu, N. Thapliyal, T.E. Chiwunze, R. Karpoormath, S. Karunanidhi, S. Cherukupalli, Materials Science and Engineering: C 77 (2017) 394-404.

[21] N.B. Thapliyal, T.E. Chiwunze, R. Karpoormath, S. Cherukupalli, Materials Science and Engineering: C 74 (2017) 27-35.

[22] H. Beitollahi, S. Nekooei, M. Torkzadeh-Mahani, Talanta (2018).

[23] E. Molaakbari, A. Mostafavi, H. Beitollahi, Sensors and Actuators B: Chemical 208 (2015) 195-203.

[24] H.M. Moghaddam, H. Beitollahi, S. Tajik, I. Sheikhshoaie, P. Biparva, Environmental monitoring and assessment 187 (2015) 407.

[25] H. Beitollahi, S.G. Ivari, M. Torkzadeh-Mahani, Biosensors and Bioelectronics 110 (2018) 97-102.

[26] C.O. Valente, C.A.B. Garcia, J.P.H. Alves, M.V.B. Zanoni, N.R. Stradiotto, M.L.P. Arguelho, ECS Transactions 43 (2012) 297-304.

[27] T.K. Malongo, B. Blankert, O. Kambu, K. Amighi, J. Nsangu, J.-M. Kauffmann, Journal of pharmaceutical and biomedical analysis 41 (2006) 70-76.

[28] T. Ahuja, I.A. Mir, D. Kumar, Biomaterials 28 (2007) 791-805.

[29] M. Gerard, A. Chaubey, B. Malhotra, Biosensors and bioelectronics 17 (2002) 345-359.

[30] T. Ahuja, D. Kumar, Sensors and Actuators B: Chemical 136 (2009) 275-286.

[31] K. Saranya, M. Rameez, A. Subramania, European Polymer Journal 66 (2015) 207-227.

[32] Y. Huang, H. Li, Z. Wang, M. Zhu, Z. Pei, Q. Xue, Y. Huang, C. Zhi, Nano Energy 22 (2016) 422-438.

[33] Ö.A. Yokuş, F. Kardaş, O. Akyıldırım, T. Eren, N. Atar, M.L. Yola, Sensors and Actuators B: Chemical 233 (2016) 47-54.

[34] L. Fang, B. Liu, L. Liu, Y. Li, K. Huang, Q. Zhang, Sensors and Actuators B: Chemical 222 (2016) 1096-1102.

[35] Q. Zhou, A. Umar, A. Amine, L. Xu, Y. Gui, A.A. Ibrahim, R. Kumar, S. Baskoutas, Sensors and Actuators B: Chemical 259 (2018) 604-615.

[36] X. Wang, S. Uchiyama, Polymers for biosensors construction, State of the art in biosensors-general aspects, InTech, 2013.

[37] P.K. Bairagi, N. Verma, Journal of Electroanalytical Chemistry 814 (2018) 134-143.

[38] K. Giribabu, Y. Haldorai, M. Rethinasabapathy, S.-C. Jang, R. Suresh, W.-S. Cho, Y.-K. Han, C. Roh, Y.S. Huh, V. Narayanan, Current Applied Physics 17 (2017) 1114-1119.

[39] K. Reddaiah, T.M. Reddy, P. Raghu, Journal of Electroanalytical Chemistry 682 (2012) 164-171.

[40] S. Ibrahim, A.S. Ayesh, Journal of Thermoplastic Composite Materials 28 (2015) 225-240.

[41] W.A. De Heer, A. Chatelain, D. Ugarte, Science 270 (1995) 1179-1180.

[42] S.J. Tans, A.R. Verschueren, C. Dekker, Nature 393 (1998) 49.

[43] J. Kong, N.R. Franklin, C. Zhou, M.G. Chapline, S. Peng, K. Cho, H. Dai, science 287 (2000) 622-625.

[44] S. Jafari, N. Nasirizadeh, M. Dehghani, Journal of Electroanalytical Chemistry 802 (2017) 139-146.

[45] I. Mustafa, I. Lopez, H. Younes, R.A. Susantyoko, R.A. Al-Rub, S. Almheiri, Electrochimica Acta 230 (2017) 222-235.

[46] A.A. Ensafi, M. Taei, T. Khayamian, F. Hasanpour, Analytical Sciences 26 (2010) 803-808.

[47] R.T. Kachoosangi, G.G. Wildgoose, R.G. Compton, Electroanalysis 20 (2008) 1714-1718.

[48] Z.A. Alothman, N. Bukhari, S.M. Wabaidur, S. Haider, Sensors and Actuators B: Chemical 146 (2010) 314-320.

[49] A. Üğe, D.K. Zeybek, B. Zeybek, Journal of Electroanalytical Chemistry (2018).

[50] V. Gautam, K.P. Singh, V.L. Yadav, Carbohydrate Polymers (2018).

[51] S.A. Kumar, S.-F. Wang, T.C.-K. Yang, C.-T. Yeh, Biosensors and Bioelectronics 25 (2010) 2592-2597.

[52] J. Wang, Analytical electrochemistry, John Wiley & Sons, 2006.

[53] A. Ullah, A. Rauf, U.A. Rana, R. Qureshi, M.N. Ashiq, H. Hussain, H.-B. Kraatz, A. Badshah, A. Shah, Journal of The Electrochemical Society 162 (2015) H157-H163.

[54] J.I. Gowda, S.T. Nandibewoor, Asian Journal of Pharmaceutical Sciences 9 (2014) 42-49.

[55] S. Prashanth, K. Ramesh, J. Seetharamappa, International Journal of Electrochemistry 2011 (2011).

[56] D.K. Gosser, Cyclic voltammetry: simulation and analysis of reaction mechanisms, VCH New York, 1993.

[57] E. Laviron, Journal of Electroanalytical Chemistry and Interfacial Electrochemistry 101 (1979) 19-28.

[58] A.J. Bard, L.R. Fulkner, Electrochemical Methods Fundamentals and Aplications 2 (2004) 236

CHAPTER 6

Electrochemical determination of an anti-malaria drug amodiaquine based on gold nanoparticles decorated reduced graphene oxide and cysteamine modified sensor.

Tirivashe Elton Chiwunze [a], Atal A.S. Gill [a], Francis Kayamba [a], Thobeka Persevearance Vilakazi [a], Wendy Zulu [a], Aphelele Ngubane [a], Kajal Mohanlal [a], and Nokwanda Zenani Dhlamini [a] Venkata Narayana Palakollu [a], Neeta Bachheti Thapliyal [a], Rajshekhar Karpoormath [a*]

[a]Department of Pharmaceutical Chemistry, College of Health Sciences, University of KwaZulu-Natal, Durban 4000, South Africa

Graphical Abstract

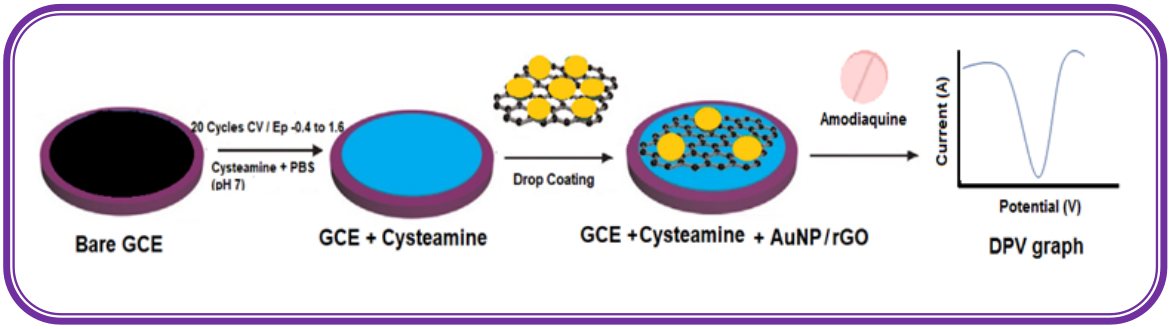

***Corresponding Author**

Dr. Rajshekhar Karpoormath

Tel: + 27-312607179, Fax: + 27-312607792

Email: karpoormath@ukzn.ac.za

Abstract

A gold nanoparticles decorated reduced graphene oxide (rGO-AuNP) and electrochemically deposited cysteamine (Cyst) modified glassy carbon electrode (rGO-AuNP/Cyst/GCE) was fabricated for the detection and quantification of amodiaquine (AQ), an antimalarial drug, The electrode modifiers were characterized using field emission scanning electron microscopy (FE-SEM) and energy-dispersive X-ray spectroscopy (EDX). The electrochemical behavior of the drug was investigated at rGO-AuNP/Cyst/GCE using cyclic and differential pulse voltammetric techniques. The electrooxidation process of AQ at the developed sensor was found to be quasi-reversible and was adsorption-controlled over the pH range of 5.5-10.0. Under optimized differential pulse voltammetric (DPV) conditions, the current response was found to be linear in the concentration ranges of 5.0×10^{-7} to 2.2×10^{-6} M and 6.6×10^{-6} to 4.5×10^{-5} M with a detection limit of 18 nM. The rGO-AuNP/Cyst/GCE demonstrated good selectivity, stability, reproducibility and practical applicability for quantification of AQ in pharmaceutical formulations. Thus, the proposed sensor can potentially be used as a quality control tool for AQ.

Keywords: Amodiaquine; Reduced graphene oxide; Gold nanoparticles; Cysteamine; Voltammetry.

1. Introduction

The study of carbon nanomaterials, such as graphene, graphene oxide and reduced graphene oxide, has been an area of interest for most researchers over the past decade owing to numerous applications of the materials. Recent studies reported the use of graphene and its derivatives in optoelectronics [1, 2], electrochemical sensors [3, 4], solar cells catalysis [5, 6], as well as in medicine as a potential cure for cancer [7, 8]. Due to their good physicochemical properties, a variety of nanocomposites have been derived for different applications. Reduced graphene oxide with gold nanoparticles (rGO/Au-NP) is one such nanocomposite which is known to have diverse applications and is easy to synthesize [9-13]. A number of reports have indicated that the synthesis of rGO/Au-NP can be achieved in a one-pot reaction [14, 15]. Thus, the ease to prepare this nanocomposite along with its excellent conductivity makes it a good candidate as an electrode modifier.

Another strategy that is frequently used to improve the performances of the electrochemical sensors is electrochemical deposition. This is a process by which a desired coating of chemical species (e.g. metal, oxide, or salt) is deposited onto the electroactive surface by simple electrolysis of a solution containing the desired chemical molecules, which results in a thin and tightly adherent coating layer [16]. Electrochemical deposition has demonstrated numerous advantages such as simple process, green chemistry, strong adherence of the polymer film to the electrode surface, uniform deposition and stability of the coating layer on the surface of the electrode [17, 18].

Cysteamine is a simple 1,2 disubstituted ethane compound containing an amine group on one end and a thiol group on the other. It is classified as an aminothiol drug used in the treatment of cystinosis and as an antioxidant with chemo-sensitizing and radioprotective properties [19]. The binary functional groups of the aminothiol drug typically make it a good linker and a perfect candidate for electrochemical deposition. In addition, because of gold's strong affinity for

sulphur compounds, Cyst makes a very good electrochemical deposition agent as it would help Au compound to adhere strongly to the electrode surface.

In the field of pharmaceutical research, the analytical investigation of bulk drug materials, intermediates, drug products, drug formulations, impurities and degradation products is essential. With the rise of unaccredited pharmaceutical industries, a lot of counterfeit products have hit the market and regulatory measures for consumers safety is inevitable [20]. Detection of counterfeit medicines has more than ever become of paramount importance, especially for developing countries. In this study, we envisaged developing a quantitative analysis tool for the detection and determination of amodiaquine (AQ). AQ is an antimalarial drug with quinoline scaffold used as a prophylactic treatment for people visiting malaria-infested regions. It is mostly prescribed in artemisinin-based combinations as artesunate plus amodiaquine, for the treatment of malaria [21]. Like chloroquine, AQ's mode of action is mediated by inhibiting a parasitic heme polymerase enzyme, the sole function of the enzyme is to convert heme which is lethal to the parasite to hemozoin a non-toxic substance [22]. However, long-term use of the drug is associated with hepatotoxicity, neurotoxicity and nephrotoxicity [23]. Hence, it is of paramount importance to develop an AQ sensitive point of care analytical device for quality control and assurance which is simple, cost-effective, portable and easy to operate.

Over the past few decades, various methods have been developed for AQ determination, such as high performance liquid chromatography [24-26], fluorimetry [27], mass spectrometry [24], spectrophotometry [28] and electrochemical methods [29, 30]. Compared to reported methods, electrochemical techniques have proven to be more efficacious for detection of several organic compounds due to advantages such as minimal sample preparation, the simplicity of equipment, rapid response time, sensitivity and reliability at a low cost. Furthermore, AQ possesses two functional groups (phenolic OH, secondary amine group) that can undergo oxidation, thus making it possible for analysis using voltammetric techniques.

The goal of this work was to combine the advantages of electrochemical deposition with the convenience of working with rGO/Au-NP. The combination is expected to show better electrocatalytic activity than the individual components. The present work describes the first time use of rGO-AuNP/Cyst composite as an electrode modifier to develop an electrochemical sensor for the voltammetric determination of AQ. The proposed sensor exhibited practical applicability as it was successfully utilised for the quantification of AQ in pharmaceutical formulations containing AQ. The novelty of this work lies in the use of the composite as there has been no published report using rGO-AuNP/Cyst/GCE as an electrode surface modifier.

2. Experimental

2.1 Materials and Apparatus

Graphene oxide, gold (III) chloride hydrate, potassium iodide, amodiaquine dihydrochloride dihydrate, cysteamine, hydrazine hydrate, sodium citrate were procured from Sigma-Aldrich. Phosphate buffer solution (PBS) was prepared from sodium phosphate dibasic and monosodium dihydrogen orthophosphate obtained from Merck. All other reagents used in the experiments were of analytical grade and double distilled water was used for all aqueous solutions. A CHI660E electrochemical workstation (CH instrument, USA) with a conventional three-electrode system was employed for all voltammetric experiments. All the three electrodes were obtained from CH Instruments, USA and they comprised of a bare or modified GCE (3.0 mm in diameter) as the working electrode, an Ag/AgCl as a reference electrode and a platinum counter electrode. All measurements were performed at room temperature and pressure.

2.2 Synthesis of rGO-AuNP

The synthesis of rGO-AuNP was carried out with a slight modification as described by Chen e*t al* [13]. Briefly, 40 mg of GO was suspended in 40 mL of distilled water and the solution was homogenized by sonication for an hour. The solution was then transferred into a round bottom flask containing 600µL of $HAuCl_4$ (40 mg mL^{-1}) and stirred at room temperature for an hour to

promote interaction between the graphene and gold ions. The mixture was heated to 80 ºC and 4 mL sodium citrate (0.2 mol L^{-1}) was added dropwise with stirring for the reduction of gold (III) complex. After stirring and heating for 2 h, hydrazine hydrate (60 µL) was added to reduce the GO. The reaction was kept at these conditions for 12 h. After completion, the synthesized nanocomposite was washed with distilled water, ethanol and isolated by centrifugation. The final product was obtained by drying the mixture in a hot oven at 60 ºC for 5h. The nanocomposite was then re-dispersed in distilled water by ultrasonication for drop casting onto the electrode surface.

2.3 Fabrication of rGO-AuNP/Cyst/GCE

Prior to use, the GCE was polished with 0.3 and 0.05 µm of alumina slurry to a mirror shine finish. It was then dipped in a 0.2 M solution of H_3PO_4 for two minutes, thoroughly rinsed with distilled water and left to air dry. The polished GCE was allowed to run 20 cyclic voltammetric cycles in a solution of 2.5M Cyst in 0.1M PBS (pH 7.0) at a scan rate of 0.05V s^{-1} and a potential window range of -0.4 to 1.6 V (Fig. 1)**.** Excess Cyst was washed off with distilled water leaving a conductive layer of Cyst on the electrode which was abbreviated as Cyst/GCE. The electrode was further modified by casting 5 µL of the synthesized rGO-AuNP (1mg/mL) onto the surface and drying it under an infrared lamp. The electrode was then used for the electrochemical experiments and was denoted as rGO-AuNP/Cyst/GCE.

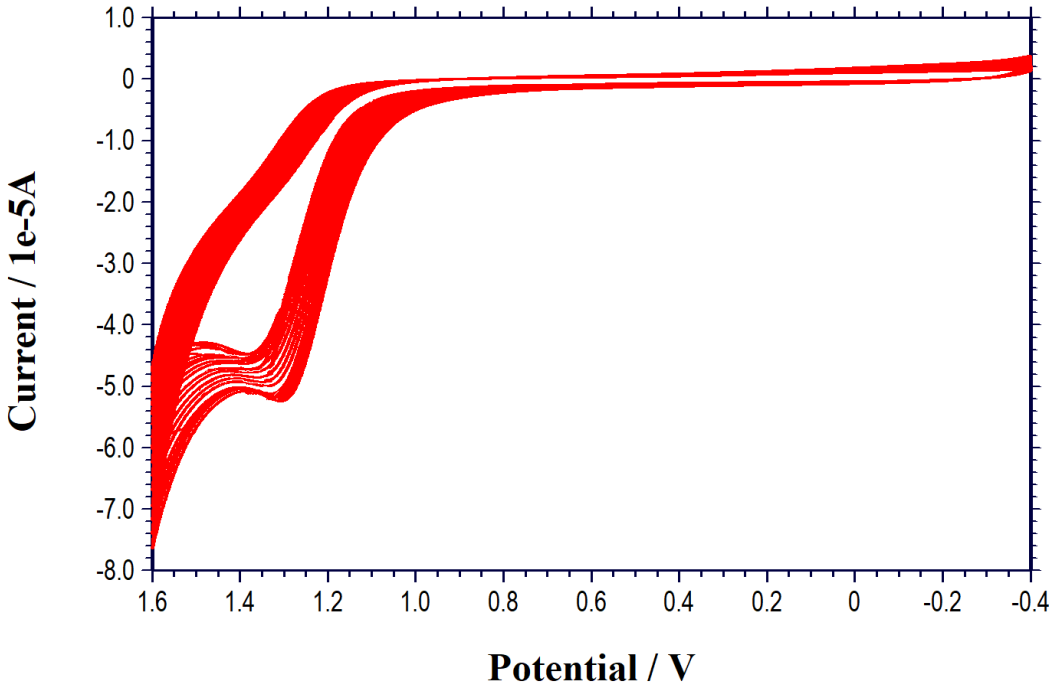

Fig. 1 Cyclic voltammograms for the electrochemical deposition of Cyst at GCE in a 2.5 M Cyst solution in 0.1M PBS (pH 7.0). Scan rate: 50 mVs^{-1}.

2.4 Sample Preparation

The contents of a commercially available amodiaquine tablet (ASAQ-Denk) were: 250mg amodiaquine hydrochloride and 250mg Artesunate (recommended dose). Two of these tablets were ground into a fine powder and 250mg of the powder was dissolved in 100 mL of distilled water to prepare a stock solution. Appropriate dilutions of the stock solution were carried out to obtain a sample solution with a concentration that falls within the observed linear concentration range. The content of AQ in the sample was then calculated by extrapolation from the calibration curve.

3. Results and discussion

3.1 Characterization of rGO-AuNP/Cyst/GCE

Field emission scanning electron microscopy (FE-SEM) was used to provide a complete imagery of the surface morphologies of the prepared materials. Fig. 2 (A to C) depict the micrographs of Cyst and rGO-AuNP composite. As can be seen in Fig. 2 (A) electrochemically

deposited Cyst possesses a flaky structure. The FE-SEM images of the synthesized rGO-AuNP (Fig. 2 (B-C)) indicate the presence of uniformly distributed and well-embedded gold nanoparticles that are spotted as shiny bright spheres. The nanocomposite was further characterised using EDX where two major peaks for carbon and gold were obtained, which confirmed the presence of GO and AuNP respectively (Fig. 2 (D)). The small oxygen peak on the EDX spectra indicates that the graphene oxide was fully reduced. Thus, the successful preparation of AuNP embedded in rGO was confirmed.

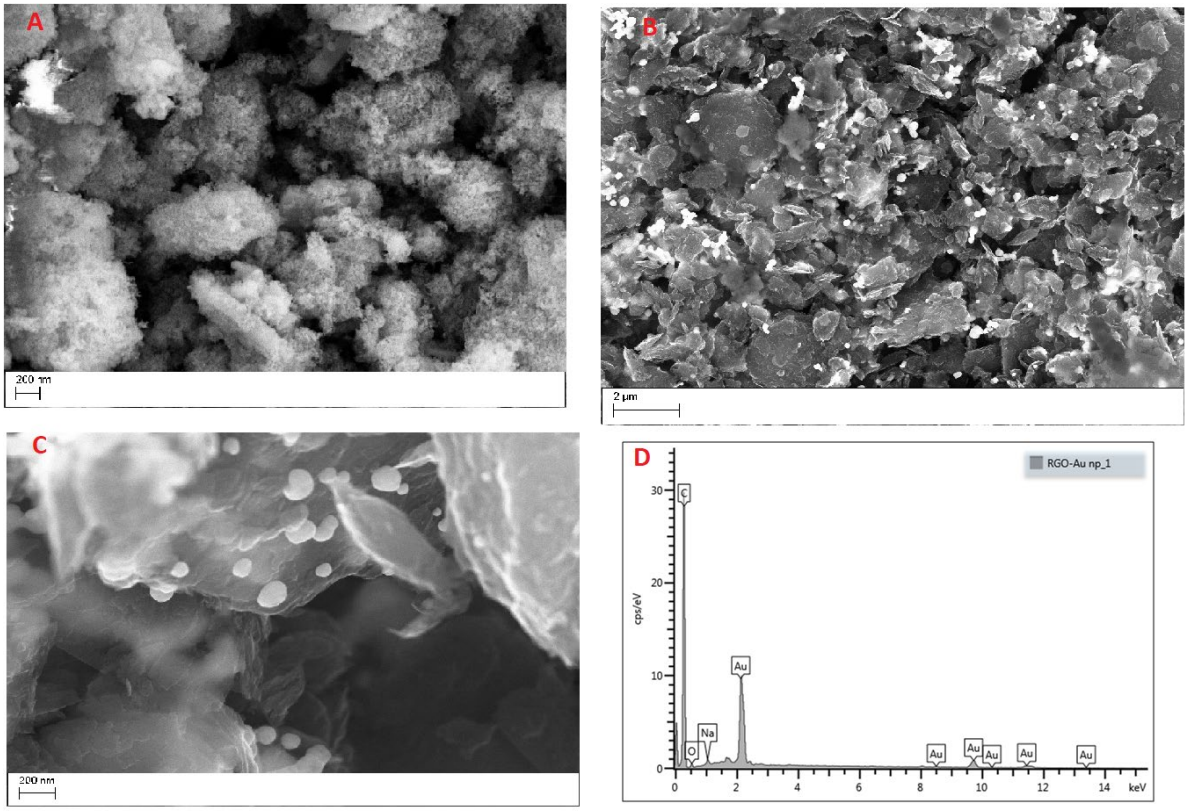

Fig. 2 FE-SEM images of **(A)** electrochemically deposited Cyst on GC, **(B)** rGO-AuNP at low magnification, **(C)** rGO-AuNP at high magnification respectively, and **(D)** EDX spectra of the rGO-AuNP.

3.2 pH study

The pH of the solution proved to have a significant influence on the oxidation peaks' potentials of AQ. Fig. 3 illustrates the relationship of CV oxidation peak potentials with the pH of the

solution. As can be observed, the peak potential for the oxidation peaks shifted negatively with the increase in pH. The dependence of E_p on pH can be expressed in the following linear equations:

E_p (V) = 0.8087 – 0.0646 pH $R^2 = 0.9922$ (peak O_1) (1)

E_p (V) = 1.2523 – 0.0596 pH $R^2 = 0.9913$ (peak O_2) (2)

The slopes for both peaks (O_1 and O_2) are approximately equal to the theoretical value of 59 mV which shows that the oxidation of AQ involves the participation of an equal number of protons and electrons. Thus, it is proposed that the oxidation process of AQ at rGO-AuNP/Cyst/GCE is facilitated by two protons and two electrons, as illustrated in Scheme 1.

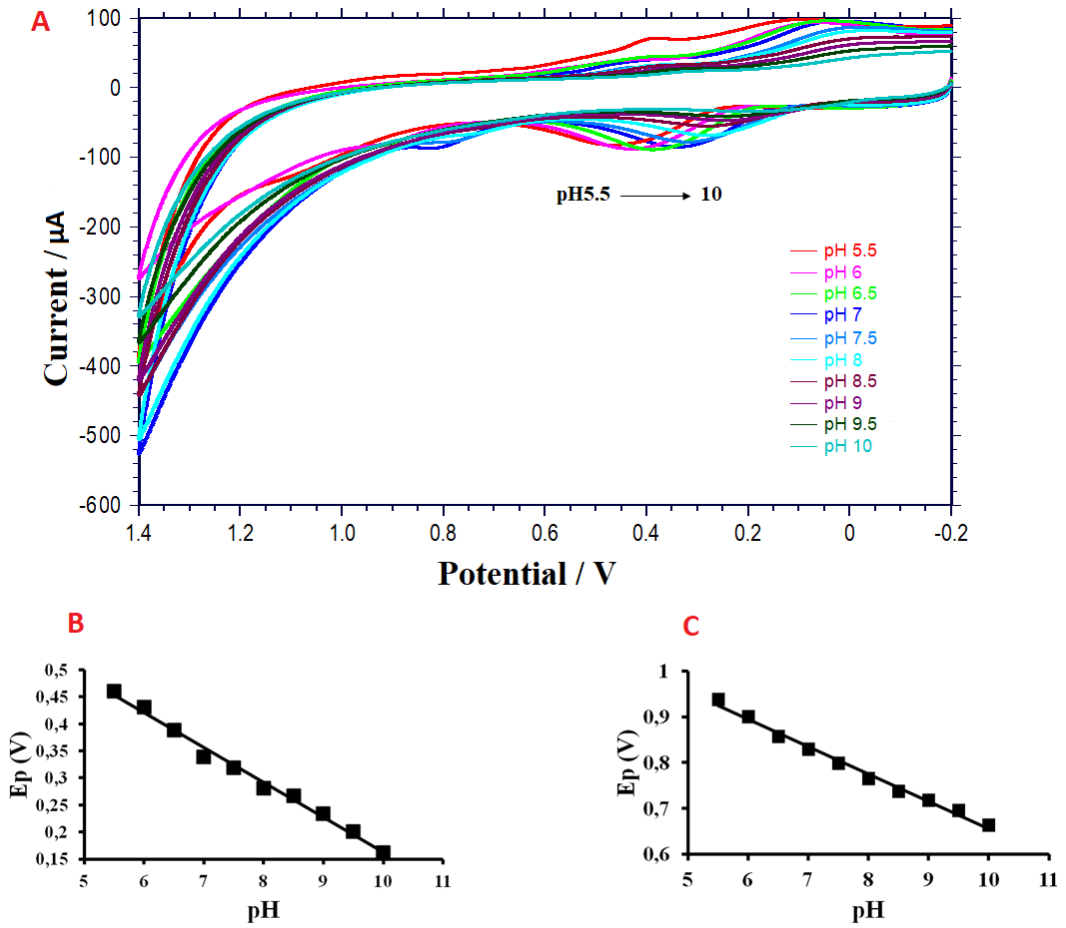

Fig. 3 (A) Effect of pH on the oxidation peak response for 0.1 mM MQ at rGO-AuNP/Cyst/GCE. **(B)** The linear relationships between the pH and the E_p values of peaks O_1. **(C)** The linear relationships between the pH and the E_p values of peaks O_2.

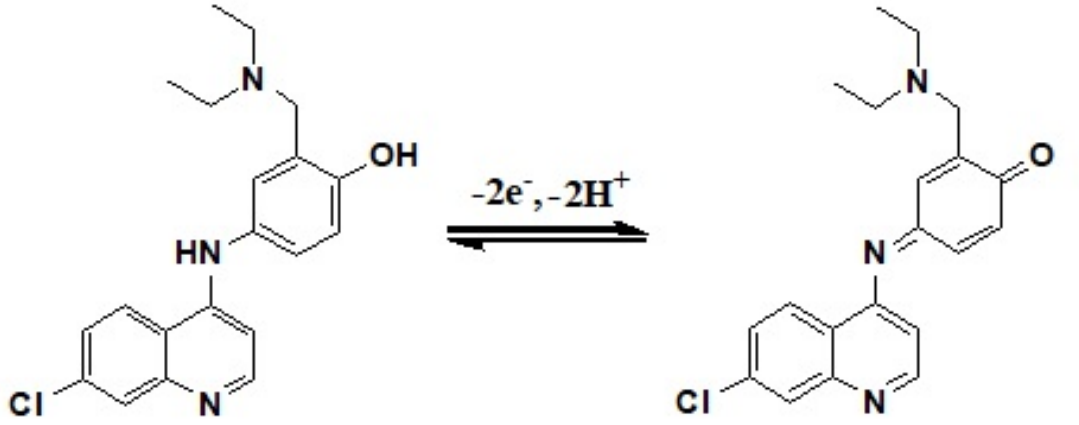

Scheme 1. Electrochemical oxidation of AQ.

3.3 Electrochemical behaviour of AQ at of rGO-AuNP/Cyst/GCE

Initial investigation of the electrochemical behaviour of AQ was performed using CV. Fig. 4 (A) shows a comparison of typical cyclic voltammograms recorded for 0.5mM AQ in PBS (pH 7.0) at various working electrodes (i.e. bare GCE, Cyst/GCE, rGO-AuNP/GCE and rGO-AuNP/Cyst/GCE). Two poorly defined oxidation peaks at 0.29 and 0.89V and one peak at 0.02V for reduction were observed at GCE as shown in Fig. 4 (A). After modification with Cyst, improved oxidation and reduction peaks were observed demonstrating an improved conductivity at Cyst/GCE. Moreover, at the rGO-AuNP/GCE the anodic peaks were found to shift negatively and the cathodic peak shifted positively with a significant increase in the peak current. A remarkable enhancement in peak current response was observed at rGO-AuNP/Cyst/GCE with a similar shift in peaks potentials as seen at the rGO-AuNP/GCE electrode. As expected, combining the two materials exhibited better electrocatalytic activity than the individual components. The shift in peak potentials and increased peak currents serve as a clear indication that rGO-AuNP/Cyst/GCE acts as a promoter and accelerates electron transfer at the electrode interface. This exceptionally high electrocatalytic activity is attributed to the good electron shuttling nature of GO materials. Hence, rGO-AuNP/Cyst/GCE was selected for all subsequent electrochemical studies. The separation between the oxidation and

the reduction peak was noticed to be greater than at the bare electrode, suggesting that the electro-oxidation process of AQ at rGO-AuNP/Cyst/GCE is quasi-reversible [31].

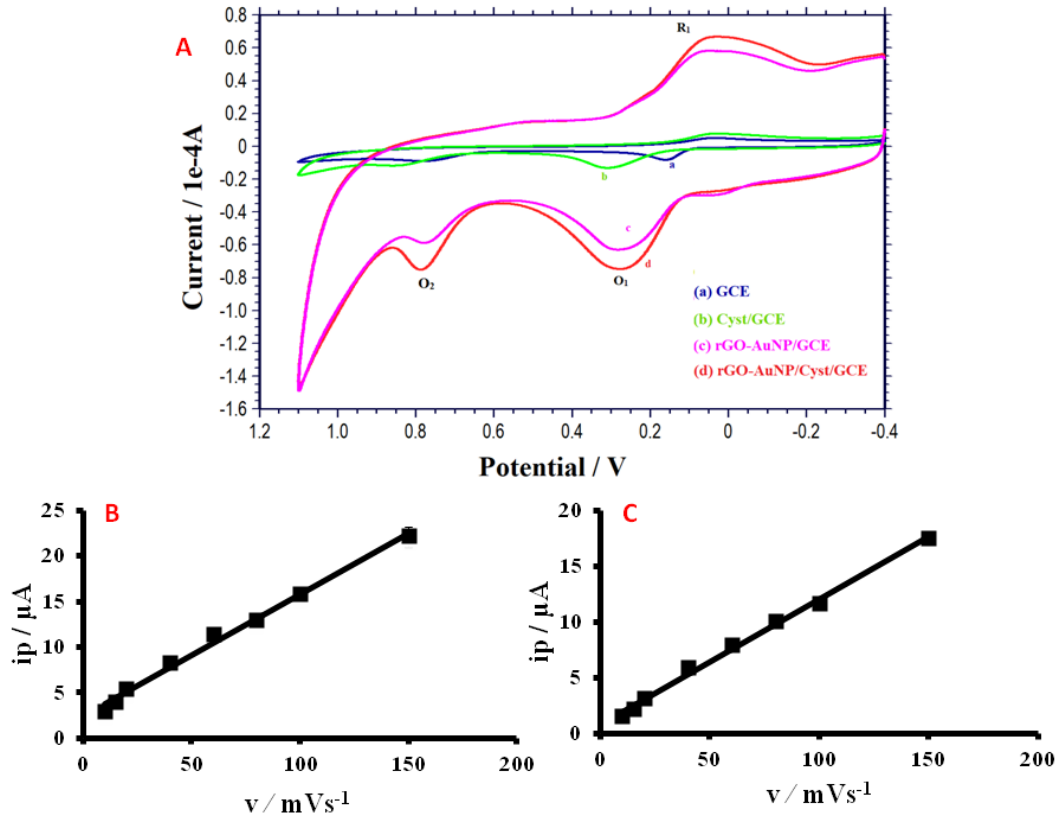

Fig. 4 (A) Cyclic voltammograms of 5 mM AQ in PBS (pH 6.5) at (a) bare GCE, (b) Cyst/GCE, (c) rGO-AuNP/GCE and (d) rGO-AuNP/Cyst/GCE. **(B)** Variation of peak currents (O_1) with scan rate. **(C)** Variation of peak current (O_2) with scan rate at rGO-AuNP/Cyst/GCE in 1.5 mM AQ.

3.4 Effect of scan rate

Useful information regarding electrochemical behaviour can be acquired from the relationship between scan rate and peak current or peak potential. Cyclic voltammograms were recorded with scan sweeps varying in the range 10-150 mV s^{-1}. A linear correlation was observed (Fig. 4 (B) and (C)) between the peak currents (i_p) of both oxidation peaks (O_1 and O_2) and scan rate (v) suggesting that the charge transfer process at the modified electrode surface is adsorption-controlled. This was further supported by the plots of log i_p vs log v which were linear and gave

slopes close to the theoretical value 1 for an ideal adsorption-controlled process[32]. The linear plots observed between i_p vs v and log (i_p) vs log (v) are as follows:

$$i_{pa} = 0.1345v + 2.3561; \qquad R^2 = 0.9927 \text{ (peak } O_1) \qquad (3)$$

$$i_{pa} = 0.1122v + 0.8134; \qquad R^2 = 0.9952 \text{ (peak } O_2) \qquad (4)$$

$$\log (v) = 0.7775 \log (i_p) - 0.2991 \qquad R^2 = 0.9927 \text{ (peak } O_1) \qquad (5)$$

$$\log (v) = 0.894 \log (i_p) - 0.6973 \qquad R^2 = 0.996 \text{ (peak } O_2) \qquad (6)$$

The relationships between E_p and log v were linear displaying slopes of 0.0455 (peak O_1) and 0.07021 (peak O_2). According to Laviron, E_p can be defined by the following equation [33],

$$Ep = E^{\circ} + \left(\frac{2.303RT}{\alpha nF}\right) Log \left(\frac{RTk^{\circ}}{\alpha nF}\right) + \left(\frac{2.303RT}{\alpha nF}\right) Log\ \upsilon \qquad (7)$$

where α, k^0 and $E^{0'}$ are electron transfer coefficient, standard rate constant of the surface reaction and the formal potential, respectively. The other symbols stated in the equation have their standard meanings. The gradient of Ep versus log v was used to deduce the value of αn.

$$\alpha = \frac{47.7}{Ep - Ep_{1/2}} \qquad (8)$$

where $Ep1/2$ is the potential at which the current is half the peak value [34]. The value of n which indicated the number of electrons was calculated to be two in total (one electron for each oxidation peak). This indicates that the electrooxidation of AQ at rGO-AuNP/Cyst/GCE involves a transfer of two electrons as proposed in scheme 1 previously.

3.5 Analytical Performance

To study the effect of concentration on the oxidation peak current of AQ, we only focused on the oxidation peak O_1 as it showed better reproducibility than oxidation peak O_2. The measurements were recorded using DPV mode at pH 6.5 in the range of $5x10^{-7}$ – $4.5x10^{-5}$ M at

rGO-AuNP/Cyst/GCE sensor as illustrated in (Fig. 5). As displayed in Fig. 5 the peak current (i_p) increased linearly with an increase in the AQ concentration. The plot of i_p vs AQ concentration showed two linear response ranges, thus a break between $2.2x10^{-6}$ – $6.6x10^{-6}$ M was observed. The two linear ranges can be expressed by the following equations

$$i_p\,(\mu A) = 13.851\ C(\mu M) + 30.135 \qquad (R^2 = 0.9918) \qquad (9)$$

$$i_p\,(\mu A) = 2.6973\ C(\mu M) + 83.709 \qquad (R^2 = 0.9874) \qquad (10)$$

where C is the concentration of AQ and R^2 is the correlation coefficient. The limit of detection (LOD) of AQ at rGO-AuNP/Cyst/GCE was calculated using the formula 3S/N, where N is the gradient of the calibration curve and S is the standard deviation of the peak currents of three blank solutions. The LOD was found to be $1.8x10^{-8}$ M, proving that the developed sensor has a high sensitivity. Table 1 shows a comparison of electrochemical performances for AQ quantification at rGO-AuNP/Cyst/GCE with the other previously reported electrochemical sensors. From the tabulated results it is evidently clear that the proposed sensor is highly sensitive and reliable for detection of low-levels of AQ in comparison to the reported ones.

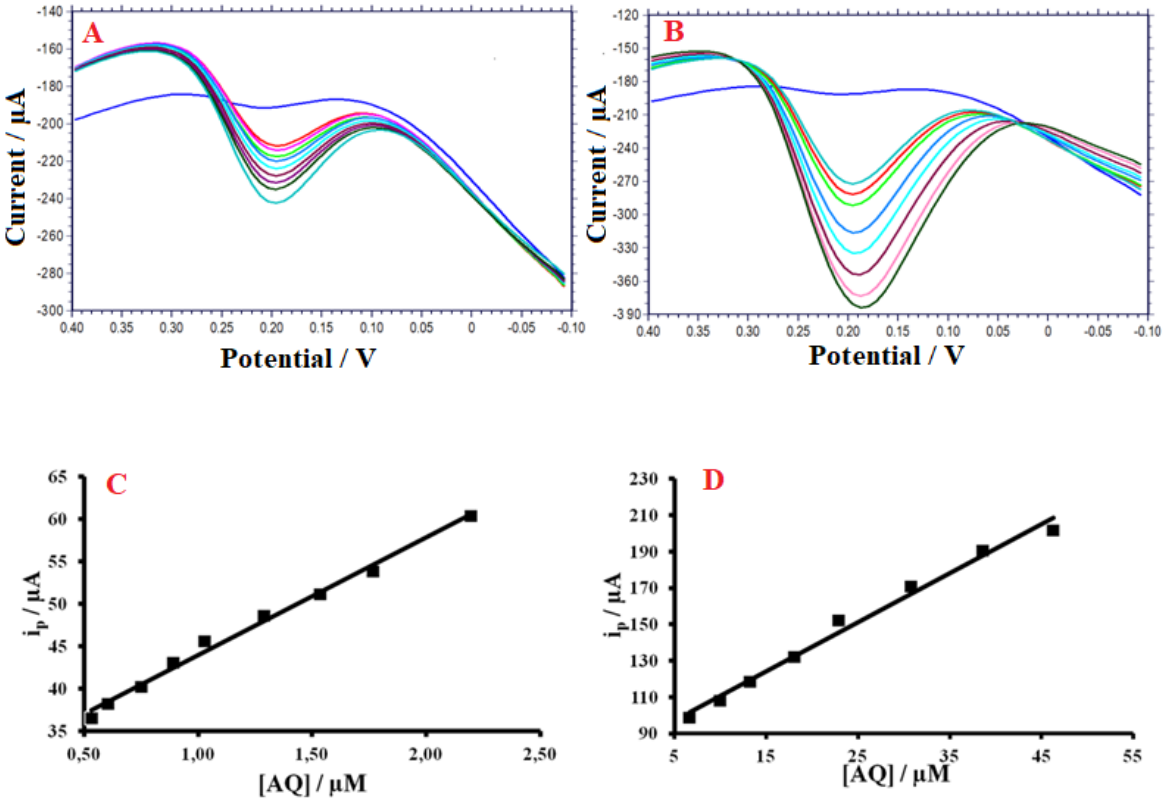

Fig. 5 DPV voltammograms of AQ with the different concentrations in 0.1M PBS of pH 6.5 **(A)** lower concentration segment (**B)** higher concentration segment. Calibration plot of AQ concentration vs i_p **(C)** lower concentration segment (**D)** higher concentration segment.

Table 1: A comparison of electrochemical methods reported for the determination of AQ.

Sensor	Concentration range (M)	*LOD (M)	Ref.
Hemin-Based Electrode	1.9×10^{-5} to 1.0×10^{-4}	7.04×10^{-6}	[29]
#PVC membrane sensors	3.2×10^{-6} to 2.0×10^{-2}	NR	[30]
***MWCNT/PMO/GCE**	1.0×10^{-7} to 3.5×10^{-6}	8.9×10^{-8}	[35]
rGO-AuNP/Cyst/GCE	5.0×10^{-7} to 2.2×10^{-6} 6.6×10^{-6} to 4.5×10^{-5}	1.8×10^{-8}	Present work

*#PVC: Poly vinyl chloride; NR: not reported, *MWCNT: Multiwalled carbon nanotubes;PMO: poly methyl orange*

3.6 Interference study

Effect of interferents on the determination of 5 µM AQ at rGO-AuNP/Cyst/GCE was carried out by assessing the effect of various potential interfering compounds that are commonly present in

biological media. The tolerance limit was defined as the maximum concentration of various potential interferents that result in an error of ±5%. The results indicated that the addition of 200 fold of Na^+, K^+, Ca^{2+}, Mg^{2+}, Cl^-, SO_4^{2-}, glucose, starch, caffeine, uric acid and ascorbic acid does not affect the detection of AQ. Thus, the developed electrode is highly selective for the target analyte in the presence of various possible common entities.

3.7 Reproducibility and stability of the electrode

The reproducibility of the rGO-AuNP/Cyst/GCE was investigated by performing DPV measurements with the same experimental parameters using three identically prepared electrodes in a solution containing 5 μM of AQ. The sensor displayed good reproducibility as the relative standard deviation (RSD) was found to be 3.1 % (n = 3). The evaluation of the sensor's stability was carried out by storing the modified electrode in a refrigerator at 5 ^oC for one month. The sensor was then used after the stipulated time and no noticeable change in current responses was observed for the same AQ solution (5 μM), indicating that the sensor has good stability.

3.8 Real sample analysis

In order to investigate the analytical applicability of the sensor, quantification of AQ in commercially available tablets was carried out. The AQ tablet was processed as described in the experimental section and optimized DPV conditions were employed. The results were found to be in good agreement with the label claim (Table 2). Thus, the proposed method is selective, accurate and can be applied as an analytical tool for quantification of AQ in pharmaceutical formulations.

Table 2: Determination of AQ in a commercially available tablets at rGO-AuNP/Cyst/GCE

Parameters	Results
Labelled AQ (mg)	250.00
AQ content found (mg)	243.60
Bias (%)	2.6
Spiked (µM)	1.00
Found (µM)	0.96
Recovery (%)	96.0
Bias (%)	4.0

4. Conclusion

In the present study, electrochemically deposited Cyst and chemically synthesized rGO-AuNP composite were employed for the fabrication of an electrochemical sensor for the detection of AQ in pharmaceutical formulations. The composite was characterized using FE-SEM and EDX spectroscopy techniques. The electrochemical investigation of AQ at the surface of rGO-AuNP/Cyst/GCE was carried out using CV. The electrooxidation process was found to be adsorption controlled and it involved two electrons and two protons. The fabricated sensor was further applied for the determination of AQ using optimised DPV conditions. The DPV peak current response was found to be linearly proportional to the AQ concentrations in the ranges of 5.0×10^{-7} to 2.2×10^{-6} and 6.6×10^{-6} to 4.5×10^{-5}. The rGO-AuNP/Cyst/GCE sensor exhibited a very low detection limit of 1.8×10^{-8} M that is by far more superior to AQ sensors previously reported in literature. Finally, the utility of the proposed method was demonstrated by determination of AQ in pharmaceutical formulations. Good recovery percentages were obtained indicating that the rGO-AuNP/Cyst/GCE sensor can be successfully used as a quality control

tool for AQ. The present study demonstrated a promising approach for quality assurance and quality control of AQ.

Acknowledgment

The authors would like to thank the College of Health Sciences University of Kwazulu-Natal, Nanotechnology platform University of KwaZulu-Natal and the National Research Foundation of South Africa (Grant No: 103728, 112079).

References

[1] N. Maity, R. Ghosh, A.K. Nandi, Langmuir (2018).

[2] S. Aslam, F. Mustafa, M.A. Ahmad, Ceramics International 44 (2018) 6823-6828.

[3] H.-C. Chen, H.-W. Yang, K.-H. Yang, C.-H. Chen, C.-C. Hou, Y.-M. Tu, Sensors and Actuators B: Chemical 240 (2017) 1153-1159.

[4] P. Bollella, G. Fusco, C. Tortolini, G. Sanzò, G. Favero, L. Gorton, R. Antiochia, Biosensors and Bioelectronics 89 (2017) 152-166.

[5] T. Mahmoudi, Y. Wang, Y.-B. Hahn, Nano Energy (2018).

[6] J. Yang, Y. Pang, W. Huang, S.K. Shaw, J. Schiffbauer, M.A. Pillers, X. Mu, S. Luo, T. Zhang, Y. Huang, ACS nano 11 (2017) 5510-5518.

[7] C.-C. Liu, J.-J. Zhao, R. Zhang, H. Li, B. Chen, L.-L. Zhang, H. Yang, American journal of translational research 9 (2017) 5197.

[8] L. Wu, H. Ji, Y. Guan, X. Ran, J. Ren, X. Qu, NPG Asia Materials 9 (2017) e356.

[9] L. Rout, A. Kumar, R.S. Dhaka, G.N. Reddy, S. Giri, P. Dash, Applied Catalysis A: General 538 (2017) 107-122.

[10] X. Zhao, W. Hu, Y. Wang, L. Zhu, L. Yang, Z. Sha, J. Zhang, Carbon 127 (2018) 618-626.

[11] S. babu Maddinedi, B.K. Mandal, S.H. Patil, V.V. Andhalkar, S. Ranjan, N. Dasgupta, Journal of Photochemistry and Photobiology B: Biology 166 (2017) 252-258.

[12] H. Wang, S. Zhang, S. Li, J. Qu, Talanta 178 (2018) 188-194.

[13] N. Chen, Y. Cheng, C. Li, C. Zhang, K. Zhao, Y. Xian, Microchimica Acta 182 (2015) 1967-1975.

[14] Y. Guo, X. Sun, Y. Liu, W. Wang, H. Qiu, J. Gao, Carbon 50 (2012) 2513-2523.

[15] R.B. Hurtado, M. Cortez-Valadez, J. Aragon-Guajardo, J. Cruz-Rivera, F. Martínez-Suárez, M. Flores-Acosta, Arabian Journal of Chemistry (2017).

[16] C.A.D. Rodriguez, G. Tremiliosi-Filho, Encyclopedia of Tribology (2013) 918-922.

[17] K. Hong, H. Zhang, J.W. Mays, A.E. Visser, C.S. Brazel, J.D. Holbrey, W.M. Reichert, R.D. Rogers, Chemical communications (2002) 1368-1369.

[18] P. Kubisa, Progress in Polymer Science 29 (2004) 3-12.

[19] M. Besouw, R. Masereeuw, L. van den Heuvel, E. Levtchenko, Drug Discovery Today 18 (2013) 785-792.

[20] R. Zumoff, Nephrology news & issues 21 (2007) 22-22.

[21] C. Falade, A. Ogundele, B. Yusuf, O. Ademowo, S. Ladipo, Tropical Medicine & International Health 13 (2008) 635-643.

[22] H. Ginsburg, O. Famin, J. Zhang, M. Krugliak, Biochemical pharmacology 56 (1998) 1305-1313.

[23] T.J. Monks, D.C. Jones, Current drug metabolism 3 (2002) 425-438.

[24] V. Dhiman, D.K. Singh, M.K. Ladumor, S. Singh, Journal of separation science 40 (2017) 4530-4540.

[25] D.A. Godin, Development of an UFLC/MS/MS method for the comparative analysis of oxytocin and artesunate-amodiaquine for validation of field detection systems, 2016.

[26] O. Minzi, M. Rais, J. Svensson, L. Gustafsson, Ö. Ericsson, Journal of Chromatography B 783 (2003) 473-480.

[27] F. Ibrahim, F. Belal, A. El-Brashy, Microchemical journal 39 (1989) 65-70.

[28] M.T. Ansari, T.M. Ansari, A. Raza, M. Ashraf, M. Yar, Chemia Analityczna 53 (2008) 305.

[29] C.O. Valente, C.A.B. Garcia, J.P.H. Alves, M.V.B. Zanoni, N.R. Stradiotto, M.L.P. Arguelho, ECS Transactions 43 (2012) 297-304.

[30] T.K. Malongo, B. Blankert, O. Kambu, K. Amighi, J. Nsangu, J.-M. Kauffmann, Journal of pharmaceutical and biomedical analysis 41 (2006) 70-76.

[31] J. Wang, Analytical electrochemistry, John Wiley & Sons, 2006.

[32] D.K. Gosser, Cyclic voltammetry: simulation and analysis of reaction mechanisms, VCH New York, 1993.

[33] E. Laviron, Journal of Electroanalytical Chemistry and Interfacial Electrochemistry 101 (1979) 19-28.

[34] A.J. Bard, L.R. Faulkner, J. Leddy, C.G. Zoski, Electrochemical methods: fundamentals and applications, wiley New York, 1980.

[35] T.E. Chiwunze, V.N. Palakollu, A.A. Gill, F. Kayamba, N.B. Thapliyal, R. Karpoormath, Materials Science and Engineering: C 97 (2019) 285-292.

CHAPTER 7

1. Summary and Conclusion

Drug counterfeit is a global predicament that affects almost every country from the richest to the poorest; but it has a worse adverse effect on the third world and developing countries. Poor-quality drugs have greatly contributed to the development of resistance in many infectious diseases, with malaria at the top of that list. Bogus drugs have deters and undermines all efforts and investments to eradicate malaria. This stands to show there is a greater need to tighten the quality assurance and quality control of drugs globally, which makes the development of cheaper and more effective analytical techniques imperative.

The aim of this entire study was to develop electrochemical sensors for antimalarial drugs. In chapter 2 we carried out a comprehensive literature review of the electrochemical techniques for determination of antimalarial drugs revealing the current status and trends in their development. This literature outcome showed that nanomaterials, conducting polymers and presence of surfactants made significant contributions to voltammetric determination of antimalarial drugs suggesting promising future for use of chemically-modified electrode based sensors for the detection. Future progress in quantification of antimalarial drugs in biological fluids is expected to drastically improve the applicability of electrochemical methods for routine clinical analysis.

In chapter 3 we manage to synthesize urchin-shaped gold nanostructures and used them for the first time as sensing material for MQ. The synthesized material was characterized by ultraviolet-visible spectroscopy, energy-dispersive X-ray spectroscopy, field emission scanning electron microscopy, zeta-sizer and electrochemical techniques (electrochemical impedance spectroscopy and cyclic voltammetry). It was discovered that AuNUs are better electrode modifiers than AuNPs due to their spike-like morphology which increases their effective surface area. The proposed electrochemical sensor showed high sensitivity and selectivity, with a LOD in the nanomolar range and a wide linear concentration range. The method was

successfully applied for detection of the drug in pharmaceutical formulations and human urine with satisfactory recoveries, indicating that AuNUs is a promising candidate for the construction of an electrochemical sensor for MQ

In chapter 4, as an ongoing endeavor we used the synthesized AuNUs to design a sensitive and reliable square wave voltammetric method for quantitative analysis of PQ in real samples. The sensor exhibited wide linear concentration range of 0.01 – 1 μM and 0.001 – 1 μM, detection limits of 0.9 nM, high sensitivity and appreciable stability for the determination of PQ. The developed sensor was effectively applied to determine the drug in human urine samples and pharmaceutical formulations demonstrating its analytical applicability in clinical analysis as well as quality control

In chapter 5, this work presents a simple and highly sensitive electrochemical determination of AQ in real samples using a GCE modified with PMO and MWCNT. The proposed method was successfully utilized as an electrochemical sensor for determination of AQ with a very low detection limit of 8.9×10^{-8} mol L^{-1}. The obtained detection limit was lower than those reported in the literature. A plausible oxidation mechanism of AQ was presented for the first time. The sensor showed impressive practical applicability when evaluating AQ recoveries in pharmaceutical products as well as in urine samples.

In chapter 6 electrochemically deposited Cysteamine and chemically synthesized rGO-AuNP composite were employed for the fabrication of an electrochemical sensor for the detection of AQ in pharmaceutical formulations. DPV technique was employed and the peak current response was found to be linearly proportional to the AQ concentrations in the ranges of 5.0 x 10^{-7} to 2.2 x 10^{-6} and 6.6 x 10^{-6} to 4.5 x 10^{-5}M. The rGO-AuNP/Poly-Cyst/GCE sensor exhibited a very low detection limit of 1.8×10^{-8} M that is by far more superior to AQ sensors previously reported in literature The present study demonstrated a promising approach for quality assurance and quality control of AQ.

2. Future works

In this future work: we envisage the design of a biosensor that is sensitive and selective to malaria antigen, by fabricating nanomaterial onto a glassy carbon electrode to increase the effective surface areas and increase sensitivity. This will be followed by the immobilization of malaria antibodies (monoclonal) onto the nanomaterial modified electrode via the use of glutaraldehyde linkers. The antibodies will then detect malaria parasites in blood samples. This study stands to pave way to a design of a portable malaria diagnosis kit.

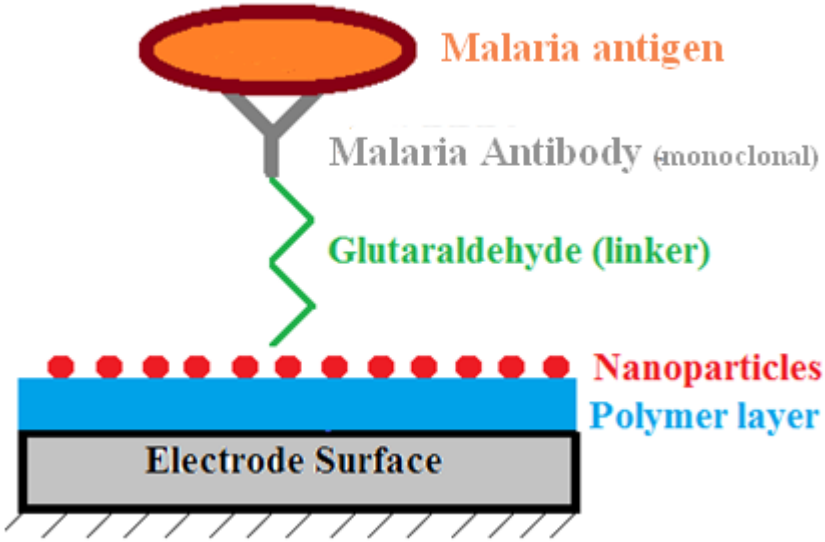

Schematic representation of the nanoparticles based electrochemical sensor for detection of malaria antigen.